

ASM-HEMT: Compact Modeling of GaN HEMTs for High Frequency and High Power Applications

Dr. Yogesh S. Chauhan

Associate Professor

Nanolab, Department of Electrical Engineering

IIT Kanpur

Email: chauhan@iitk.ac.in

Homepage – <http://home.iitk.ac.in/~chauhan/>

Outline

- Overview of Compact Modeling
- GaN HEMT
- ASM-HEMT Model Overview
- Model Validation

Joint Development & Collaboration



IIT Gandhinagar
Indian Institute of
Technology Gandhinagar



UNIVERSITY OF SEOUL



iemn
Institut d'Electronique, de Microélectronique
et de Nanotechnologie
UMR CNRS 8520



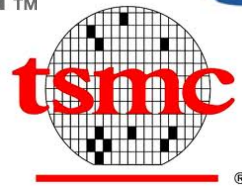
Leading Innovation >>>



KEYSIGHT
TECHNOLOGIES



maxim
integrated™



freescale™
semiconductor



TEXAS
INSTRUMENTS



GLOBALFOUNDRIES®

ON Semiconductor®



11/08/2017

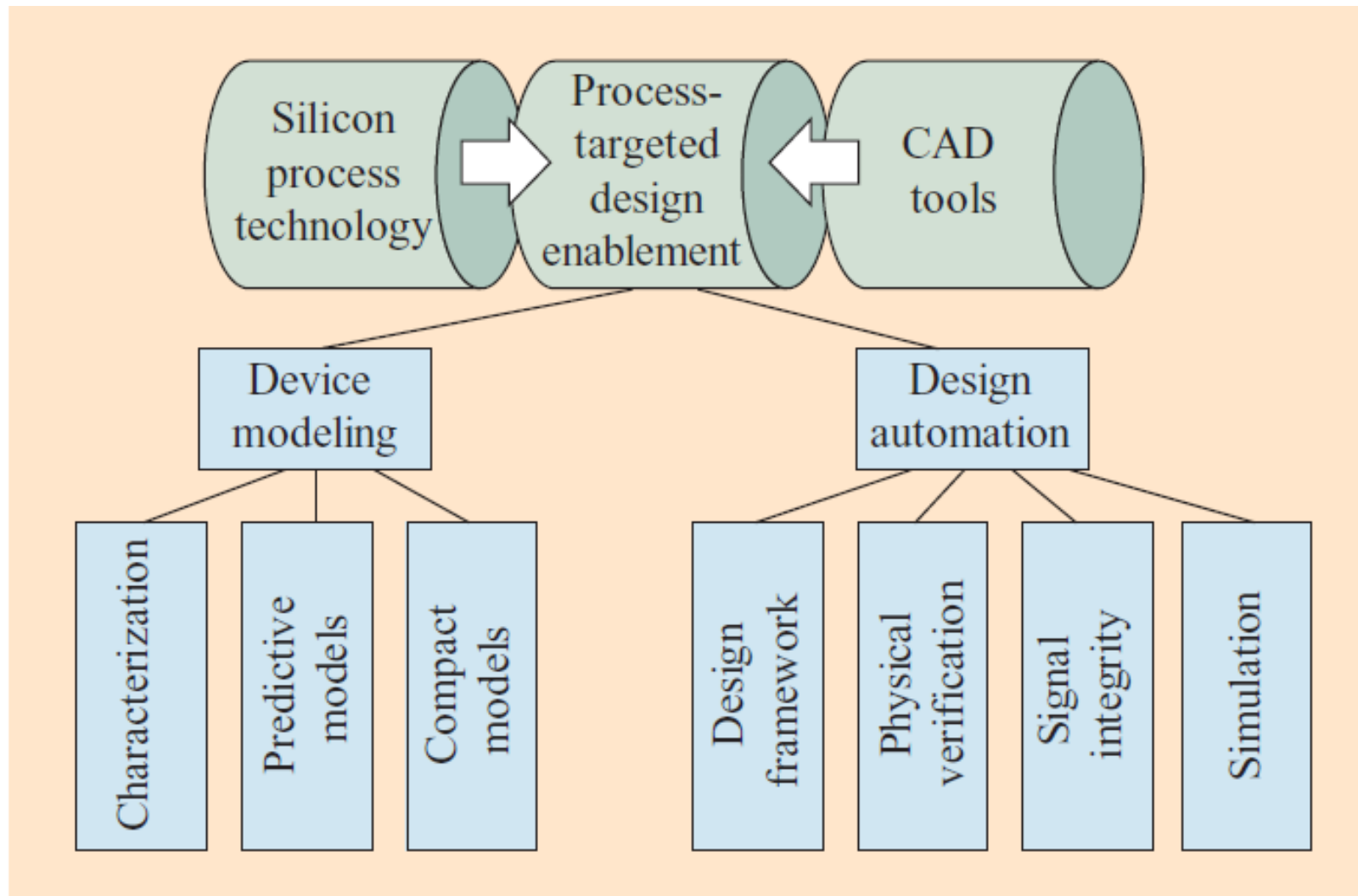
cādence™ in S.



ANALOG
DEVICES

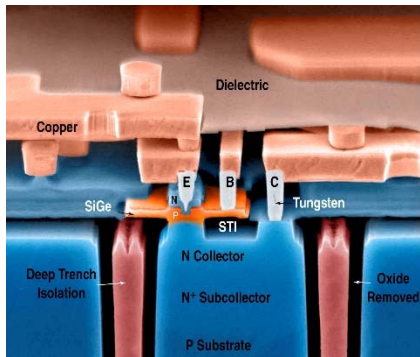
PDK and Compact Model

Enablers of a silicon chip design



Goal of a PDK – The output of Enablement

Technology Innovation



Enablement PDK
Key to Happy Designers!!

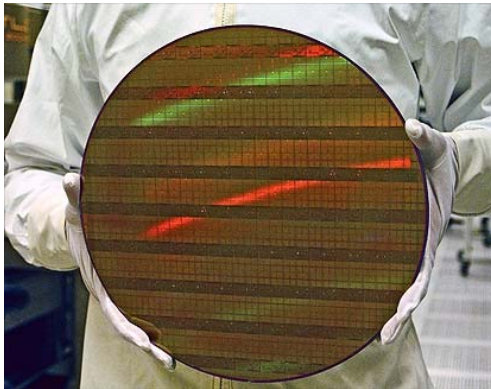


Circuit Designers



- Offer a circuit design environment that enables full exploitation of technology
 - Capture all device physics
 - Model impact of layout choices on device mean and variance
 - Include typical layout effects for simulation from schematic
 - Accurate modeling of layout effects for simulation from layout

Compact Modeling or SPICE Modeling



**Medium of
information
exchange**



- Good model should be
 - **Accurate:** Trustworthy simulations.
 - **Simple:** Parameter extraction is easy.
- Balance between accuracy and simplicity depends on end application

- **Excellent Convergence**
- **Simulation Time – $\sim \mu\text{sec}$**
- **Accuracy requirements**
 - $\sim 1\%$ RMS error after fitting
- **Example: BSIM6, BSIM-CMG**

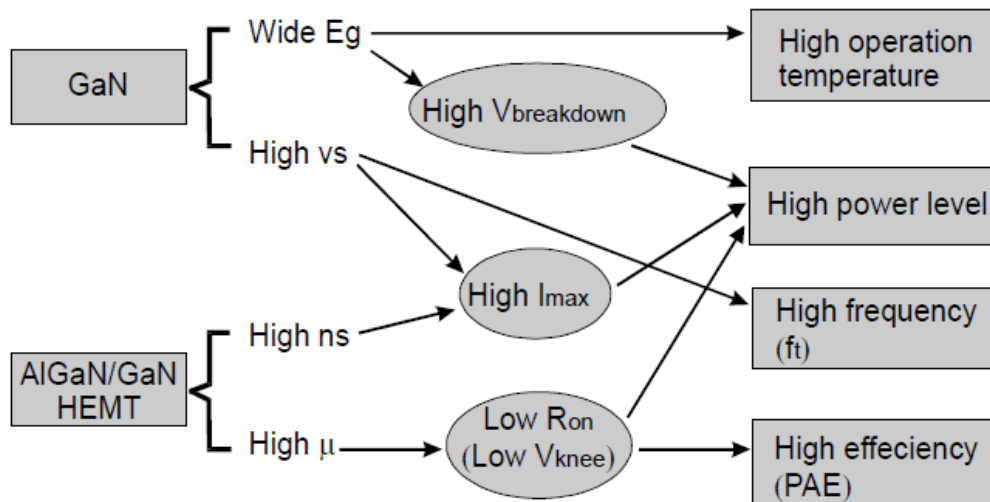
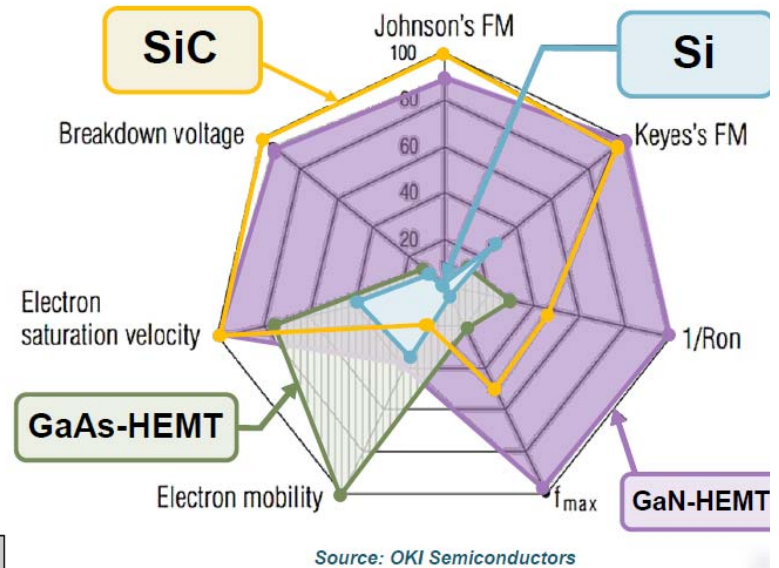
Industry Standard Compact Models

- Standardization Body – **Compact Model Coalition**
- CMC Members – EDA Vendors, Foundries, IDMs, Fabless, Research Institutions/Consortia
- CMC is by the industry and for the industry

GaN Properties

	Si	GaAs	4H-SiC	GaN
E_g (eV)	1.1	1.42	3.26	3.39
n_i (cm ⁻³)	1.5×10^{10}	1.5×10^6	8.2×10^{-9}	1.9×10^{-10}
ϵ_r	11.8	13.1	10	9.0
μ_n (cm ² /Vs)	1350	8500	700	1200(Bulk) 2000(2DEG)
v_{sat} (10 ⁷ cm/s)	1.0	1.0	2.0	2.5
E_{br} (MV/cm)	0.3	0.4	3.0	3.3
Θ (W/cm K)	1.5	0.43	3.3-4.5	1.3
$JM = \frac{E_{br} v_{sat}}{2\pi}$	1	2.7	20	27.5

Johnson's figure of merit (rel. to Si)



Device characteristics:

- High Breakdown Voltage (V_{BR})
- Low ON Resistance (R_{ON})

GaN HEMT: Advantages

600V FETs	Ron (mohm)	Ciss (nF)	FOM 1 (Ron*Ciss)	Coss (nF)@400V	FOM2 (Ron*Coss)	Qrr(uC)	FOM3 (Ron*Qrr)
Si SJ	37	7.24	267	0.38	14	36	1332
SiC MOS	120	1.2	144	0.09	10.8	0.053	6.3
GaN HFET	25	.52	13	0.13	3.25	0.113	2.8

Si SJ: Infineon IPW65R037C6. SiC MOSFET: Rohm SCT2120AF GaN HFET: GaNSystem GS66516T

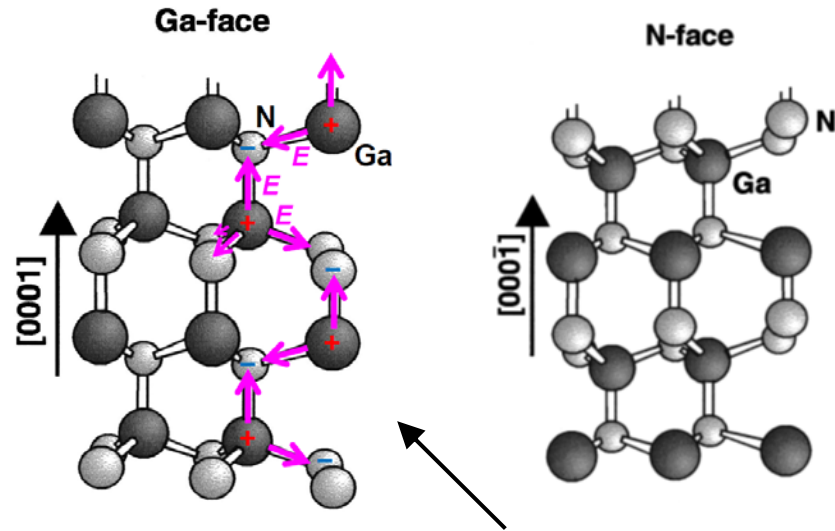
Alex Q. Huang pp. 528-531, IEDM 2016

advantage of fast gate driving capability

Reduction in switching loss in hard or soft switched converter

Reverse recovery loss reduction

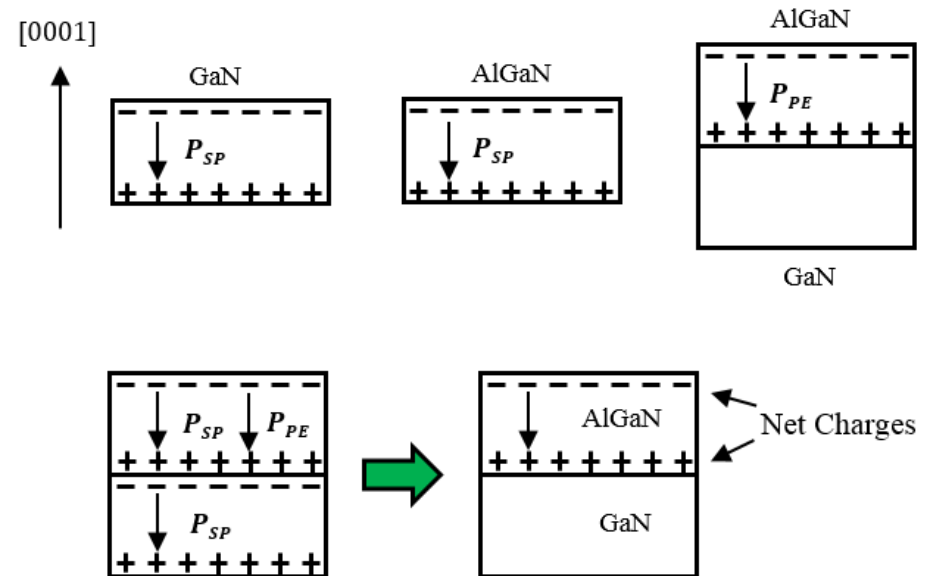
Polarization



Wurtzite

$$P_{PE} = 2 \frac{a - a_0}{a_0} \underbrace{\left(e_{31} - e_{33} \frac{C_{13}}{C_{33}} \right)}_{\text{Constant for a given } x \text{ (Al fraction)}}$$

Polarization!



GaN Wafers

- **Sapphire (Al_2O_3)**

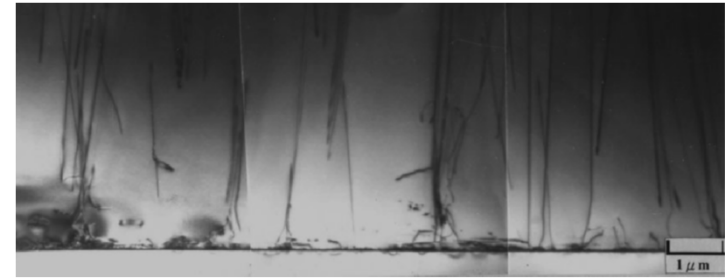
- ☺ Semi-insulating
- ☺ High growth temperatures
- ☺ Relatively cheap
- ☹ Low thermal conductivity
- ☹ Lattice mismatch
- ☹ CTE mismatch

- **Silicon (Si)**

- ☺ Low cost
- ☺ Large diameters
- ☺ Acceptable thermal conductivity
- ☺ Processing in standard silicon fabs
- ☹ Lattice mismatch
- ☹ CTE mismatch

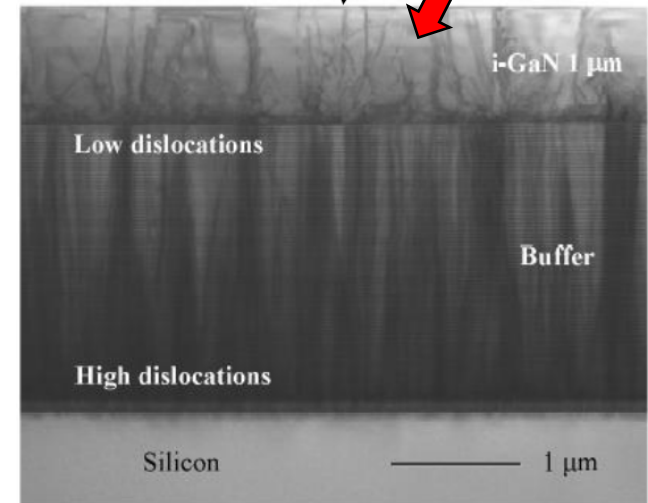
- **Silicon Carbide (SiC)**

- ☺ High thermal conductivity
- ☺ Low Lattice mismatch
- ☺ Low CTE mismatch
- ☹ Highly costly
- ☹ Smaller Wafers



TEM Image of GaN on Sapphire

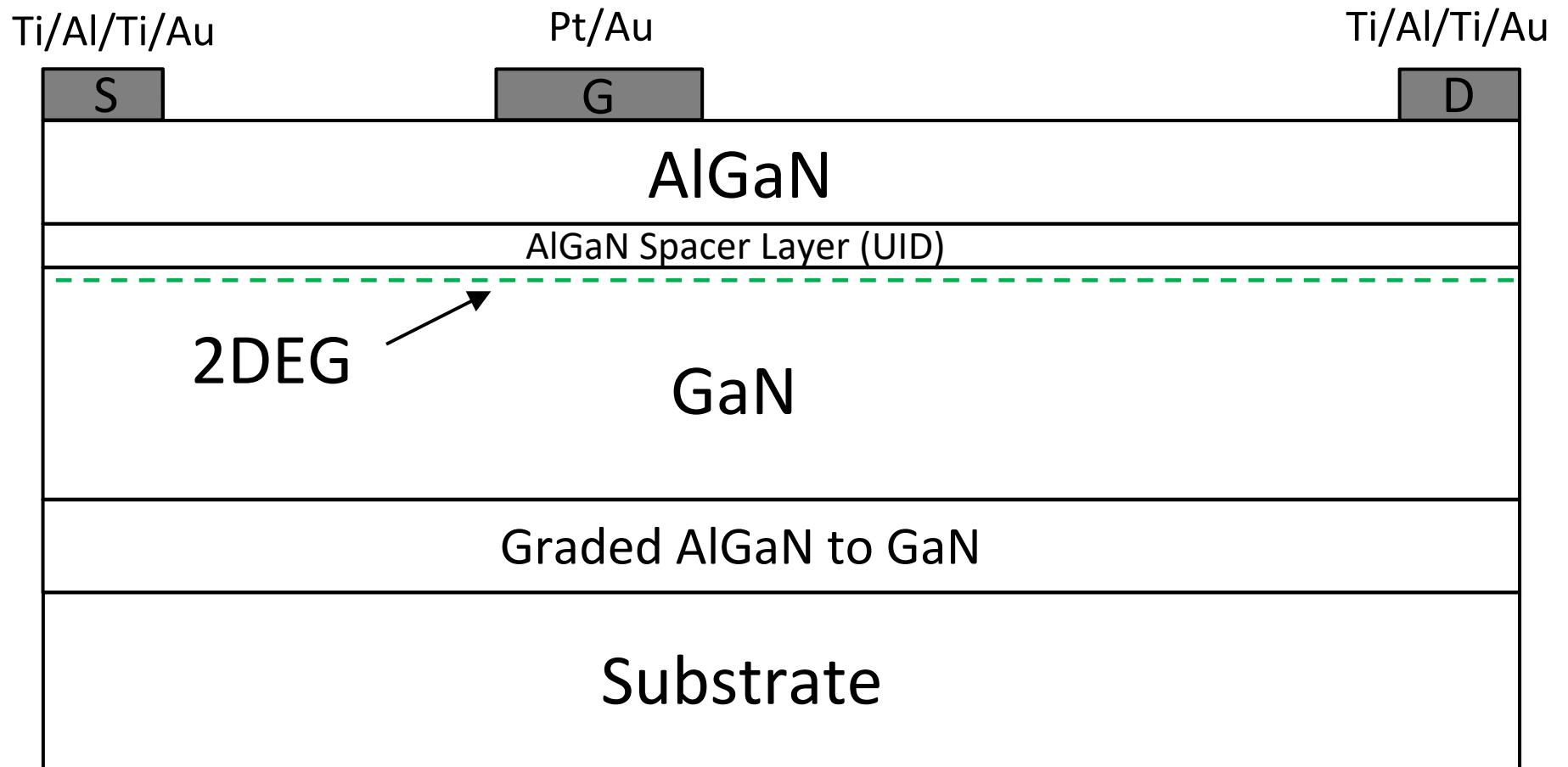
Dislocations $\sim 10^9 \text{ cm}^{-2}$



[S. Huang, JJAP, 47 (10), 7998 (2008)]

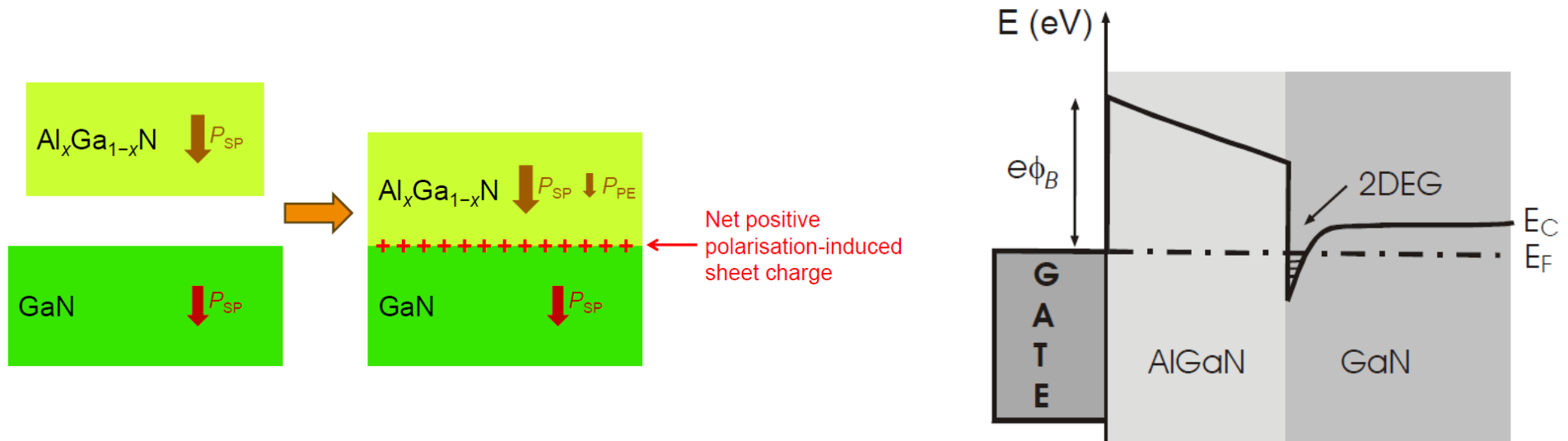
[S. L. Selvaraj et al., Proc. DRC, 12, 53 (2012)]

GaN HEMT Structure

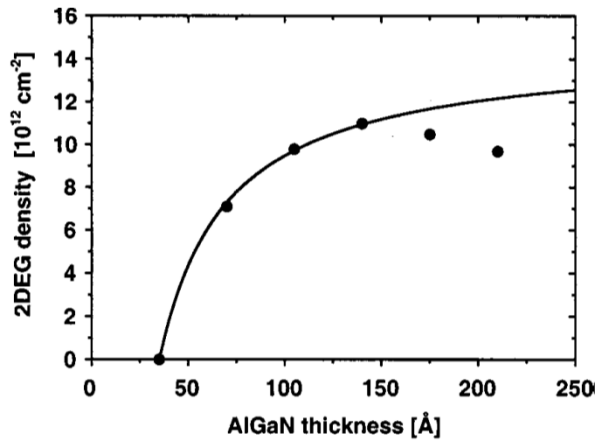
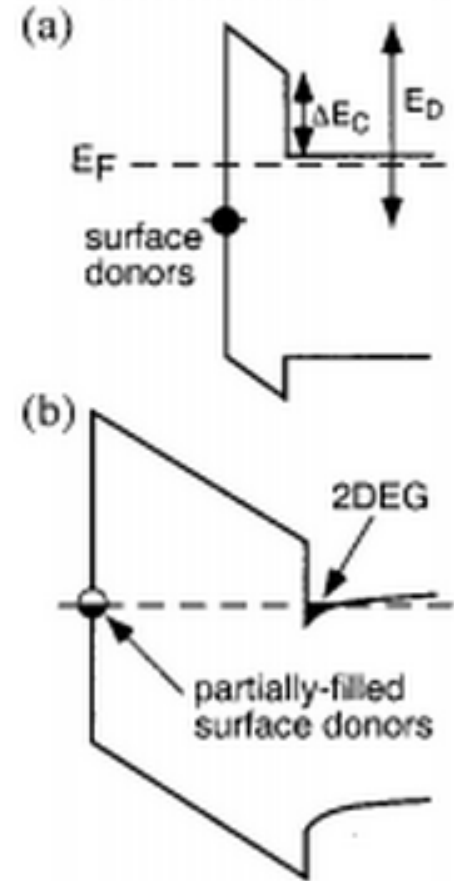
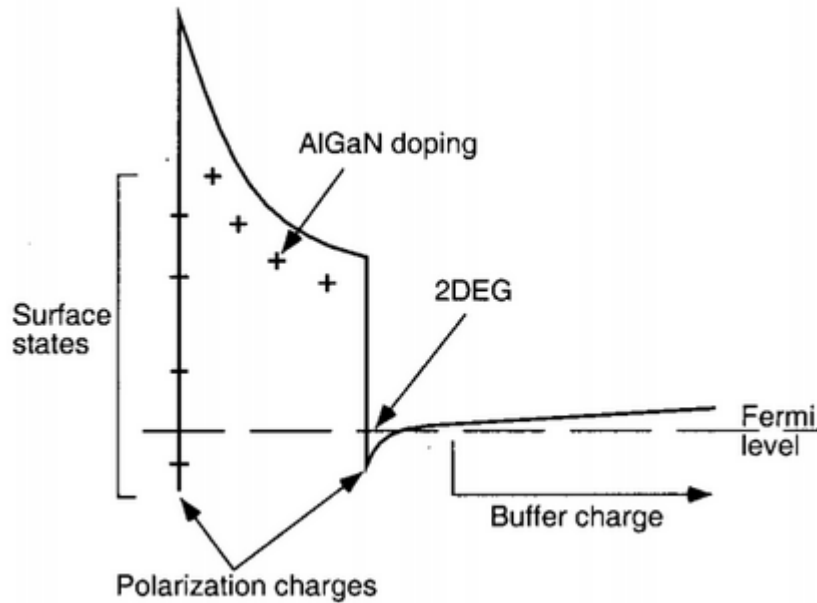


AlGa_xN/GaN Hetero-structure

- The AlGa_xN/GaN hetero-structure is used to take advantage of the **two dimensional electron gas (2-DEG)**
- AlGa_xN/GaN materials create **piezoelectric** and **spontaneous polarization** effects using an un-doped hetero-interface



2DEG Source



$$qn_s = \sigma_{pz} \left(1 - \frac{t_{cr}}{t} \right)$$

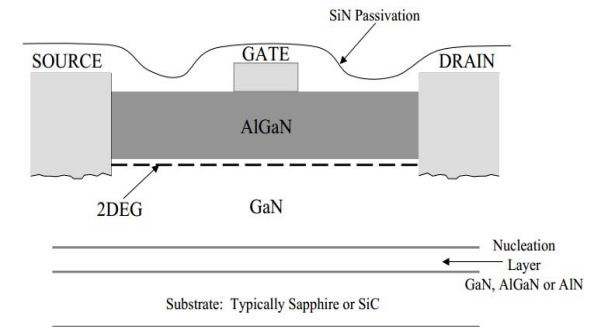
Design Rules – Materials Perspective

- Thickness of the barrier – 2DEG control
- Al Mole Fraction – 2DEG Concentration
- Nucleation and Buffer Layer – Dislocations
- Substrate – Thermal Properties

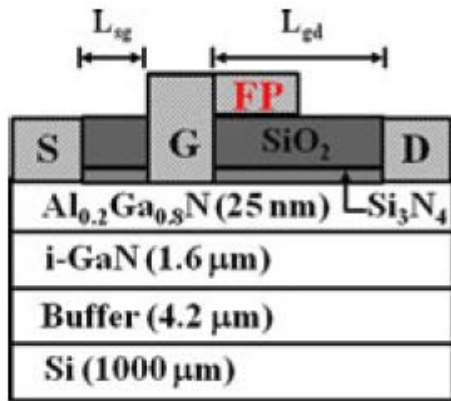
GaN HEMT

Some interesting features of III-nitride system:

- Wide bandgap
- High 2-DEG charge density
- High electron mobility
- High breakdown voltage
- Excellent thermal conductivity
- High power density per mm of gate periphery
- GaN based HEMTs are able to operate in **high frequency, high power** as well as **high temperature** device applications



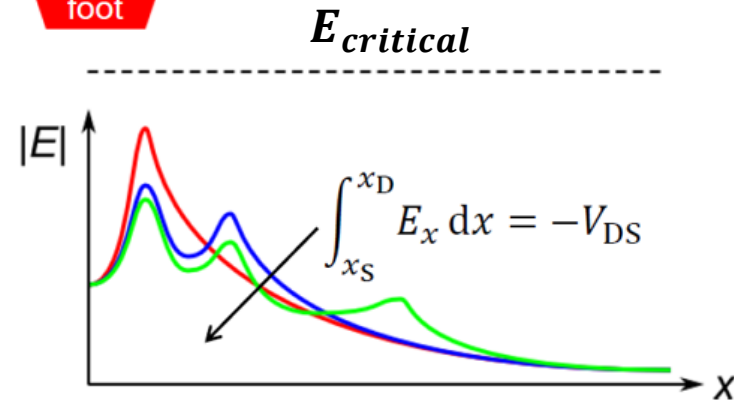
Field Plates



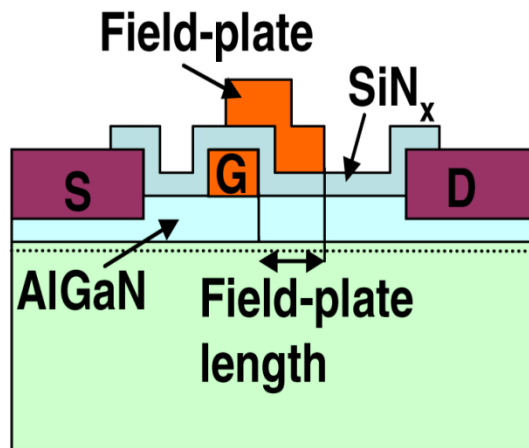
Field Plated Structure



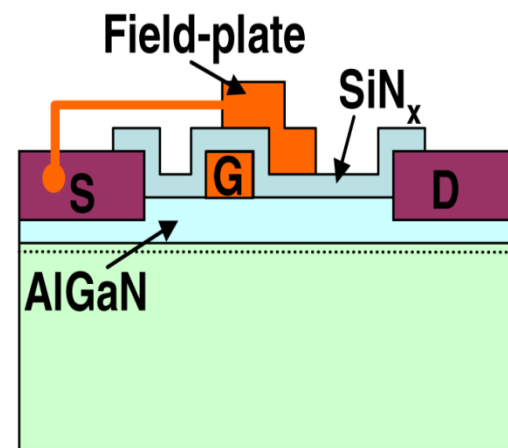
Distribution of E



C_{gd} and C_{ds}

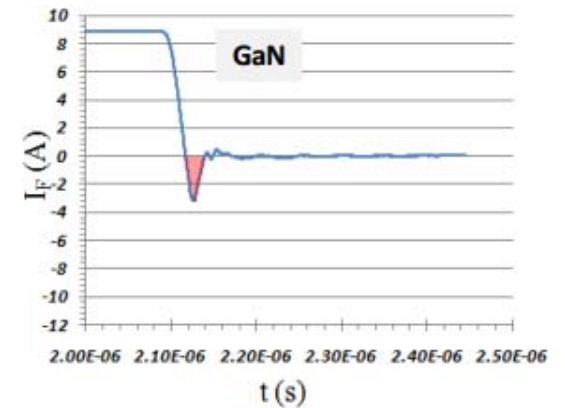
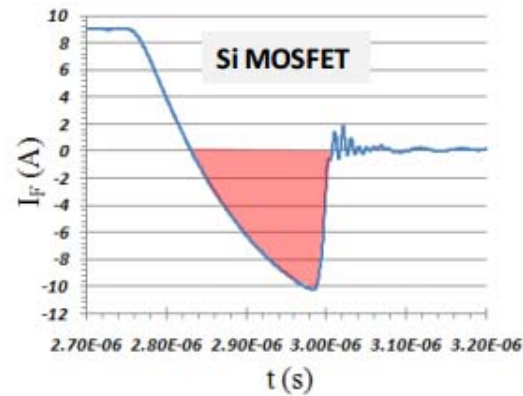
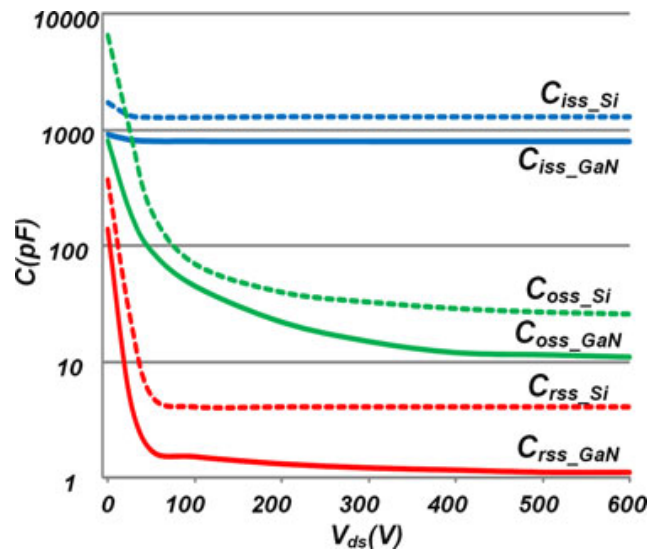


(a)



(b)

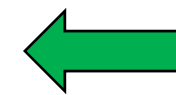
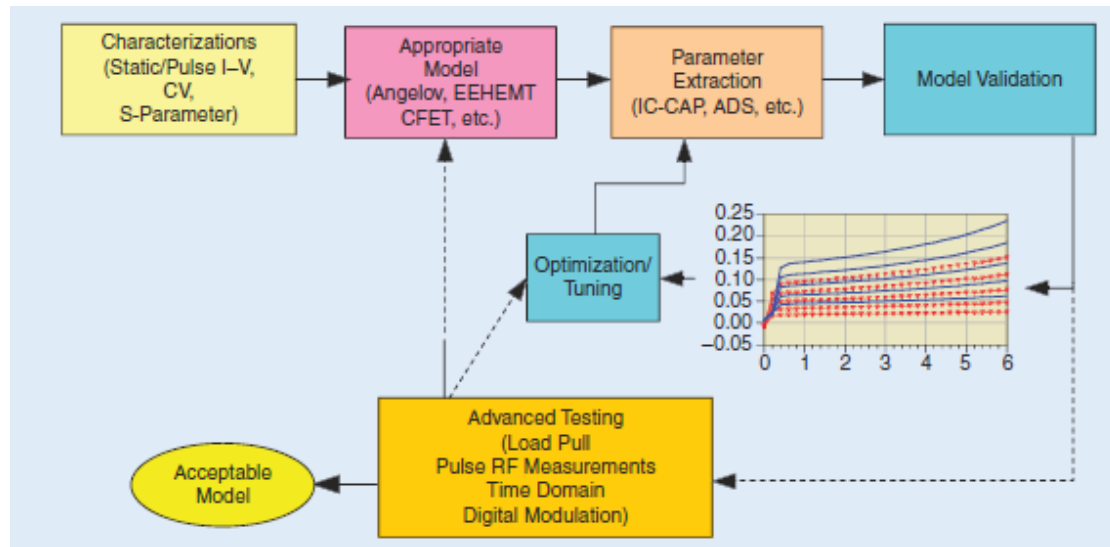
Switching applications



- Small terminal capacitances
- Less reverse recovery charge
- Power loss is low

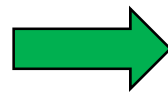
[X. Huang, *et al.*, IEEE TPEL, 29 (5), 2453 (2014)]

Modeling GaN!



Modeling Strategy

Existing Models



FET Models	Approx. Number of Parameters	Electrothermal (Rth-Cth) Model	Geometry Scalability Built-In	Original Device Context
Curtice3 [12]	59	No	No	GaAs MESFET
Motorola Electrothermal (MET) [25]	62	Yes	Yes	LD MOSFET
CMC (Curtice/Modelithics/Cree) [26]	55	Yes	Yes	LD MOSFET
BSIMSOI3 [24]	191	Yes	Yes	SOI MOSFET
CFET [5]	48	Yes	Yes	HEMT
EEHEMT [13]	71	No	Yes	HEMT
Angelov [14]	80	Yes	No	HEMT/MESFET
Angelov GaN [11]	90	Yes	No	HEMT
Auriga [4]	100	Yes	Yes	HEMT

Modeling Continued...

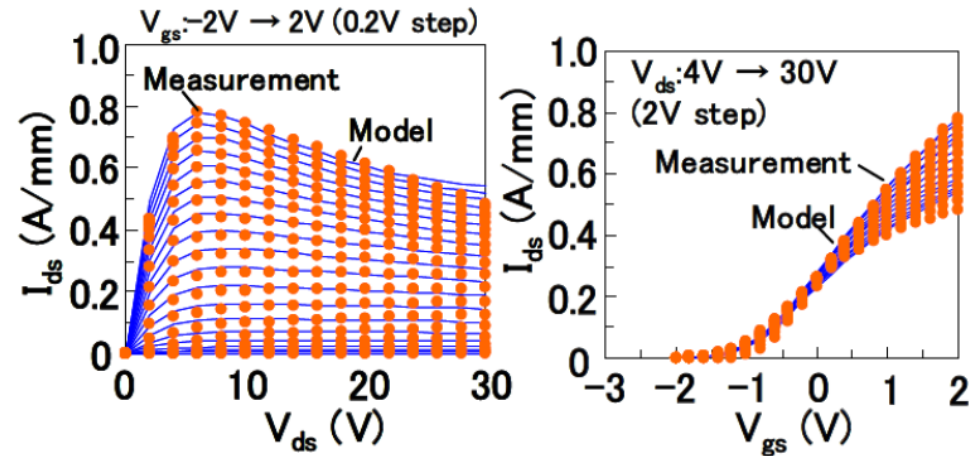
Angelov model

$$g_m = g_{mpk} (1 - \tanh^2[p_{1m} (V_{gs} - V_k)])$$

$$I_{ds} = I_{pks} (1 + \tanh(\psi_p)) \tanh(\alpha V_{ds}) (1 + \lambda V_{ds})$$

$$\psi_p = P_{1m} (V_{gs} - V_{pk0}) + P_2 (V_{gs} - V_{pks})^2 + P_3 (V_{gs} - V_{pksm})^3$$

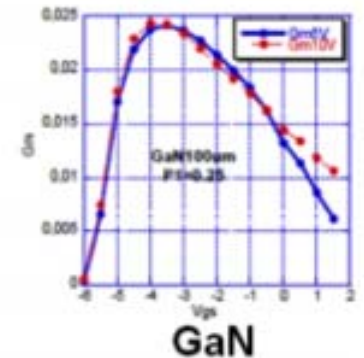
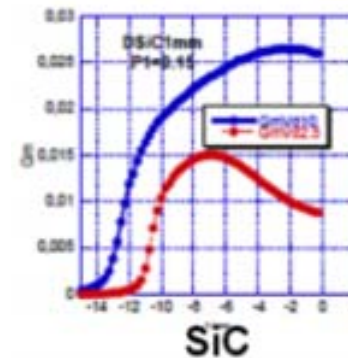
$$C_{gs} = C_{gsp} + C_{gso} (1 + \tanh(\psi_1)) (1 + \tanh(\psi_2))$$



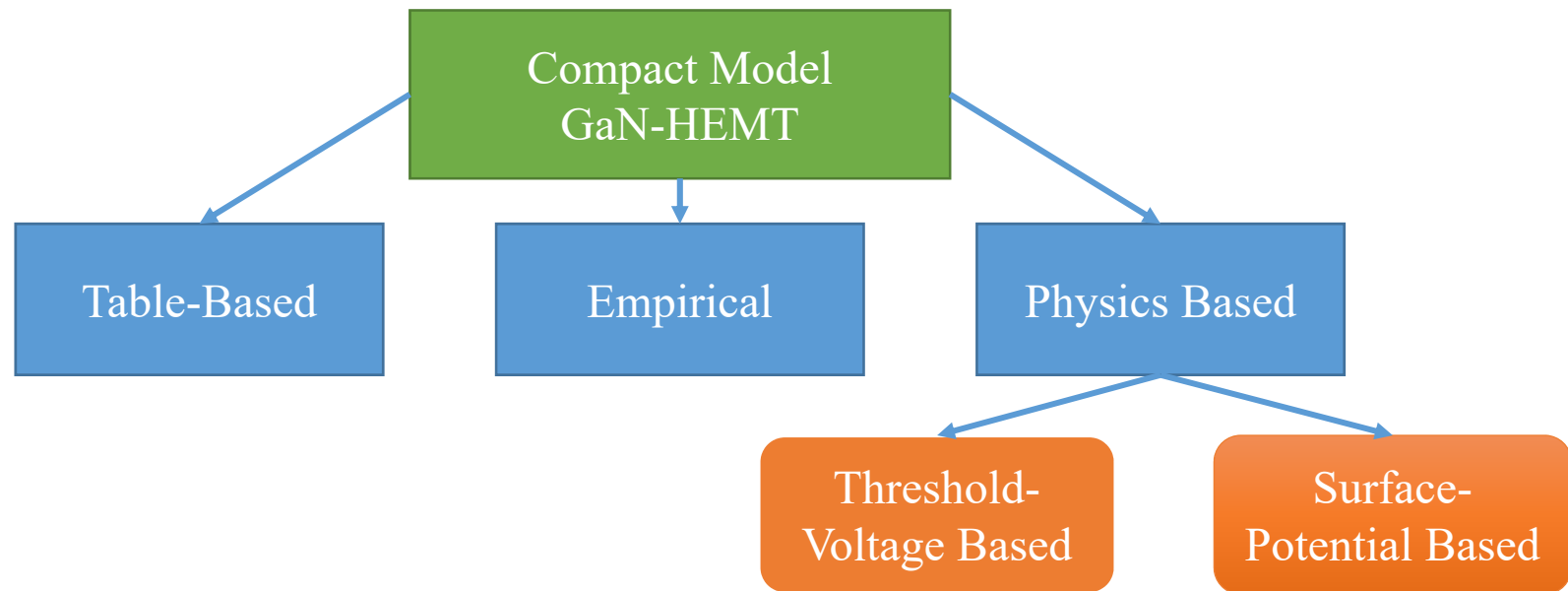
Angelov Model Deficiencies



- Empirical model with ~ 90 parameters
- Fails to capture non-linear behaviour and harmonic accuracy in power circuits
- Challenging to use for multiple device dimensions



Status of Compact Model – GaN HEMT



Advanced SPICE Model for GaN HEMT device

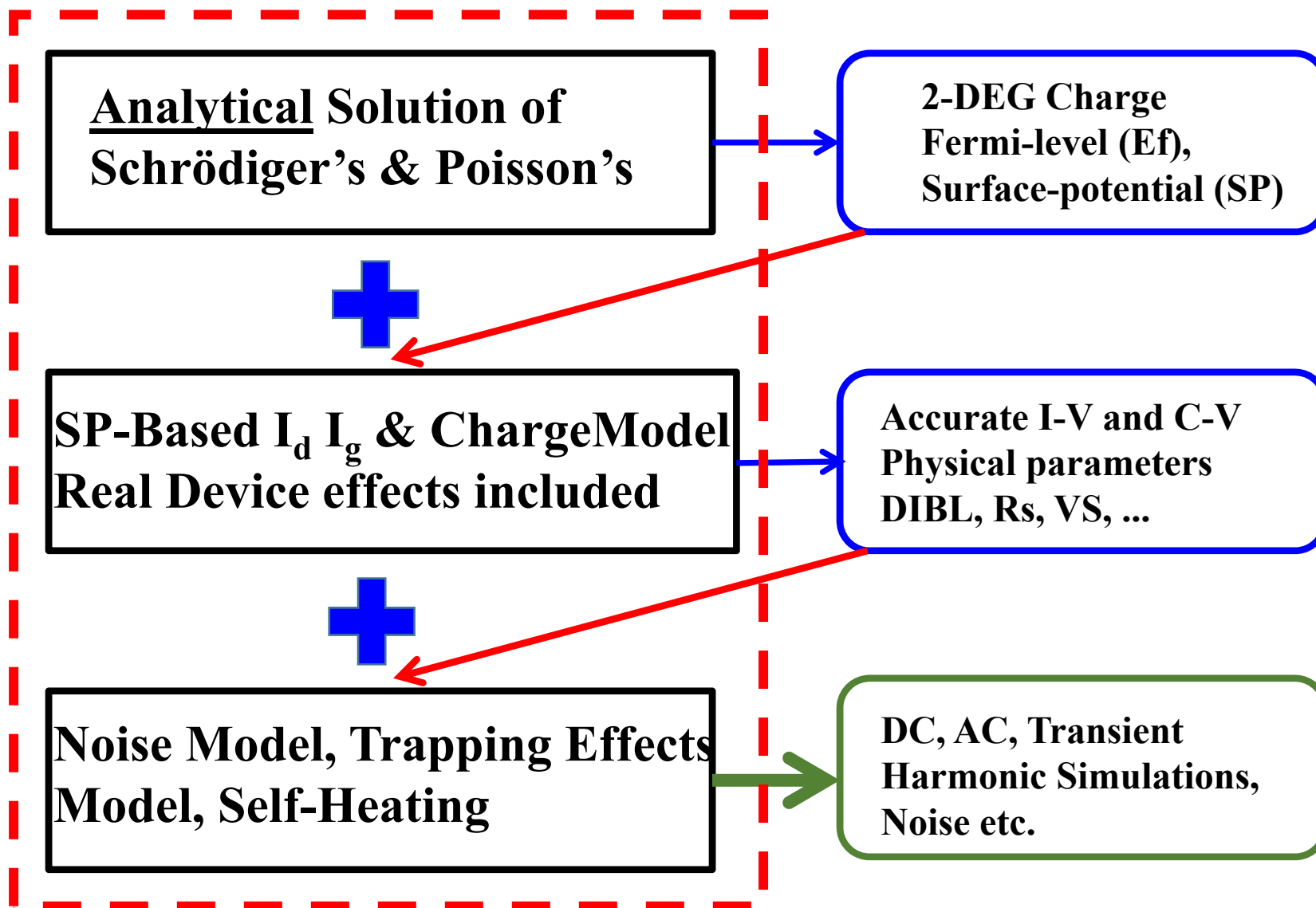
CMC candidate models for industry standardization
(Two models are in final phase)

- ASM-HEMT model: Our model
- MIT Unified VS GaNFET (MVSG) model: MIT, Prof. D. Antoniadis

Advantages of SP-Based Model

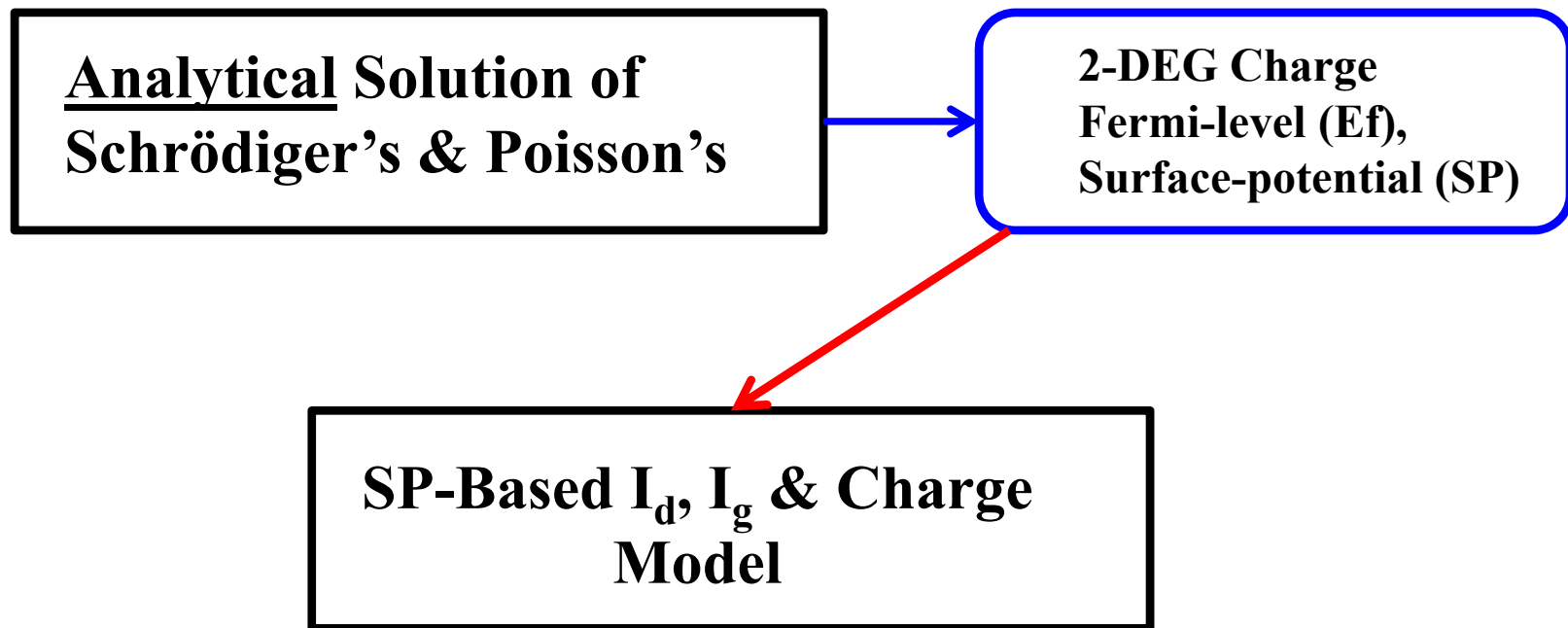
- Better Model Scalability
- Device Insight
- Better Statistical Behavior
- Accurate Charges and Capacitances
- Better Temperature Scalability
- Less number of parameters
- Easier parameter extraction
- Uses a single expression for all regions
- Inherent Model Symmetry

ASM-HEMT Model Overview



ASM-HEMT Model Overview

Core Model

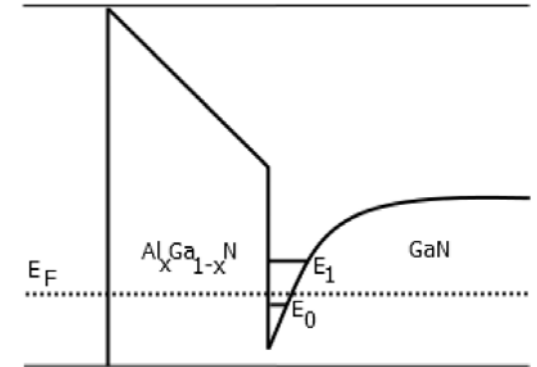


Surface-Potential Calculation

Assumptions:

- Quasi-constant electric field in the potential well (**triangular well approximation**)
- Only the contribution of the **first two sub-bands** are important

$$n_s = DV_{th} \left\{ \ln \left[\exp \left(\frac{E_f - E_0}{V_{th}} \right) + 1 \right] + \ln \left[\exp \left(\frac{E_f - E_1}{V_{th}} \right) + 1 \right] \right\}$$



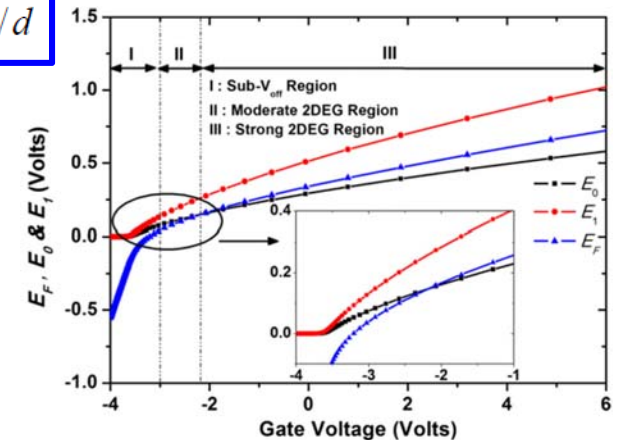
Quasi-Fermi-potential and SP

$$E_{f1} = E_{f,\text{unified}} - \frac{p}{q} \left(1 + \frac{pr}{2q^2} \right)$$

$$E_{f,\text{unified}} = V_{go} - \frac{2V_{th} \ln \left(1 + e^{\frac{V_{go}}{2V_{th}}} \right)}{1/H(V_{go,p}) + (C_g/qD)e^{-\frac{V_{go}}{2V_{th}}}}$$

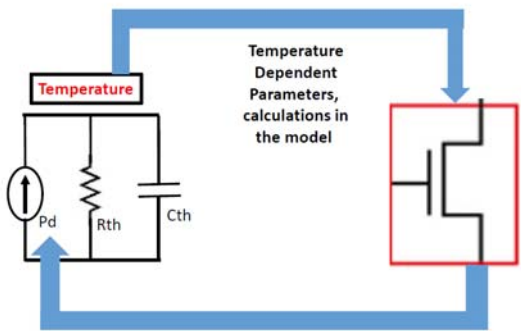
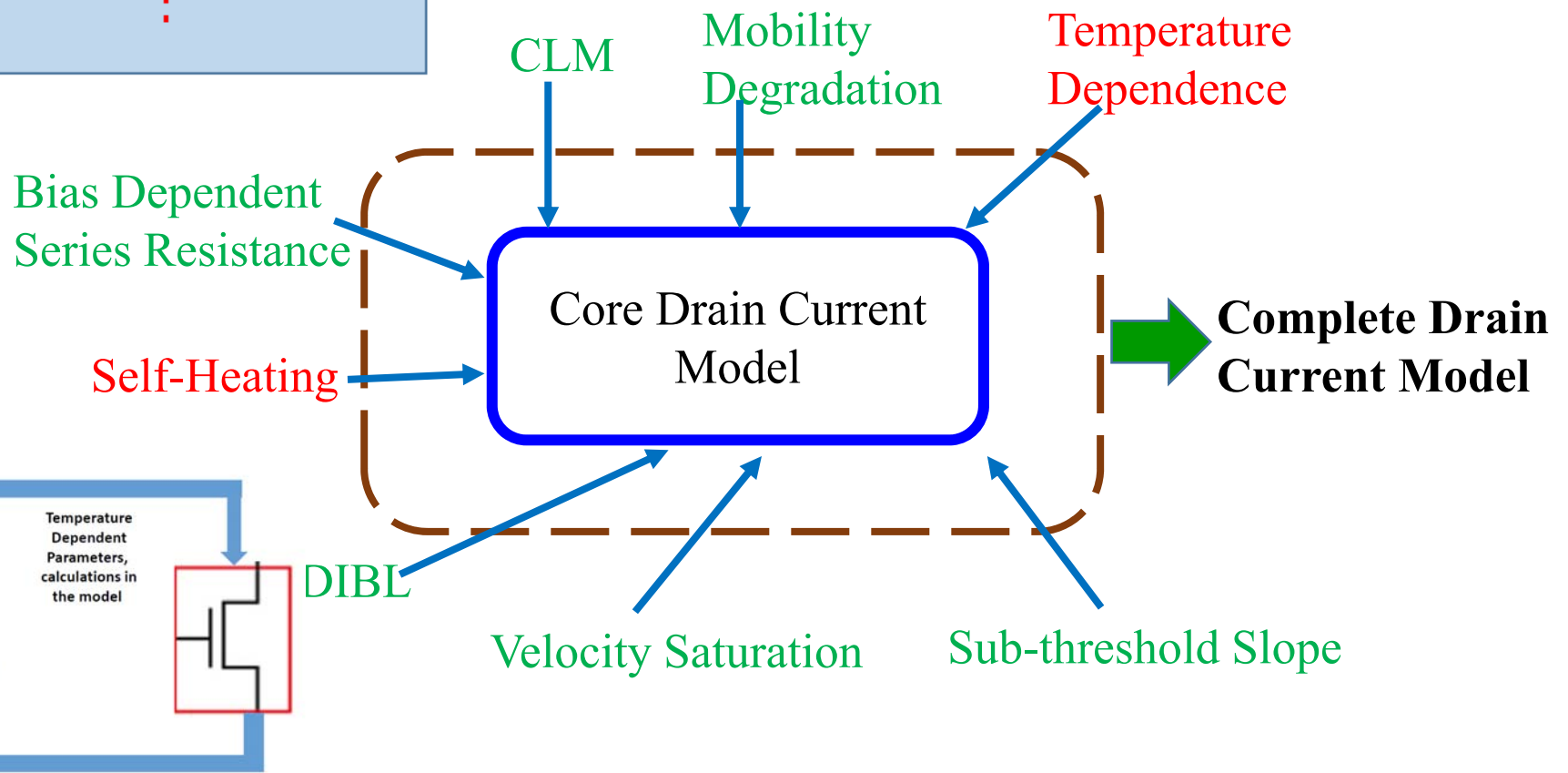
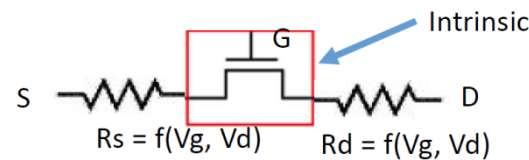
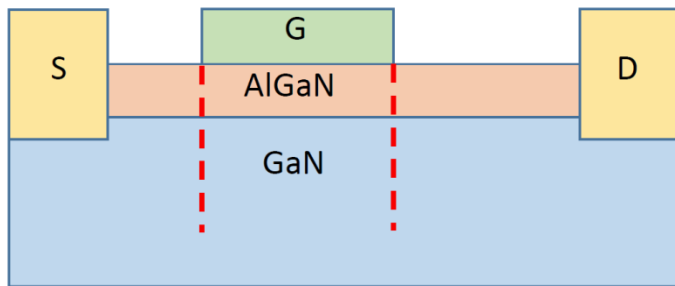
$$\psi_{s/d} = E_{f,s/d} + V_{s/d}$$

- Basic device equations are transcendental in nature
- We divide variation of E_f with V_g into **regions** to develop fully analytical expression
- Regional models are **combined in one analytical expression**
- No fitting parameters introduced, **accuracy** (order of nano-Volts)



S. Khandelwal, TED, VOL. 59, NO. 10, OCTOBER 2012

ASM-HEMT Model Overview



SP-Based Model Including Self-Heating

Drain-Current Model and Intrinsic Charges

- We apply the **drift-diffusion** framework for carrier transport
- An analytical and continuous expression for the core drain-current is developed including the **velocity-field relation** and **mobility degradation**

- Core Drain Current Model:

$$\int I_d \cdot dx = \int \mu_{\text{eff}} W \tilde{Q}_{ch} d\psi$$

$$\tilde{Q}_{ch} = V_{th} \frac{dQ_{ch}}{d\psi} - Q_{ch}$$

$$I_{ds} = \frac{\mu_{\text{eff}} C_g}{\sqrt{1 + \theta_{\text{sat}}^2 \psi_{\text{ds}}^2}} \frac{W}{L} (V_{\text{go}} - \psi_m + V_{\text{th}}) (\psi_{\text{ds}}) (1 + \lambda V_{\text{ds}})$$

- **Ward-Dutton Partitioning** for S/D charges

- Capacitances are calculated as derivatives of the terminal charges: $C_{ij} = -dQ_i/dV_j$ ($i \neq j$), $C_{ii} = dQ_i/dV_i$ ($i = j$)

Charge conservation

$$Q_g = \int_0^L W q n_s (V_g, V_x) \cdot dx$$

$$Q_d = \int_0^L \frac{x}{L} W q n_s (V_g, V_x) \cdot dx$$

$$Q_s = \int_0^L \left(1 - \frac{x}{L}\right) W q n_s (V_g, V_x) \cdot dx$$

- Velocity-Field relation and mobility-degradation:

$$\psi_{ds} = \psi_d - \psi_s \quad \psi_m = (\psi_d + \psi_s) / 2 \quad \theta_{\text{sat}} = \mu_{\text{eff}} / v_{\text{sat}} L$$

$$\mu_{\text{eff}} = \frac{\mu_0}{1 + UA (V_{\text{go}} - \psi_m) + UB (V_{\text{go}} - \psi_m)^2}$$

Temperature Dependence

$$\mu_0(T) = U_0 \cdot \left(\frac{T}{TNOM} \right)^{UTE} \quad V_{sat}(T) = VSAT \cdot [1 + AT(T - TNOM)]$$

$$V_{off}(T) = VOFF + KT1 \cdot \left(\frac{T}{TNOM} - 1 \right)$$

$$R_{source}(T) = \frac{R_{sc}(T)}{W \cdot NF} + R_{s,bias}(T)$$

$$I_{sat,acc}(T) = W \cdot NF \cdot q_{s,acc}(T) \cdot V_{sat,accs}(T)$$

$$R_{drain}(T) = \frac{R_{dc}(T)}{W \cdot NF} + R_{d,bias}(T)$$

$$q_{s,acc}(T) = q \cdot n_{s0}(T)$$

$$R_{sc}(T) = RSC \cdot \left(1 + KRSC \left(\frac{T}{TNOM} - 1 \right) \right)$$

$$n_{s0}(T) = NSOACC \cdot \left(1 - KNS0 \cdot \left(\frac{T}{TNOM} - 1 \right) \right)$$

$$R_{dc}(T) = RDC \cdot \left(1 + KRDC \left(\frac{T}{TNOM} - 1 \right) \right)$$

$$V_{sat,accs}(T) = VSATACCS \cdot [1 + ATS(T - TNOM)]$$

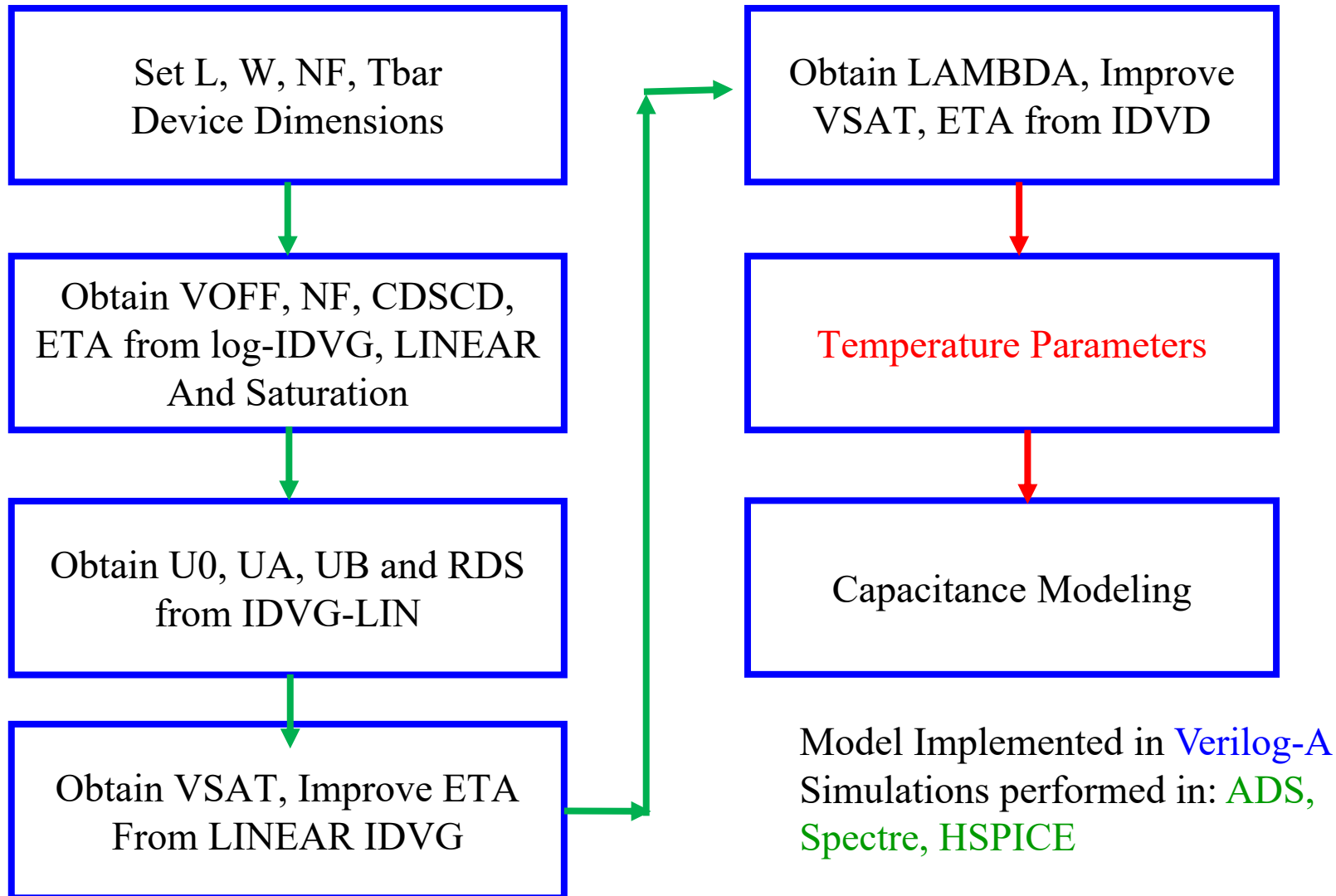
$$R_{s0}(T) = \frac{LSG}{W \cdot NF \cdot q_{s,acc}(T) \cdot \mu_{0,accs}(T)}$$

$$R_{s,bias}(T) = \frac{R_{s0}(T)}{\left[1 - \left(\frac{I_{ds}}{I_{sat,acc}(T)} \right)^{MEXPACCS} \right]^{\frac{1}{MEXPACCS}}}$$

$$R_{d0}(T) = \frac{LDG}{W \cdot NF \cdot q_{s,acc}(T) \cdot \mu_{0,accd}(T)}$$

$$R_{d,bias}(T) = \frac{R_{d0}(T)}{\left[1 - \left(\frac{I_{ds}}{I_{sat,acc}(T)} \right)^{MEXPACCD} \right]^{\frac{1}{MEXPACCD}}}$$

Model Parameter Extraction



List of Main Parameters

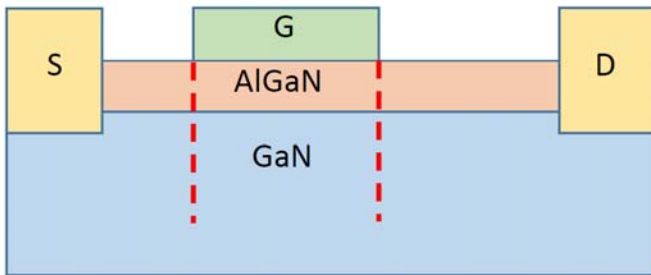
- Physical Constants
- Simulation Conditions
- Device dimensions
- Physically-Linked Parameters

Parameters	Physical Meaning
U0	Low field Mobility
UA	Mobility degradation parameter
UB	Mobility degradation parameter
VOFF	Cut-off Voltage of Device
VSAT	Saturation Velocity
RTH	Thermal Resistance
DIBL	DIBL effect parameter
LAMBDA	Channel length modulation
VOFFT	Temperature dependence of Voff
UTE	Mobility dependence of mu0
RS	Source Side Resistance
RD	Drain Side Resistance
.....

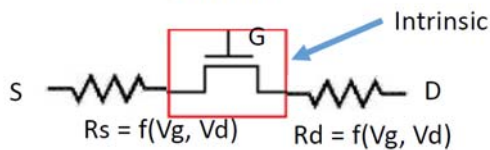
Importance of $R_{d/s}$ Model

- Aggressive lateral scaling of source-drain access regions improve the **RF performance** of GaN HEMT but at the cost of **breakdown voltage (BV)**
 - Too short L_{gd} increases electric field which is responsible for lowering of BV
 - Scaling of L_{gd} also affects the f_{max} due to increasing C_{gd} and g_{ds} of device
- As a **trade-off**, a short L_{gs} and optimized L_{gd} is required to achieve high f_T , f_{max} and BV altogether
- In GaN HEMT, gate-to-drain/source access region works as nonlinear resistance ($R_{d/s}$) which **limits maximum drain current**
- Accurate model of $R_{d/s}$ is of great importance to predict the I_d and g_m for high power as well as high frequency GaN HEMTs

Nonlinear source/drain access region resistance model



$$R_J = \frac{L_J}{q\mu_n n_{s0}} \quad J = S, D$$



$$I_{acc} = Q_{acc} \cdot v_s = Q_{acc} \cdot v_{sat} \cdot \frac{V_R/V_{Rsat}}{\left[1 + \left(\frac{V_R}{V_{Rsat}}\right)^\gamma\right]^{\frac{1}{\gamma}}}$$

$$R_{d/s} = \frac{V_R}{I_{acc}} = \frac{R_{d0/s0}}{\left[1 - \left(\frac{I_d}{I_{acc,sat}}\right)^\gamma\right]^{\frac{1}{\gamma}}}$$

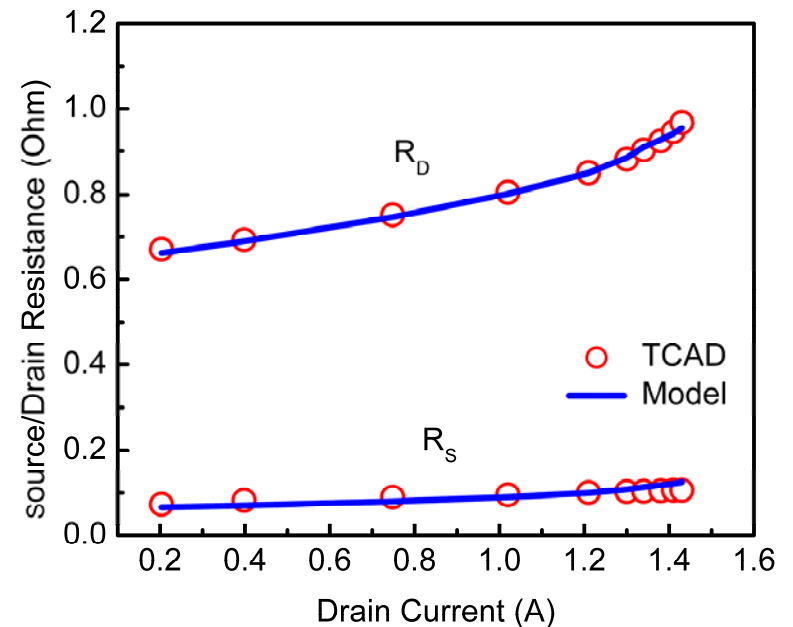


Fig. 1: Nonlinear variation of source/ drain access resistances with I_{ds} extracted from TCAD simulation and comparison with model.

$R_{d/s}$ Model Validation with Measurement

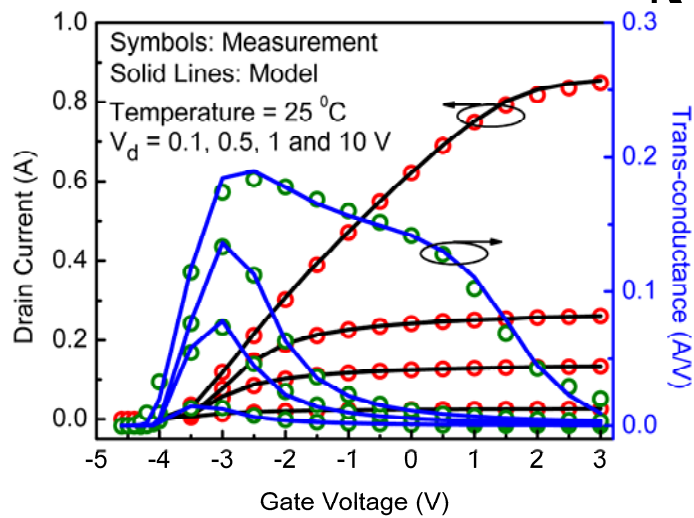


Fig. 2: $I_d - V_g$ and trans-conductance for the Toshiba power HEMT. Different slopes above V_{off} in $g_m - V_g$: self-heating governs the first slope while velocity saturation in access region affects second slope.

Effect of high access region resistance at high V_g

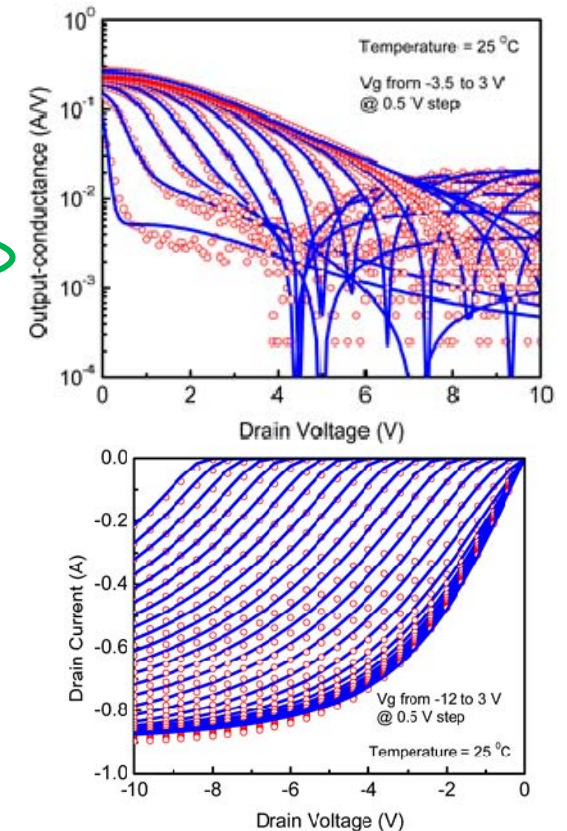
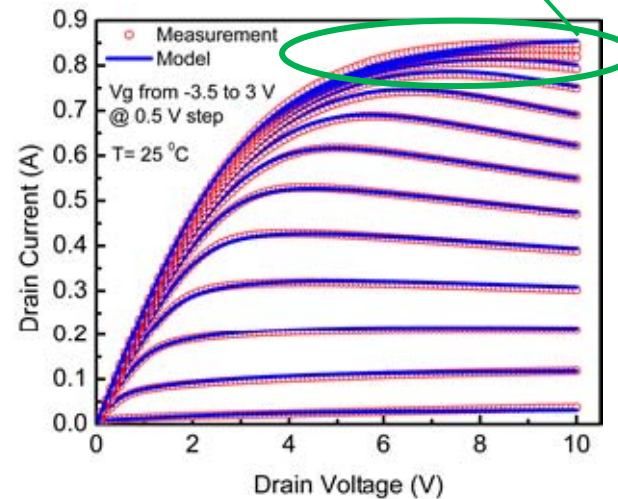


Fig. 3: (a) $I_{ds} - V_{ds}$, (b) g_{ds} and (c) reverse $I_{ds} - V_{ds}$ fitting with experimental data. The non-linear $R_{s/d}$ model shows correct behavior for the higher V_g curves in the $I_d - V_d$ plot; the S-P based model can accurately capture the reverse output characteristics.

Modeling of Temperature dependence

The temperature dependence of $R_{d/s}$ model is extremely important as it increases significantly with increasing temperature

Temperature dependence of 2-DEG charge density in the drain or source side access region:

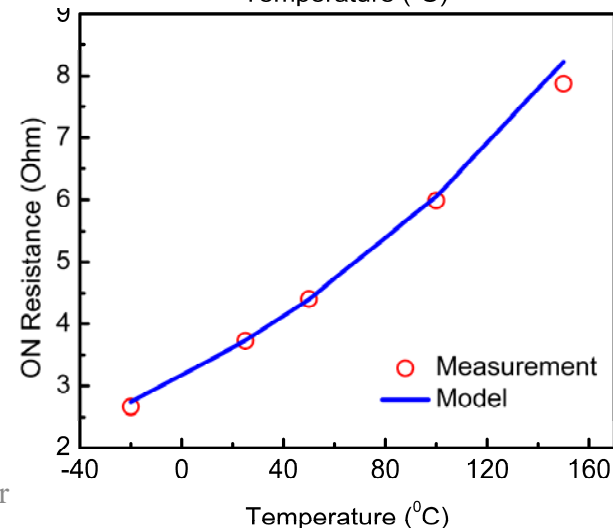
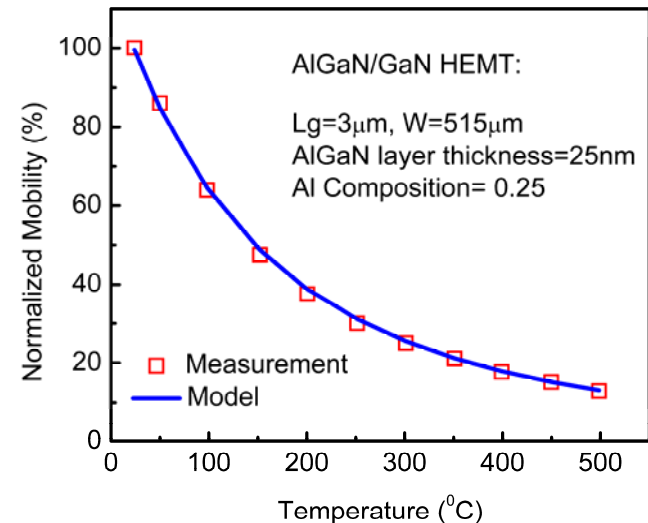
$$n_{s0}(T) = NS0ACC \cdot \left(1 - KNS0 \cdot \left(\frac{T}{TNOM} - 1 \right) \right)$$

Temperature dependence of Saturation Velocity:

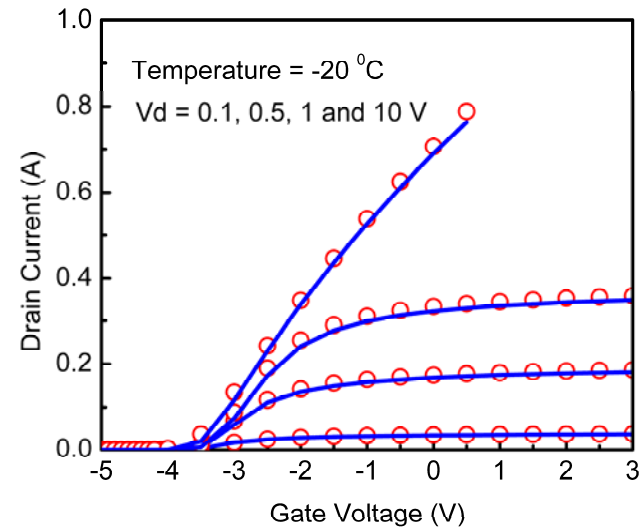
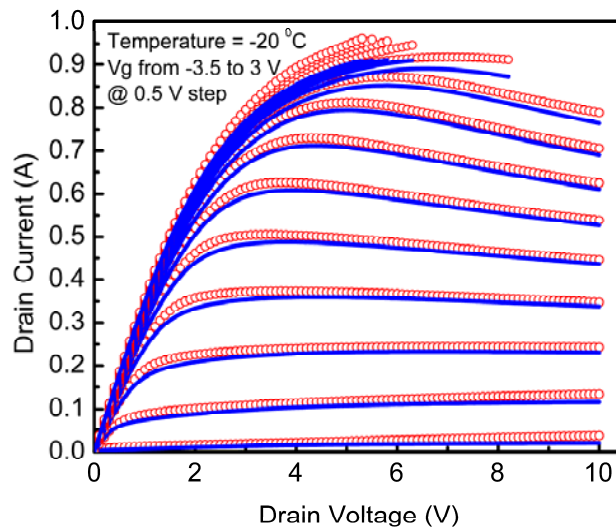
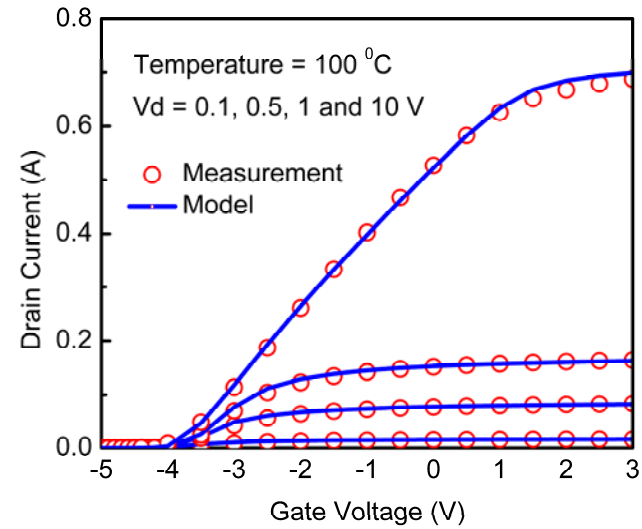
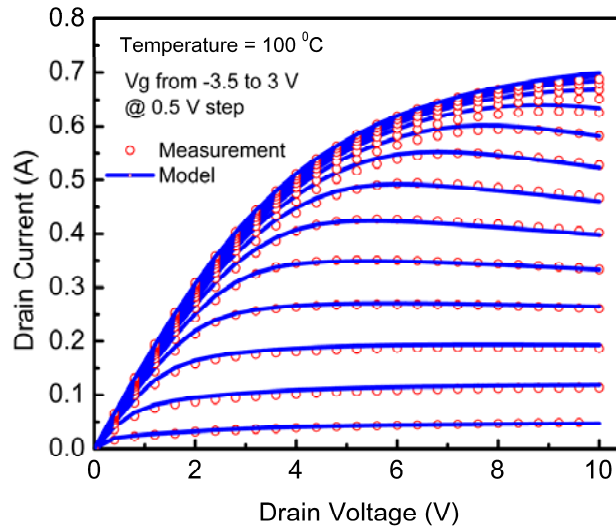
$$V_{sat}(T) = VSATACCS \cdot [1 + ATS(T - TNOM)]$$

Temperature dependence of electron Mobility:

$$\mu_{acc}(T) = U0ACC \cdot \left(\frac{T}{TNOM} \right)^{UTEACC}$$

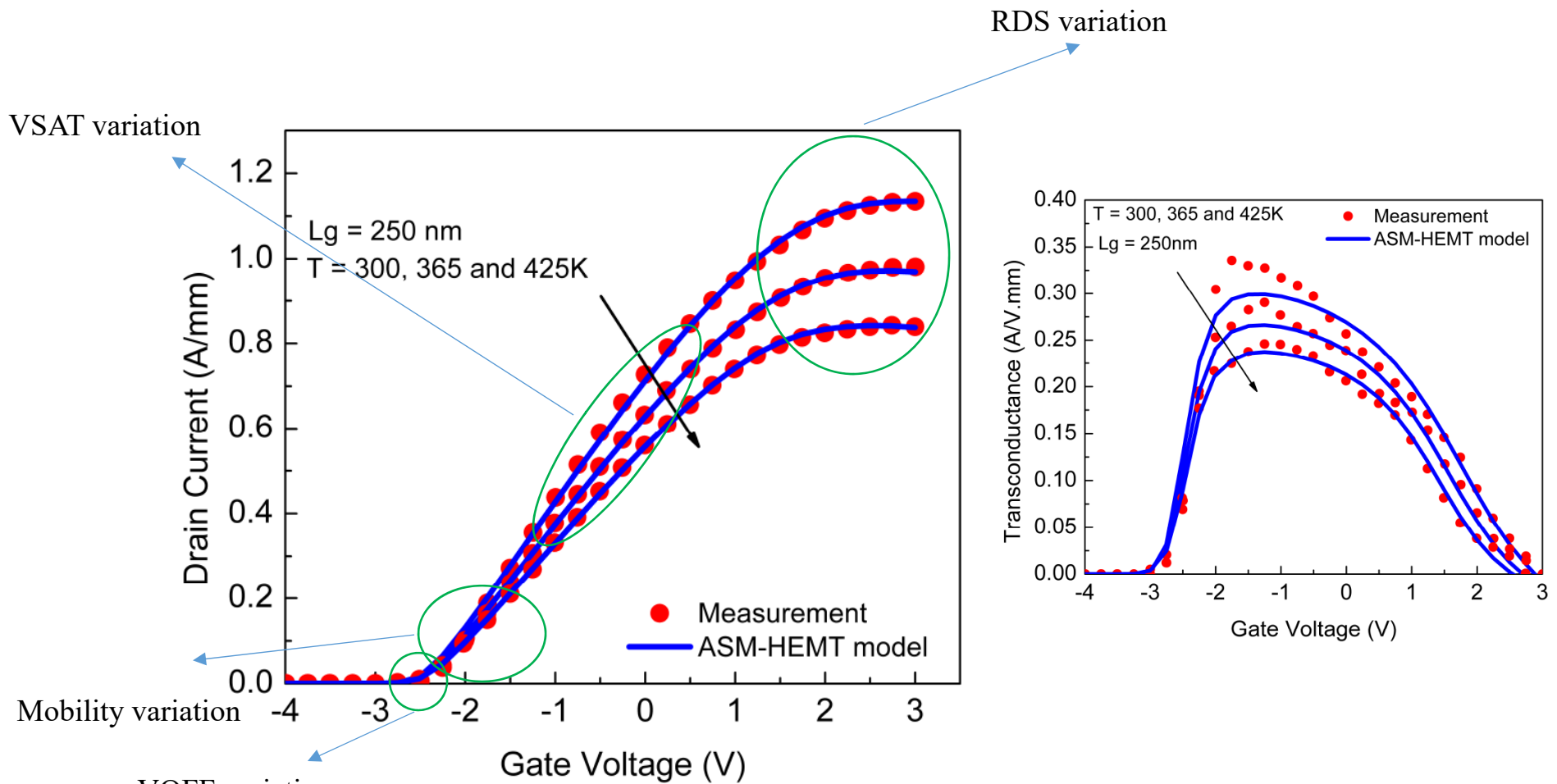


Temperature Model Validation



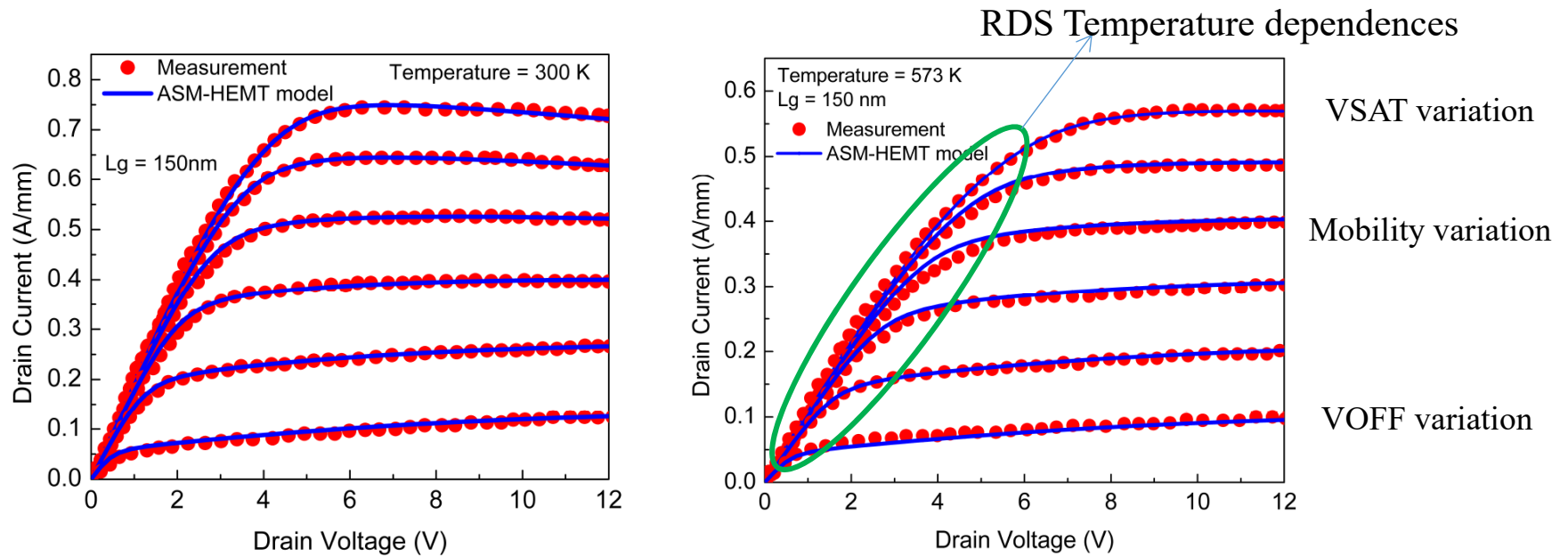
Temperature Model Validation

Id-Vg at three different temperatures 300, 365 and 425 K

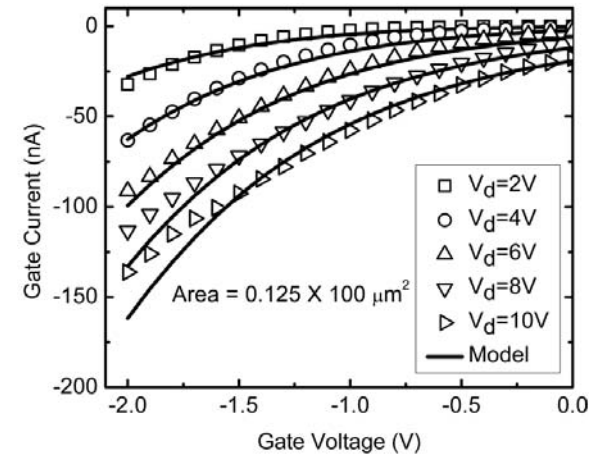
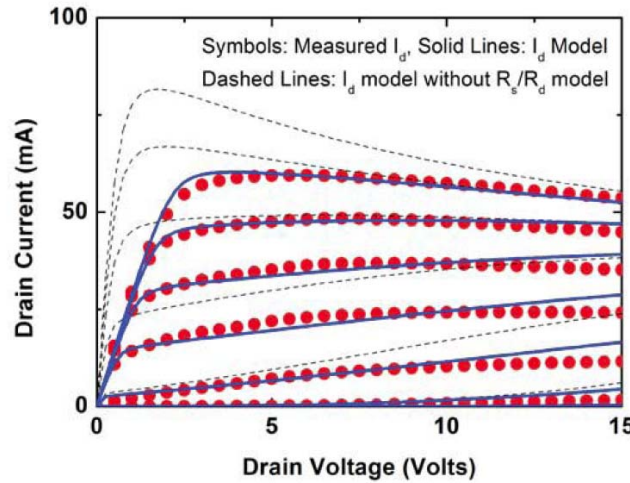
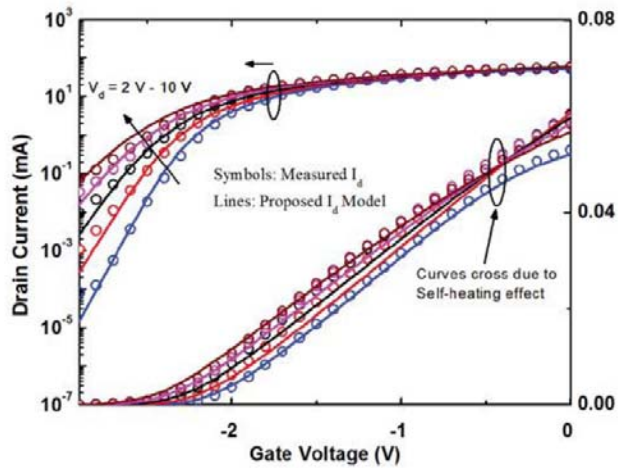


Temperature Model Validation

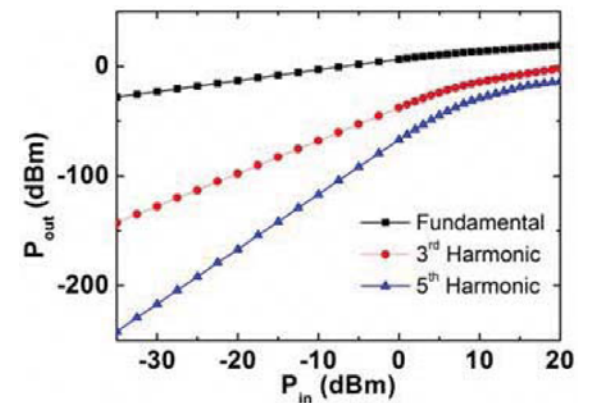
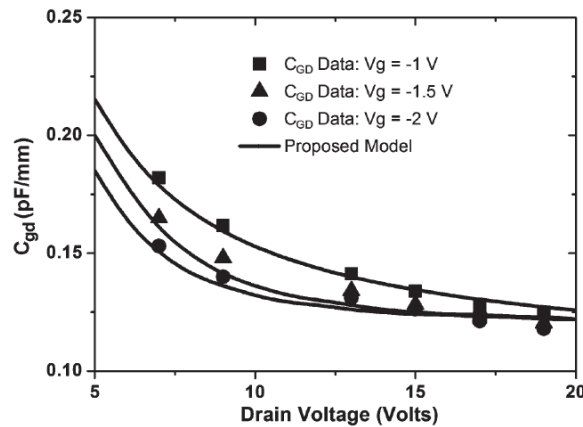
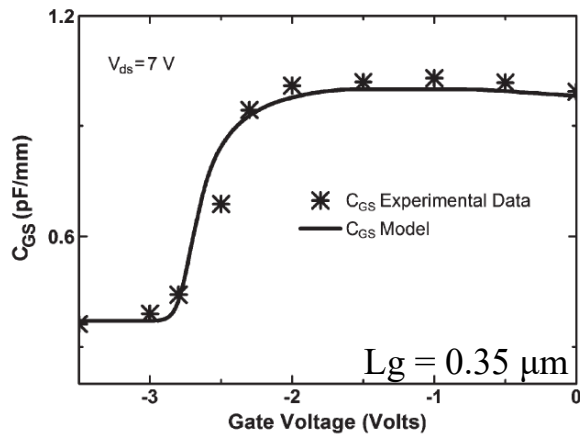
- **Id-Vd at two different temperatures 300 and 573K**



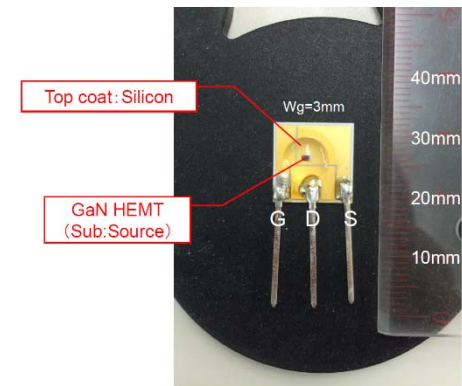
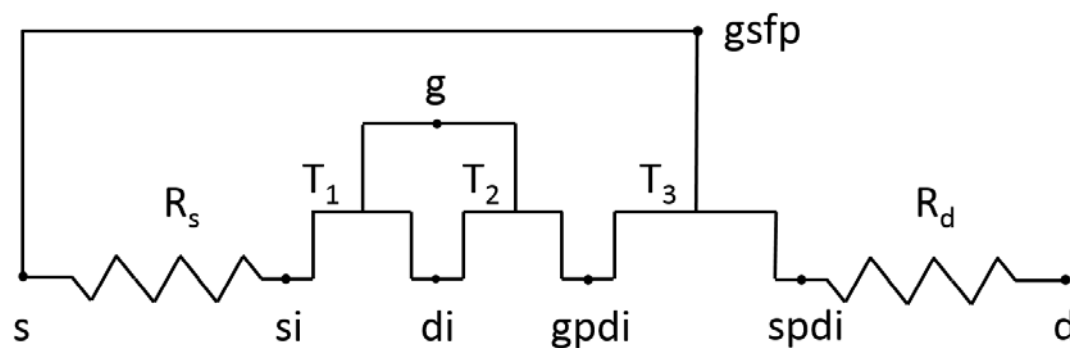
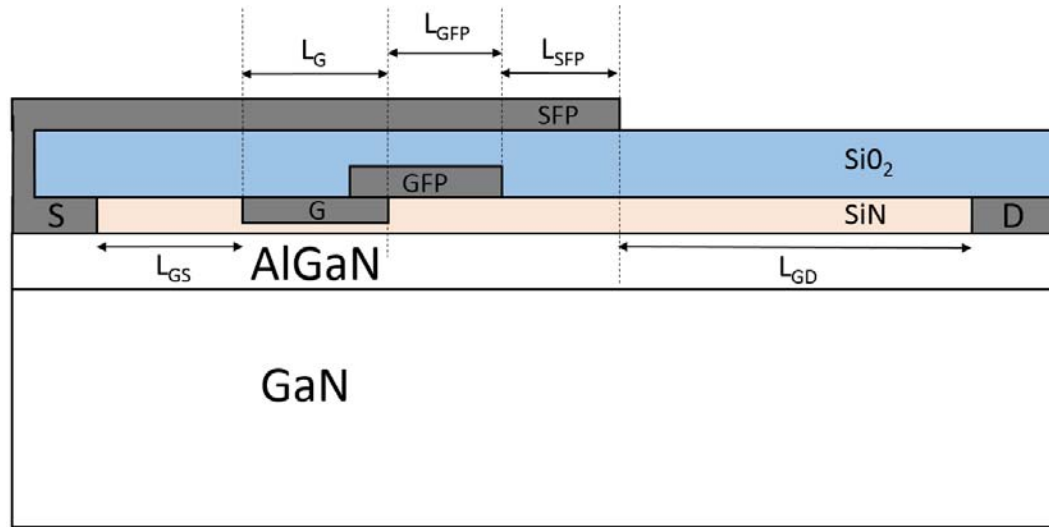
Model Validation – IEMN France data



$L_g = 0.125 \mu\text{m}$, $W = 100 \mu\text{m}$

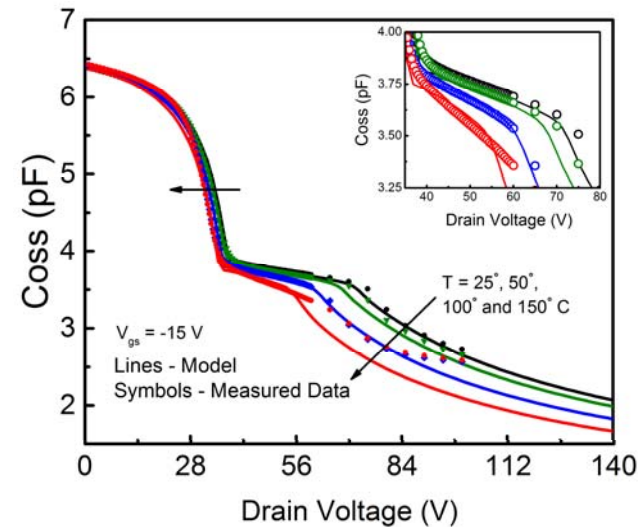
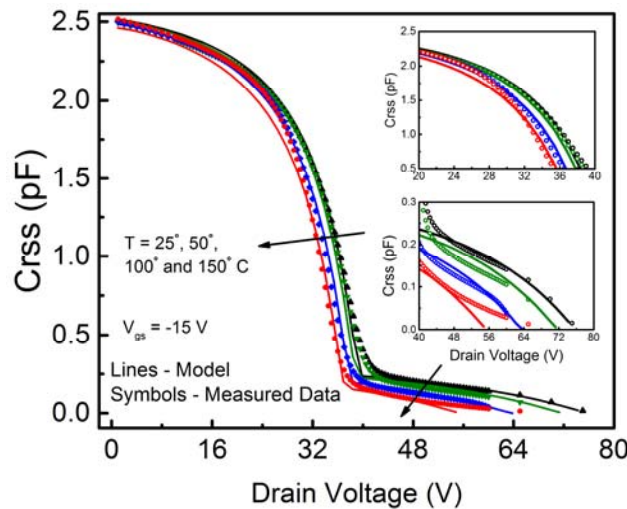
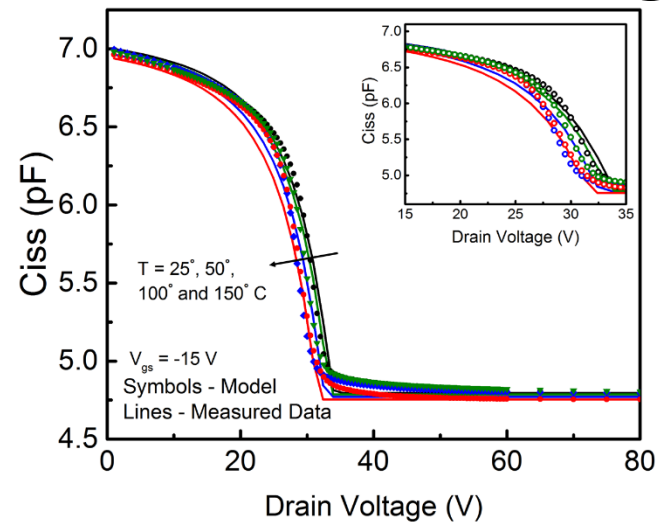
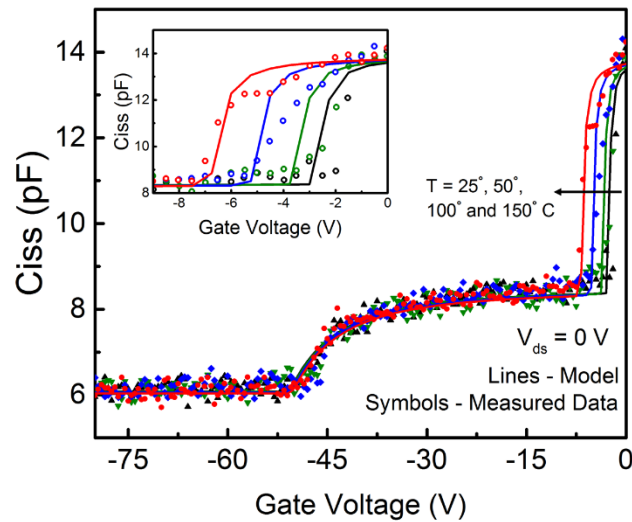


Modeling of Field-Plates in HEMTs

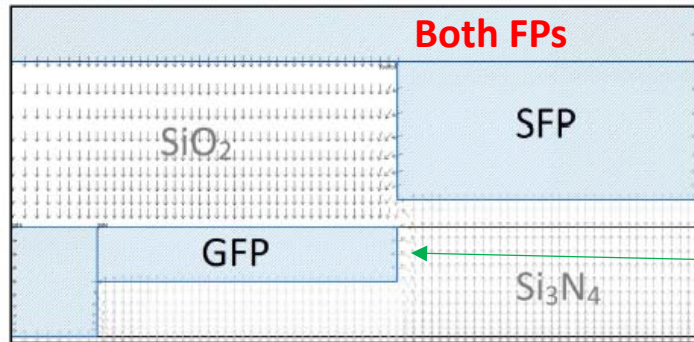


Affects capacitance and breakdown behavior.

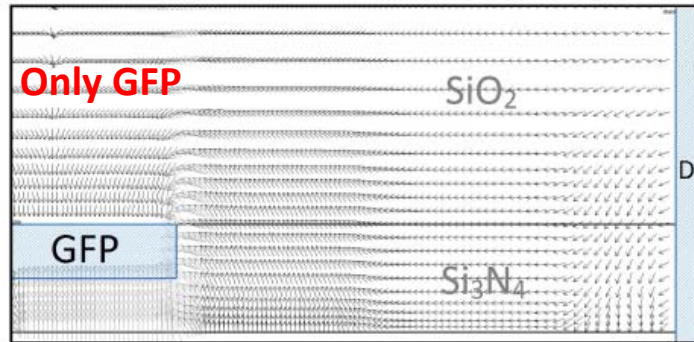
Field-Plate Capacitance Modeling



Cross-Coupling Capacitance



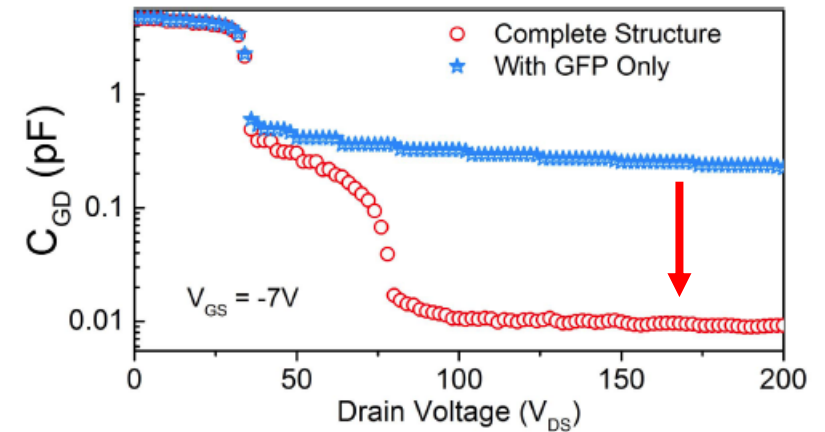
(a)



(b)



(c)



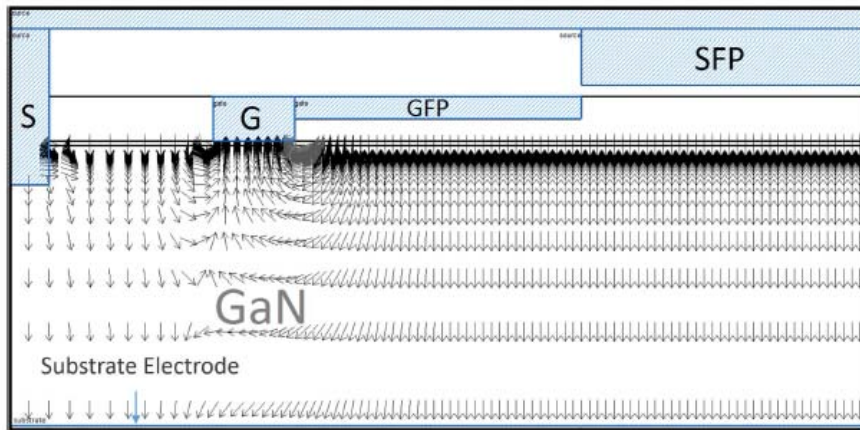
Appearance of fringing electric field between the vertical wall of the **GFP** and the 2-DEG_{SFP} causes the **cross-coupling effect** giving rise to the **second plateau**

Significant number of fringing field lines reach the GFP through the insulator stack in the **absence of SFP** causing **more fringing capacitance**

In the **presence of the SFP**, most of them end up at the SFP leading to a **reduced fringing capacitance component** in C_{gd}

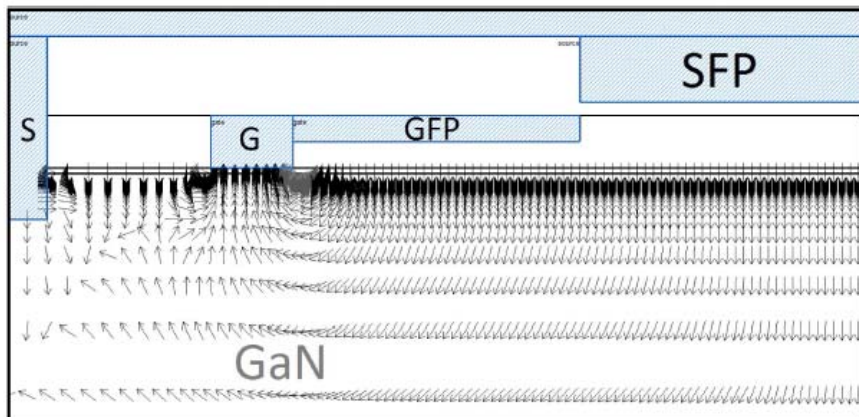
Substrate Capacitance

$V_{gs} = -7 \text{ V}$ $V_{ds} = 20 \text{ V}$



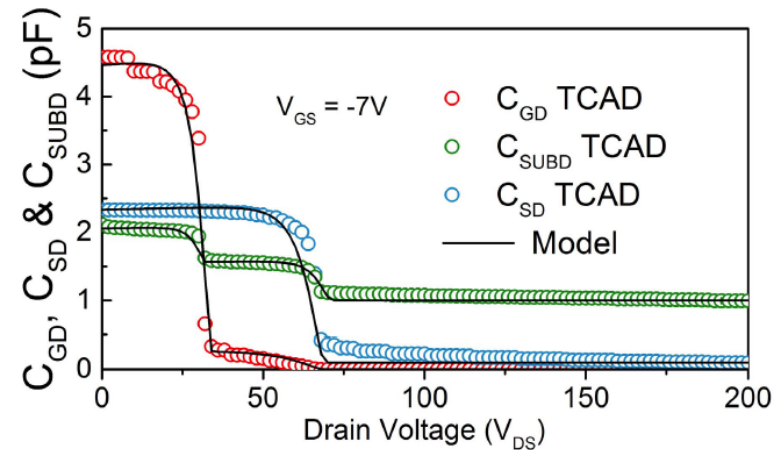
(a)

(a) Field lines originating from the 2-DEG reach the substrate electrode leading to the existence of C_{SUBD}



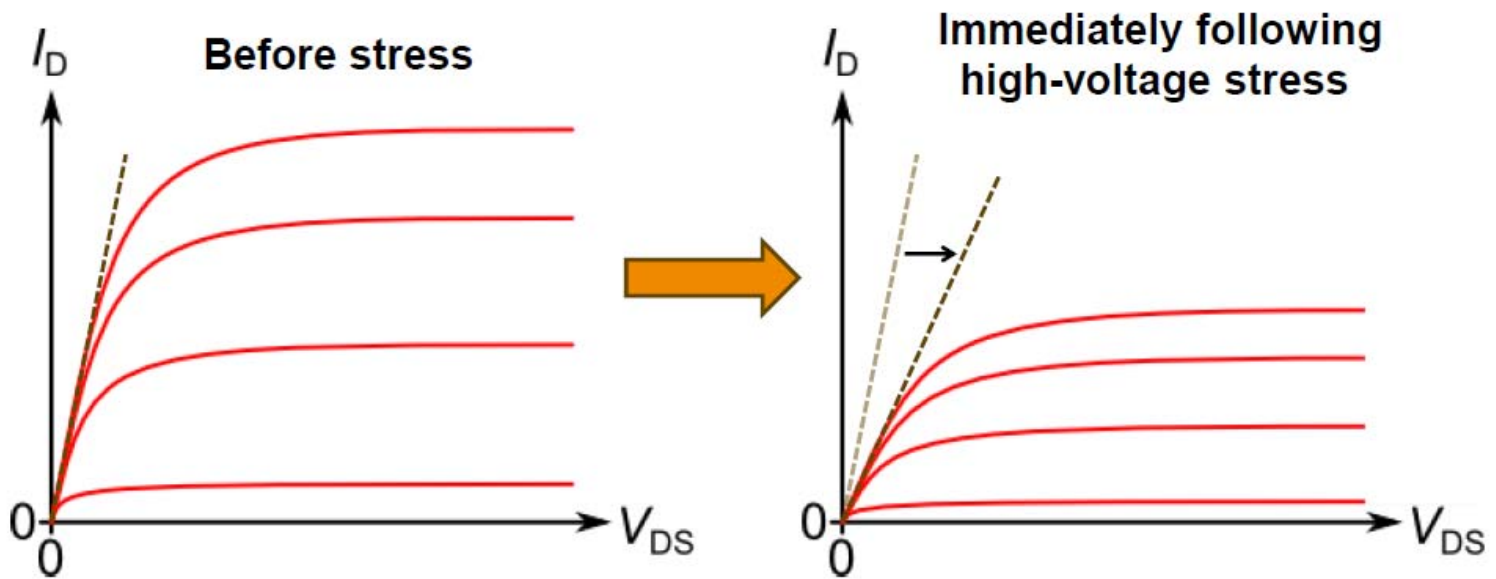
(b)

(b) whereas without substrate node, field lines from the drain side of the 2-DEG terminate at the 2-DEG on the source side through the GaN buffer



Current Collapse

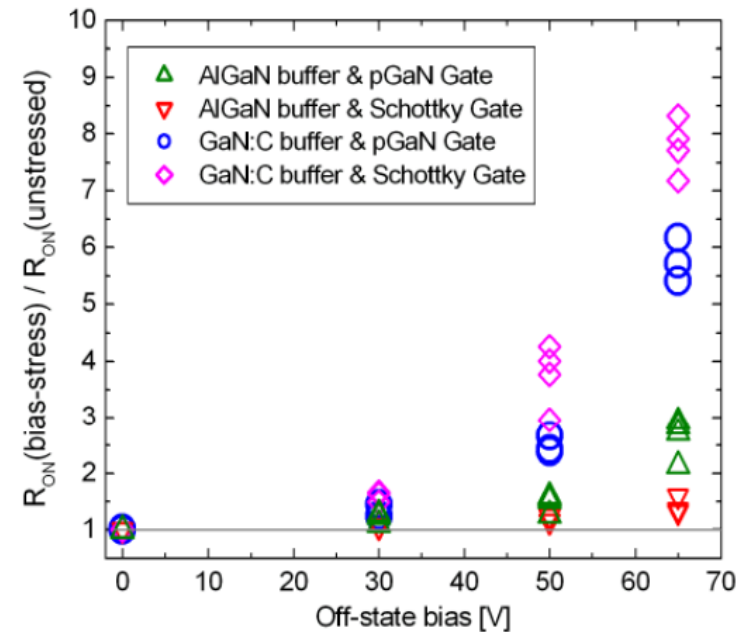
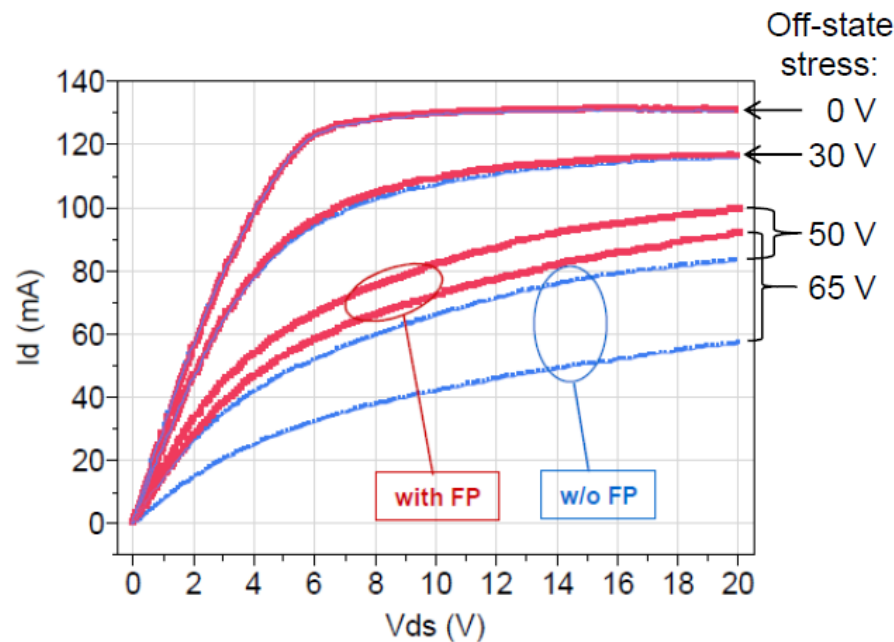
- ▶ On-state current temporarily reduced following off-state stress



- ▶ Also known as **dynamic R_{on}**
 - On-state resistance depends on recent history of device biasing

Current Collapse

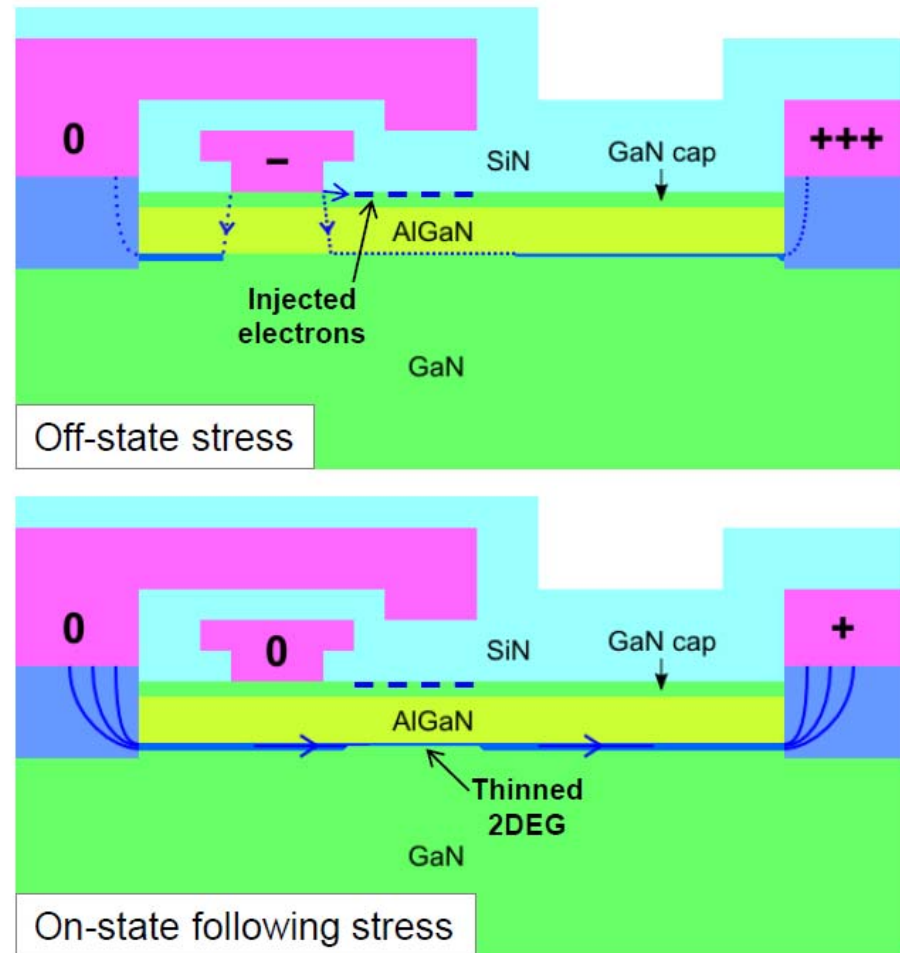
- ▶ Device design and substrate composition can have a strong influence on the magnitude of current collapse (dynamic- R_{on} increase)



[O. Hilt *et al.*, Proc. ISPSD 2012, 345 (2012)]

Issues-Virtual-gate effect

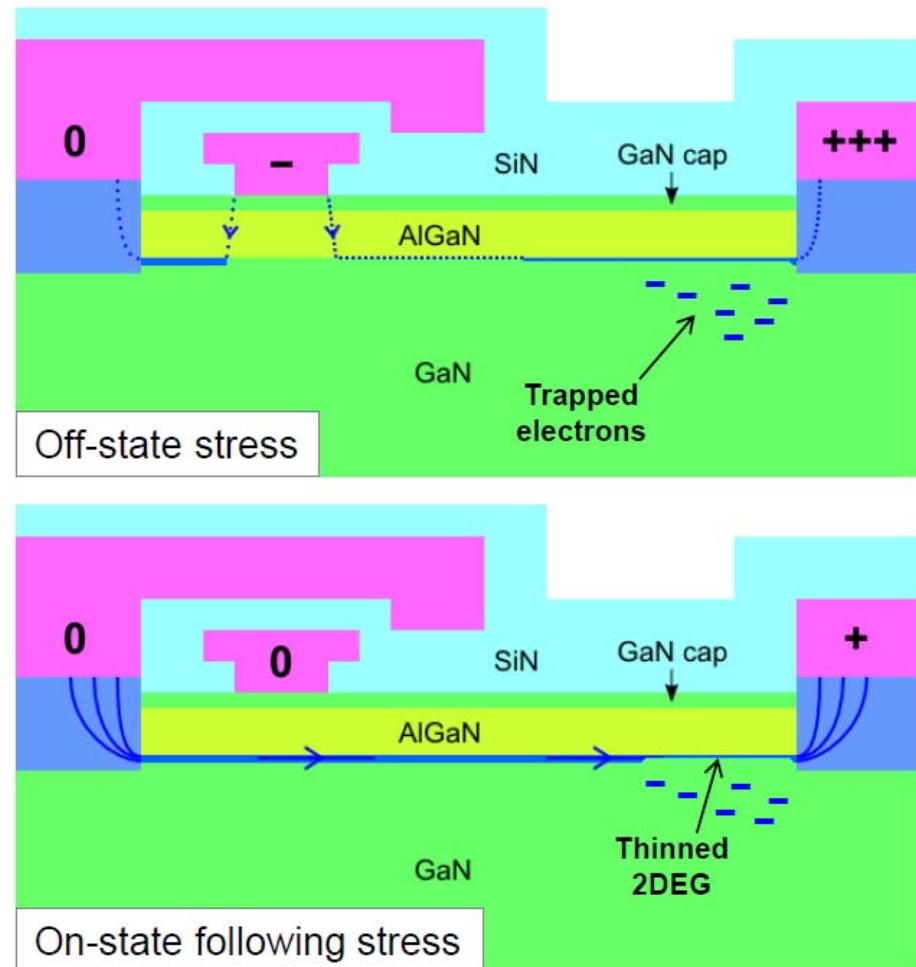
- ▶ **Off-state stress:**
 - Electrons from gate injected into trap states next to gate
- ▶ **On-state after stress:**
 - Trapped electrons act like a negatively biased gate
 - 2DEG partially depleted underneath \Rightarrow increased R_{on}
- ▶ **Later (~seconds):**
 - Electrons de-trap, 2DEG current restored



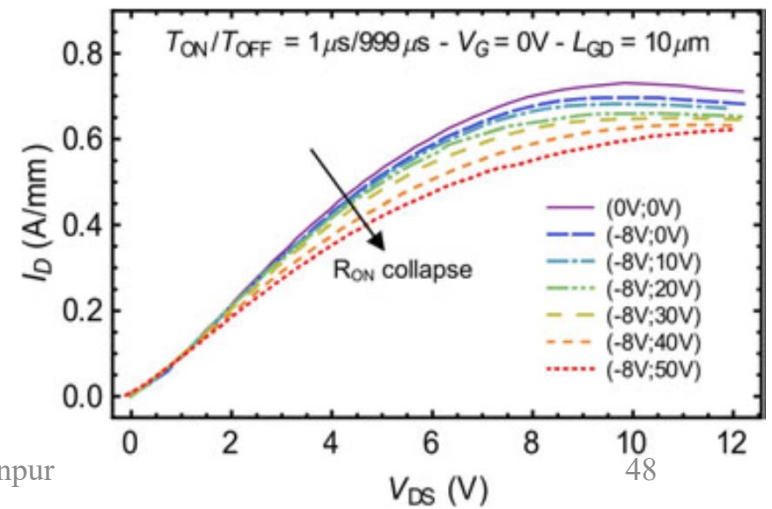
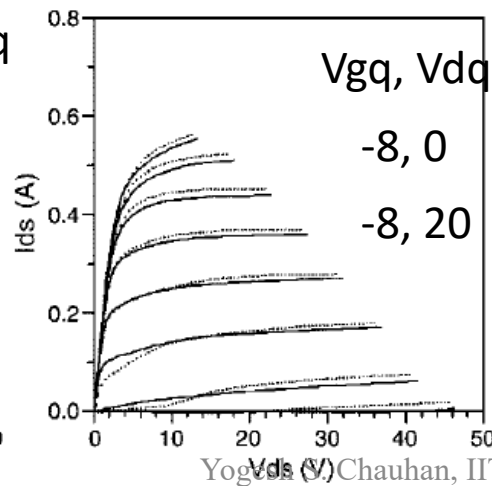
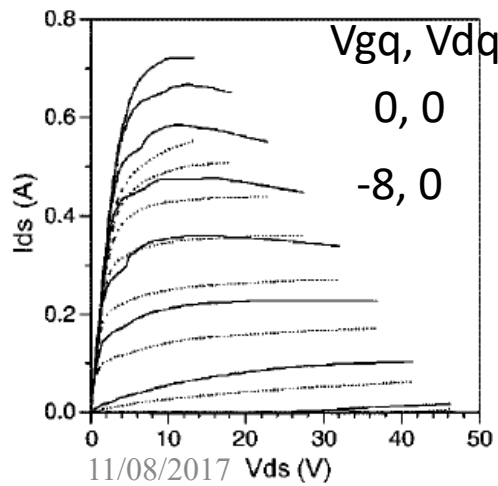
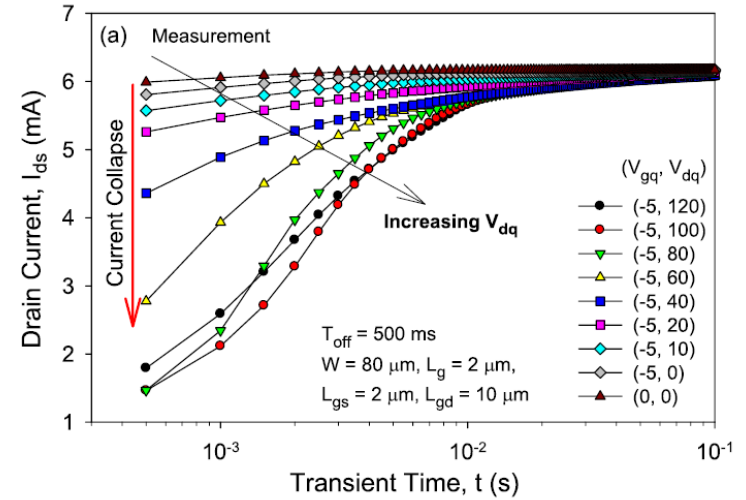
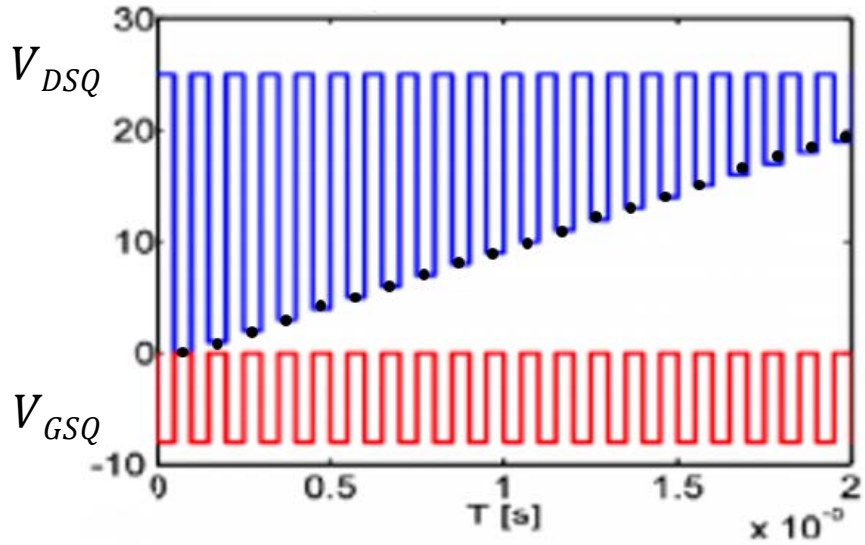
Issues-Buffer trapping

- ▶ **Off-state stress:**
 - Electrons trapped in bulk (deep donors/acceptors?)
- ▶ **On-state after stress:**
 - Trapped electrons partially deplete the 2DEG above \Rightarrow increased R_{on}
- ▶ **Later (~minutes):**
 - Electrons de-trap, 2DEG current restored

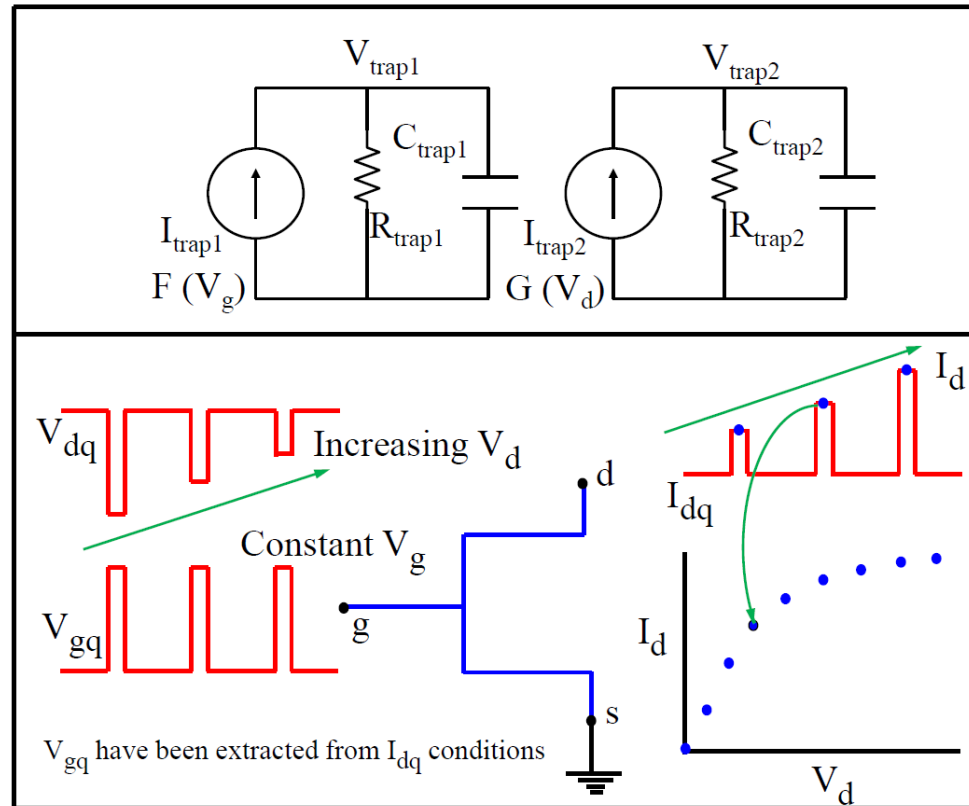
[M. J. Uren *et al.*, Trans. Elec. Dev. **59** (12), 3327 (2012)] and refs. therein



Pulsed IV Measurements



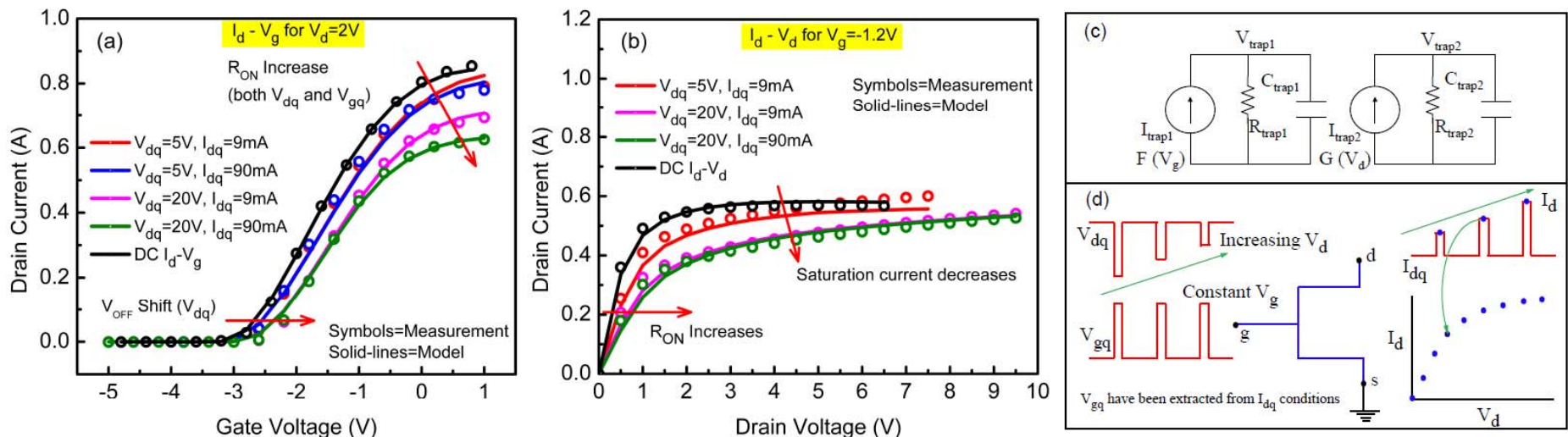
Trap Model and Pulsed IV Scheme



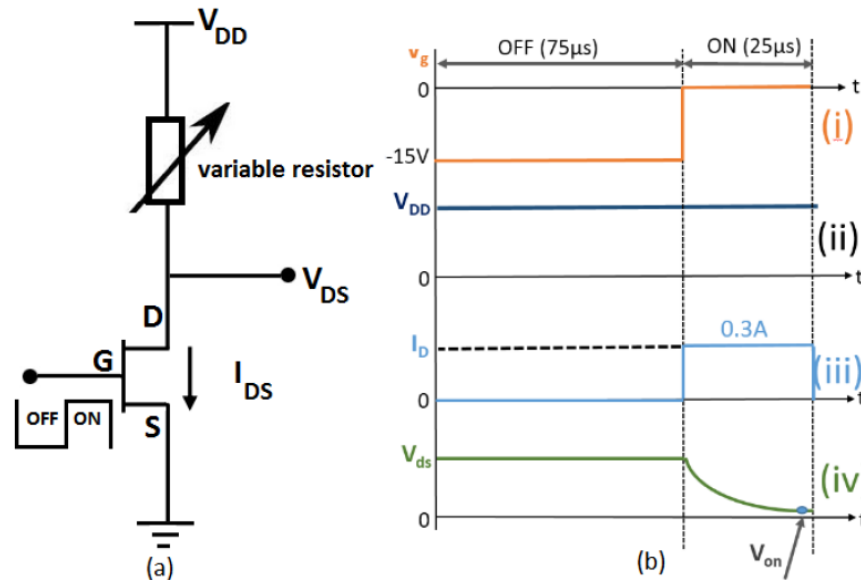
The trapping effects are modeled with the help of two R-C sub-circuits. The generated trap voltages $V_{\text{trap}1}$ and $V_{\text{trap}2}$ are fed back into the model which update parameters like the cut-off voltage, sub-threshold slope, source and drain-resistances to capture the effects of traps.

Modeling of Trapping effect

Traps in GaN HEMTs play huge role in determining the performance of the device, especially **in high frequency** operations



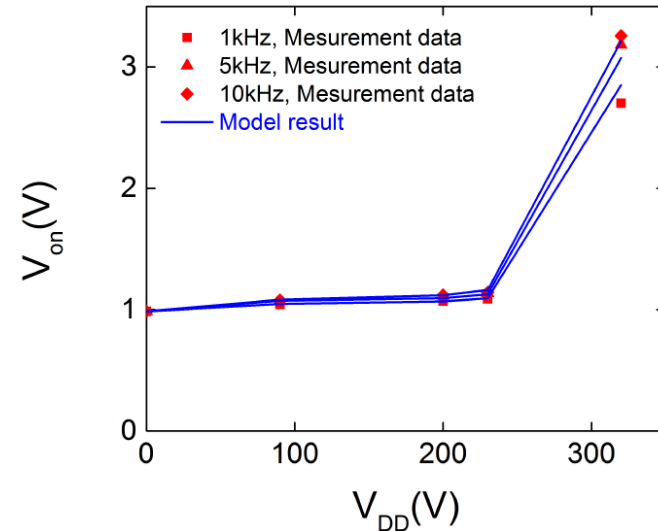
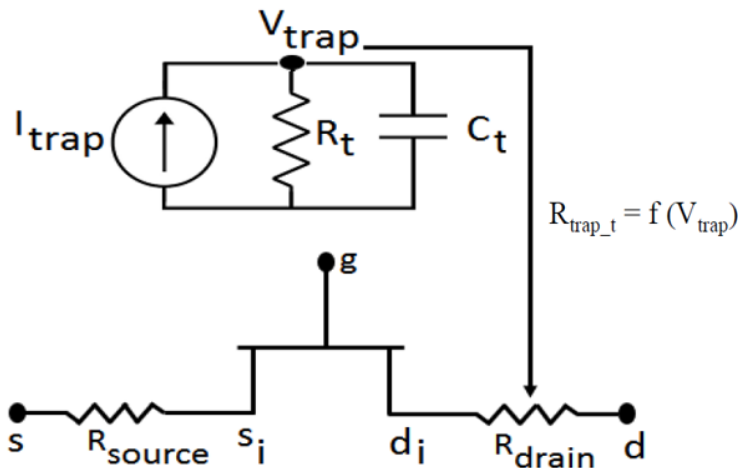
Switching Collapse Setup



Signal generator at gate terminal switches device from high negative stress voltage (V_{gsq}) to some value higher than V_{off} . Variable resistor is used to make device working in linear region of operation.

- Waveform (i) is the input at the gate, which is switching the device from ON to OFF-state and vice versa. Waveform (ii) is the constant input applied at drain terminal via a variable resistor.
- Waveform (iii) is showing the output drain current with time. The drain current is kept fixed at 0.3A with the help of variable resistor.
- Waveform (iv) is the value of V_{ds} which is equal to V_{DD} when device is in OFF-state and becomes V_{on} when device is in ON-state.
- Waveform (iv) illustrates the fact that, as the device is turning ON, capacitor assumed for the trap-states start to discharge and due to reduction in depletion of 2-DEG, V_{on} of the device recovers with

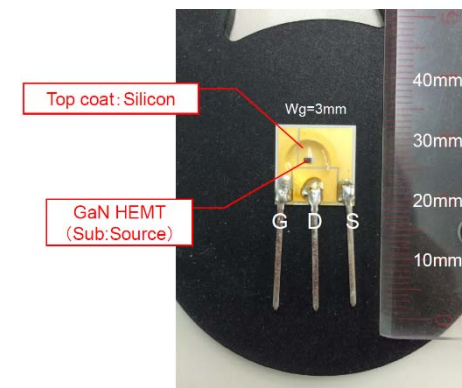
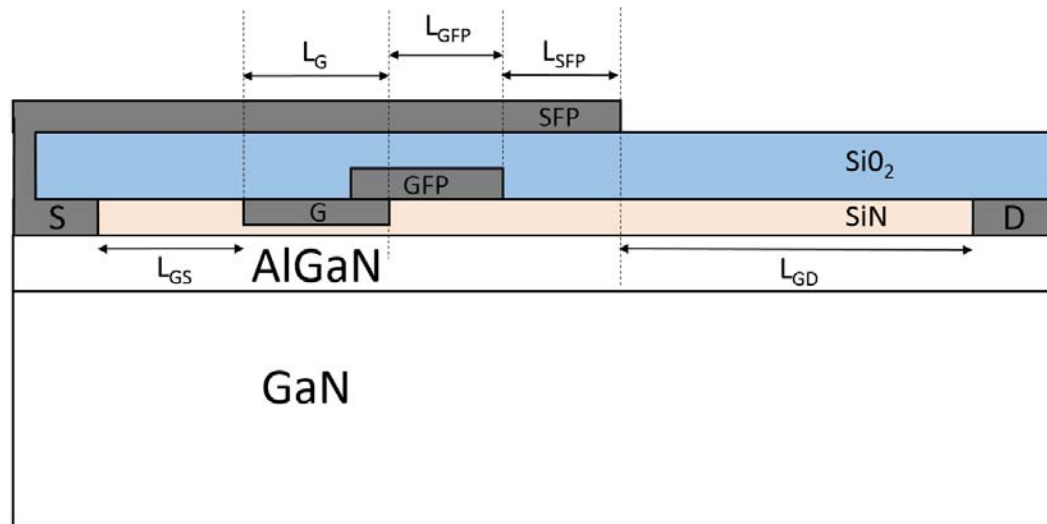
Switching Collapse Model



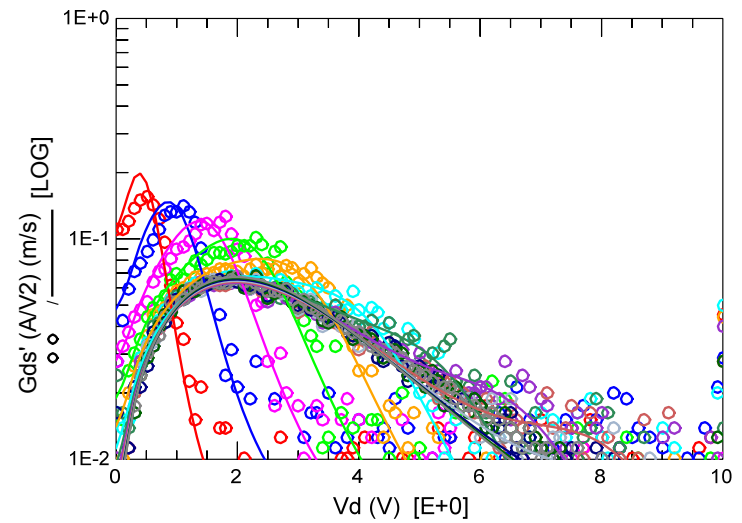
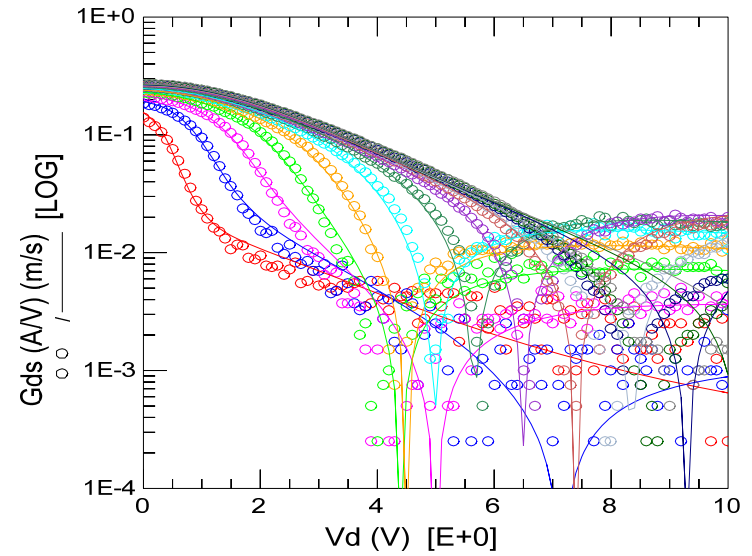
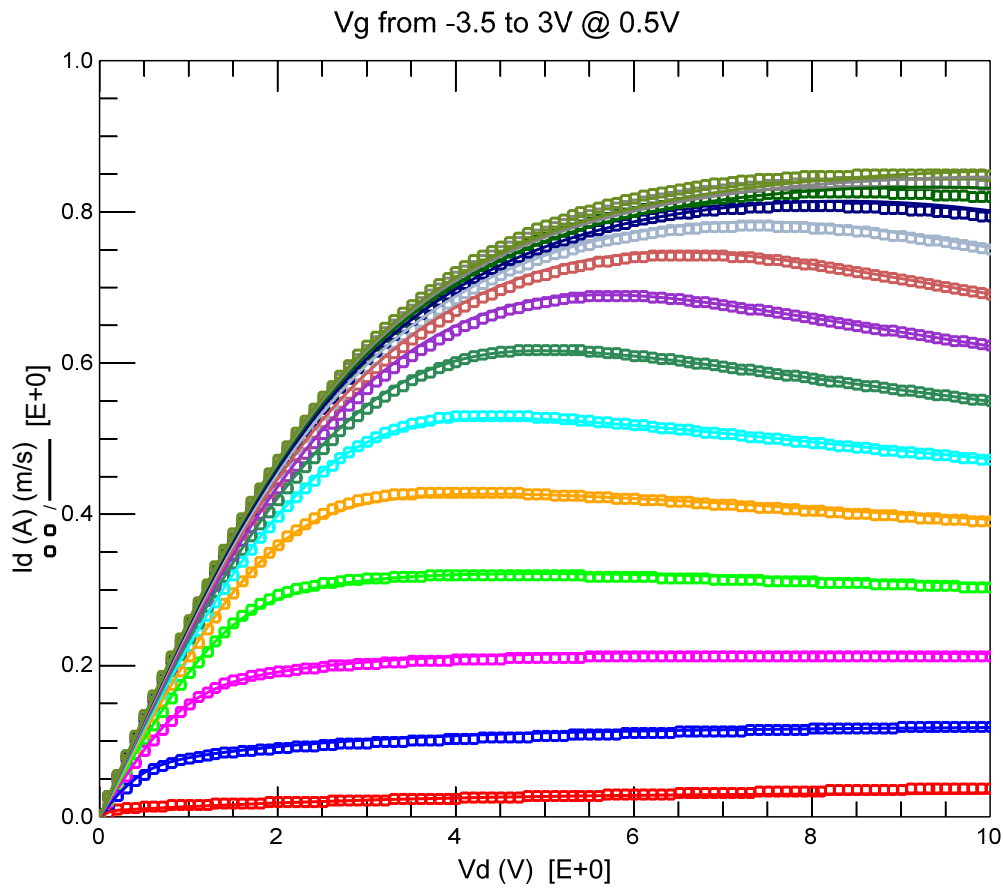
Strategy for implementation of surface trapping effect using an RC network

- Modeling of trapping effect by using RC network with different time constant. This RC network is contributing to drain-access region resistance as R_{trap} (as a function of V_{trap}) to capture the trapping effect on device ON-resistance (R_{on})
- Model-Hardware correlation for pulsed I-V, V_{on} data for 1, 5 and 10 kHz input applied at gate terminal for various V_{ds} . V_{on} is the value of V_{ds} at which the value of drain current is 0.3A. As V_{DD} is increasing, R_{on} of the device increases which results in switching collapse. Measured data is from Toshiba for CMC standardization.

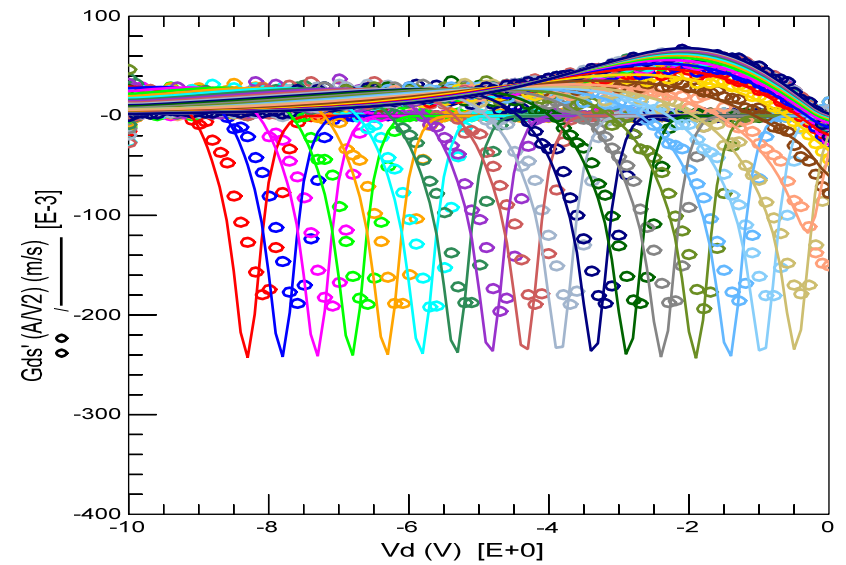
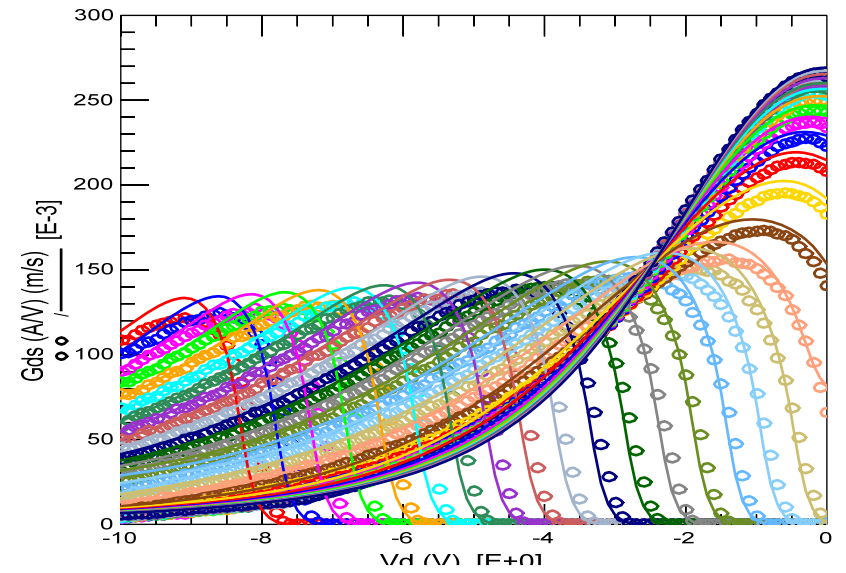
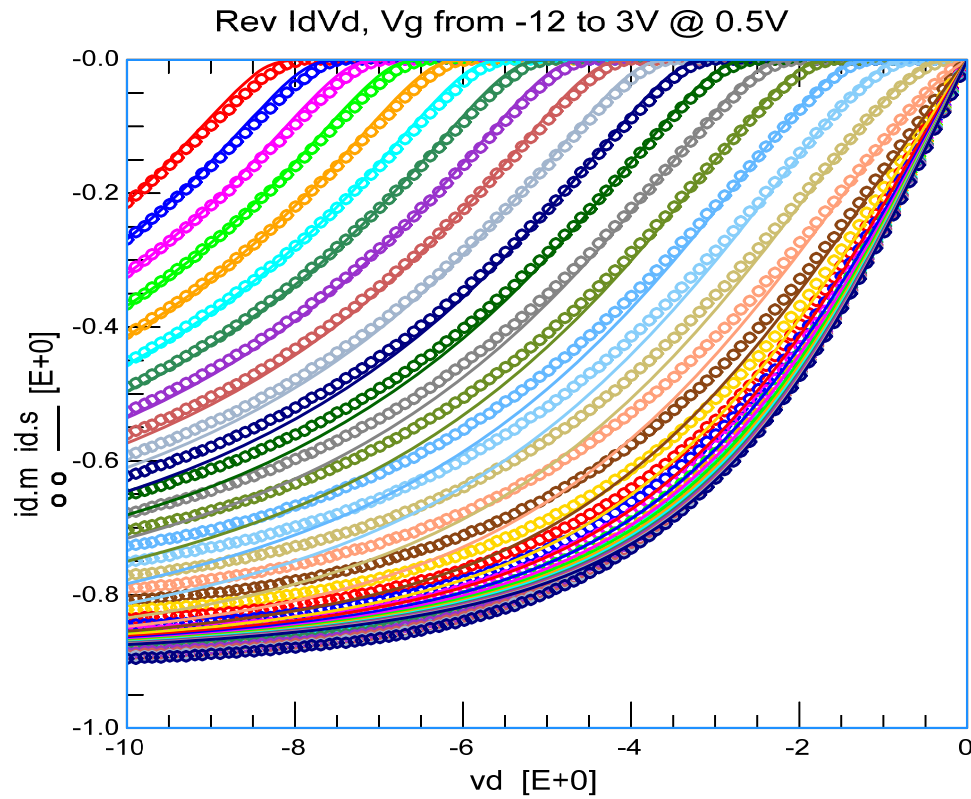
Toshiba DC I-V Results for High Power HEMT



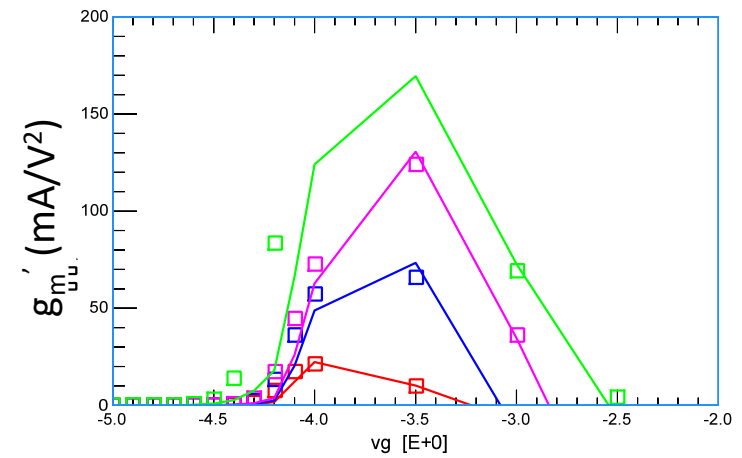
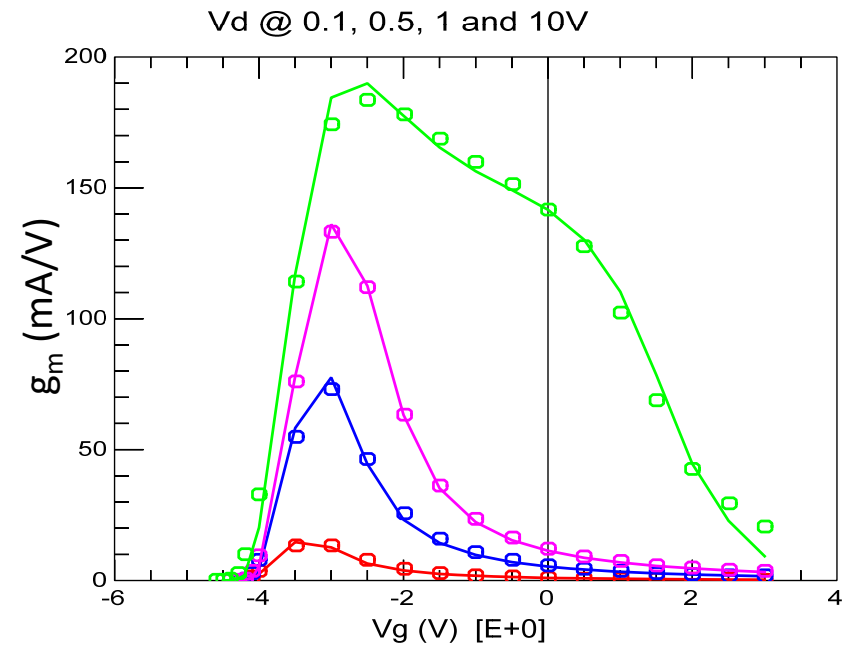
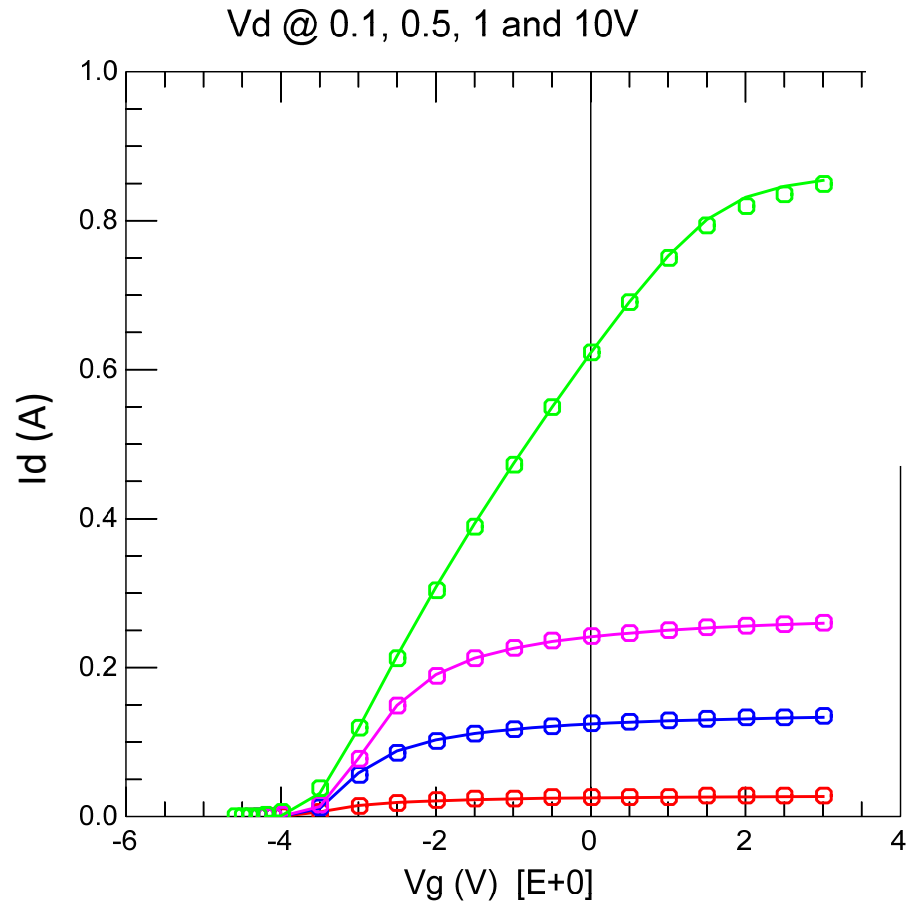
Room Temperature I-V



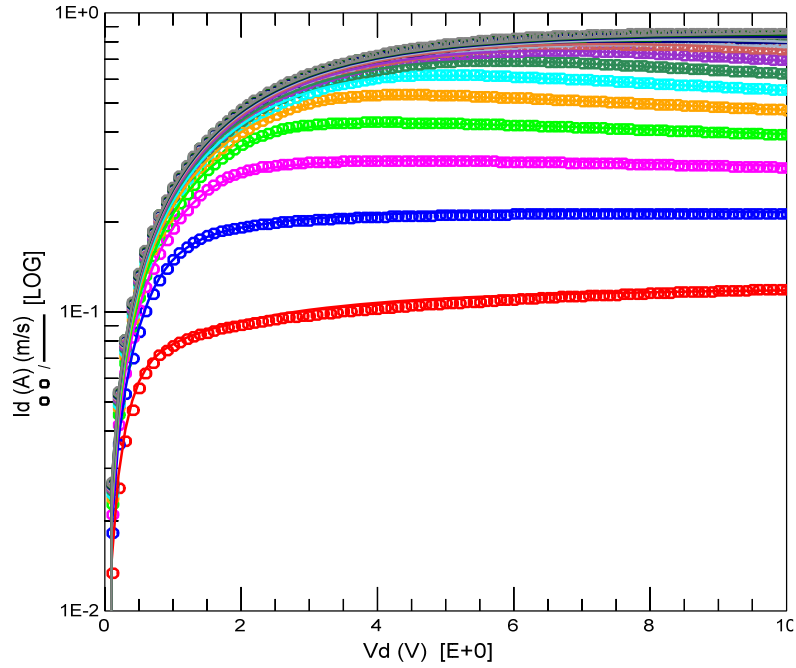
Reverse IdVd @ room temperature



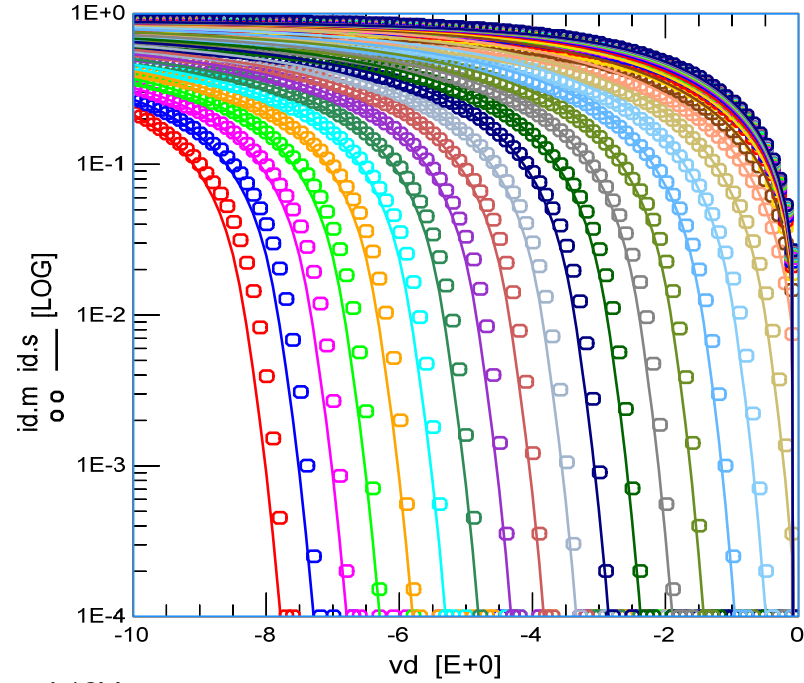
Room Temperature I-V



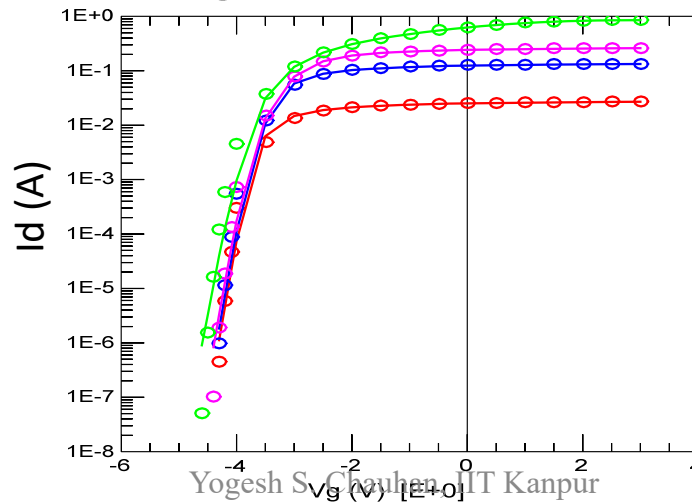
Log (Id) - Vds (Vd>0) T=25



Log (Id) - Vds (Vd<0) T=25

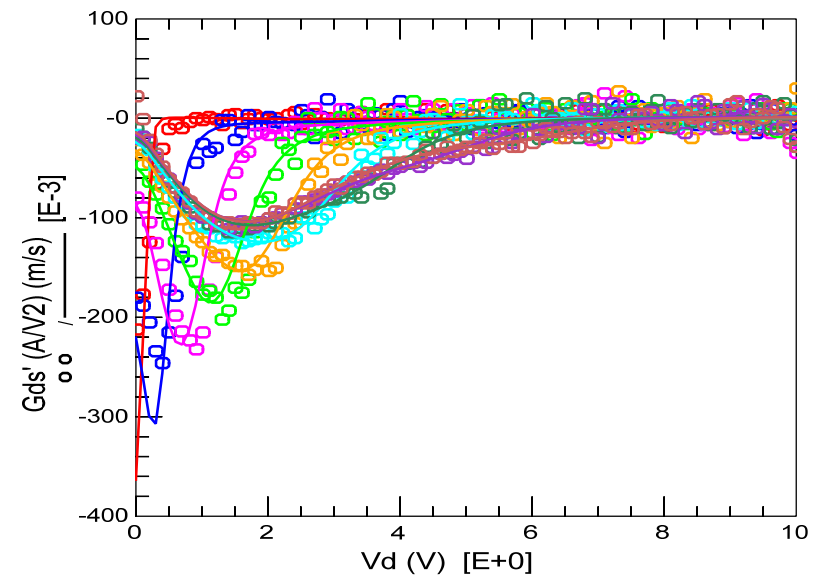
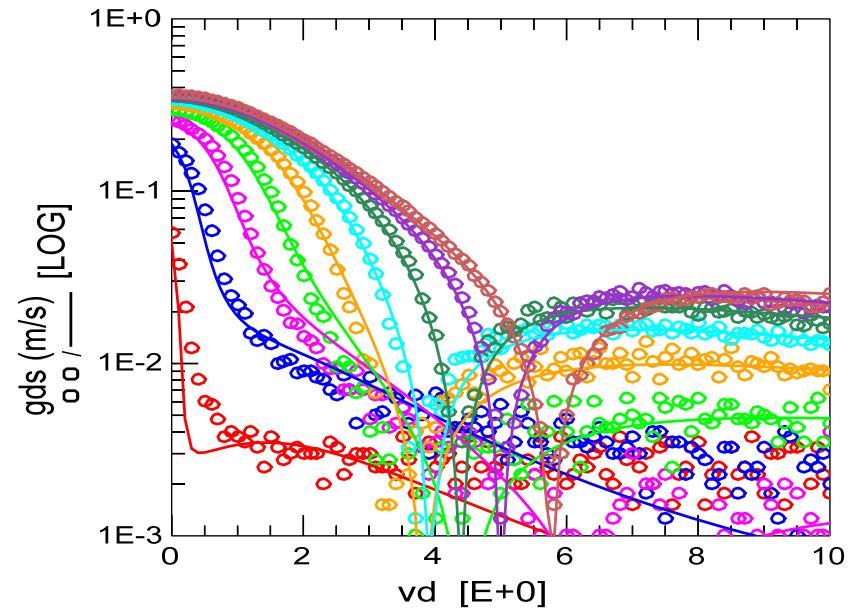
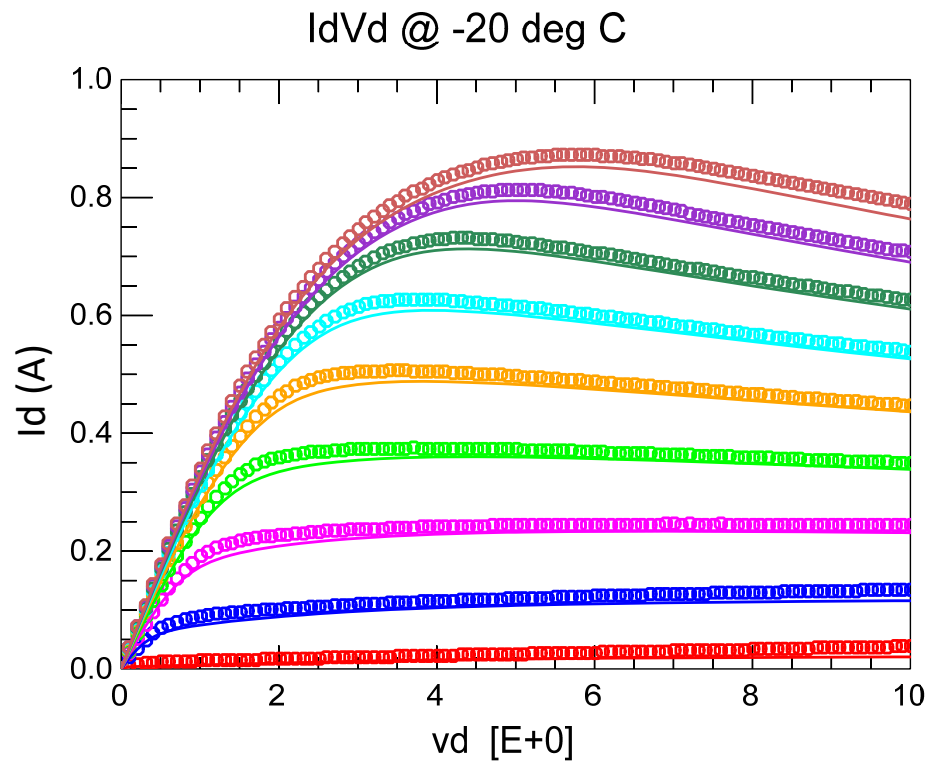


Vd @ 0.1, 0.5, 1 and 10V

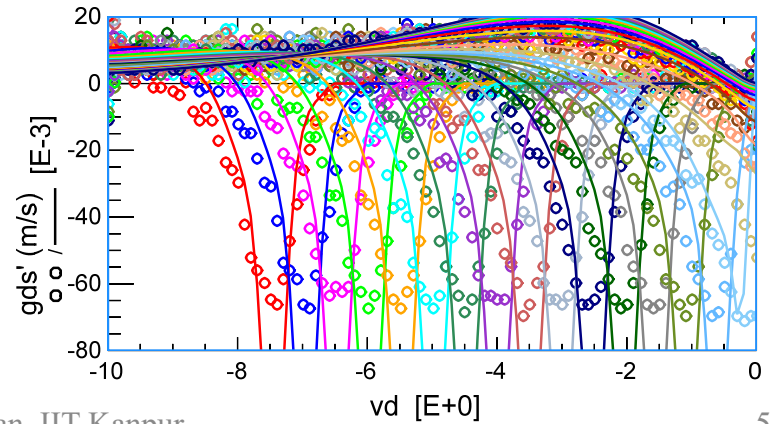
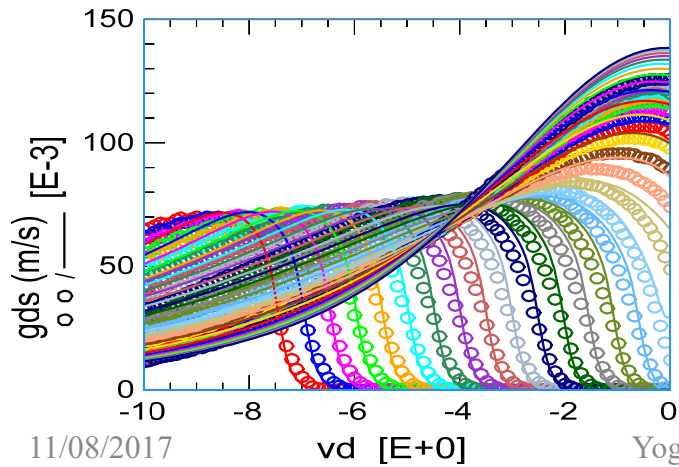
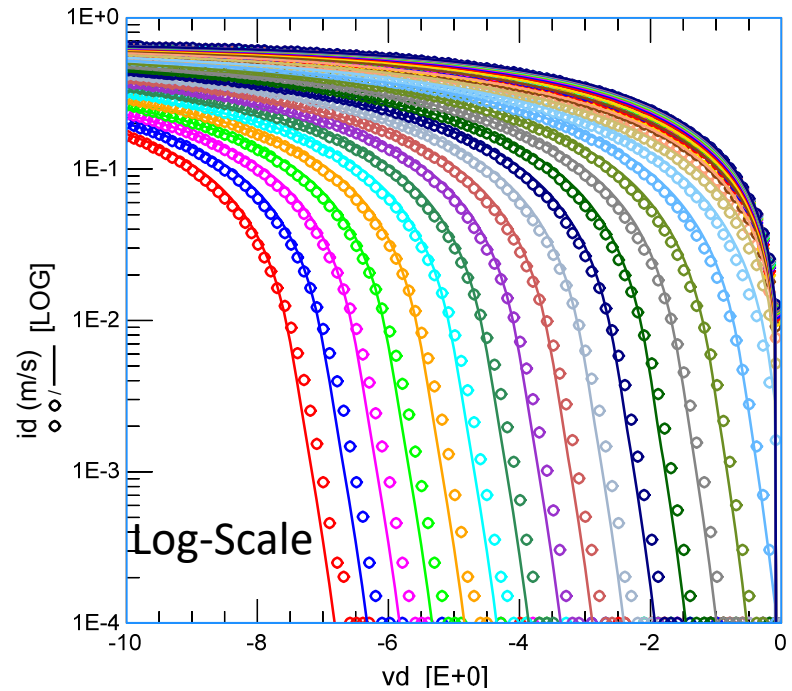
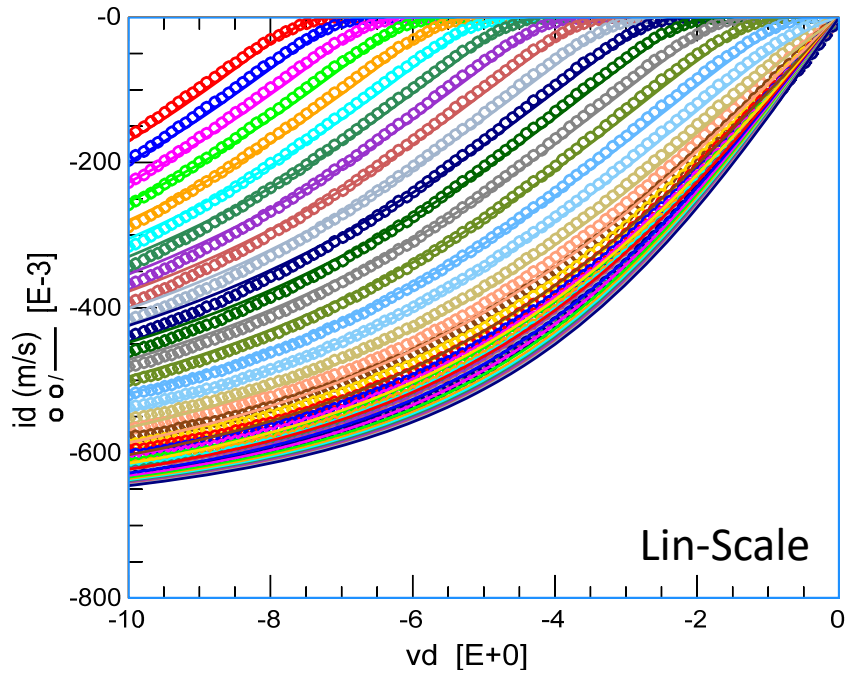


Log (Id) - Vgs T=25

I-V @ -20 deg C

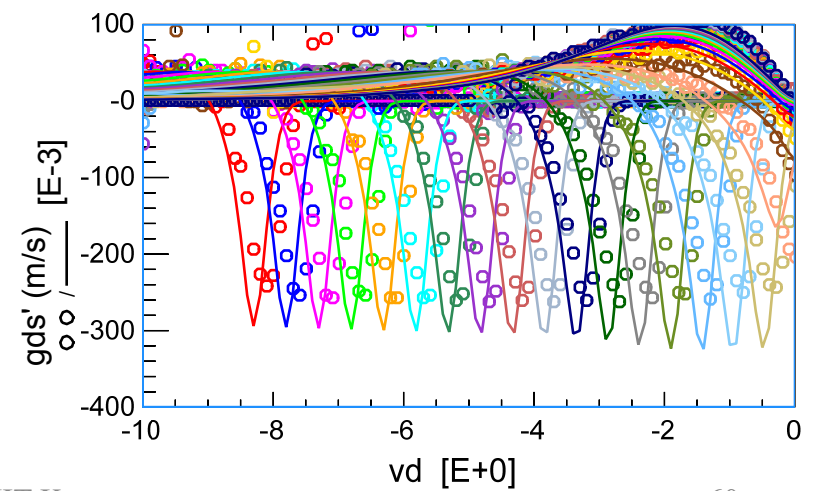
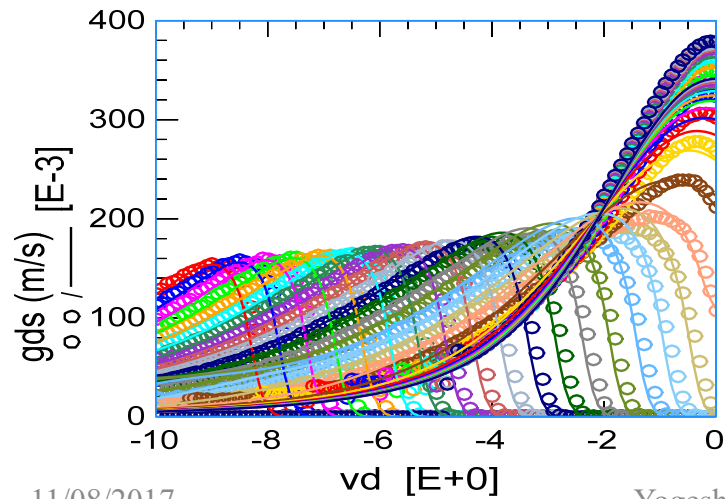
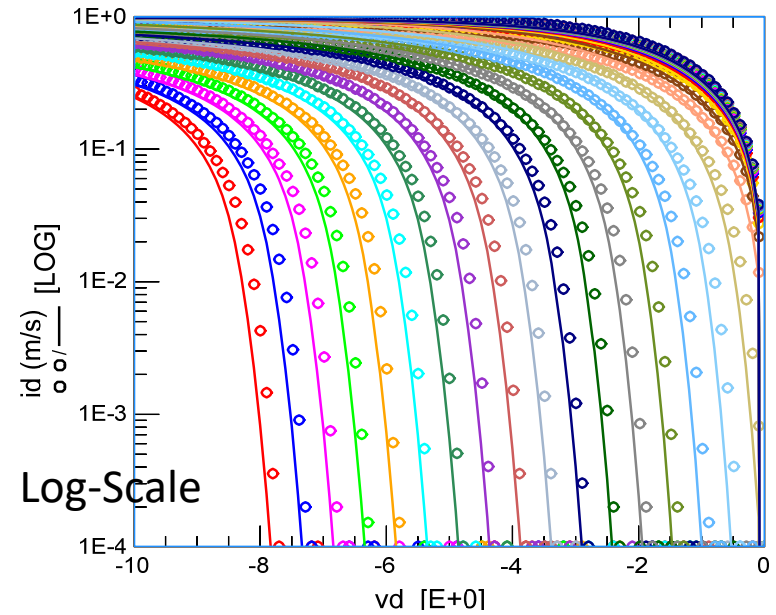
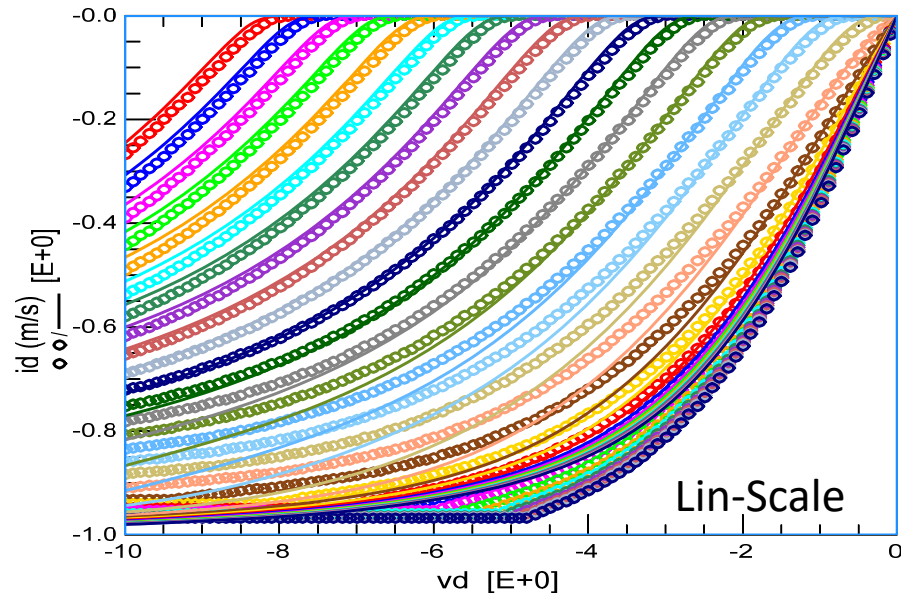


Rev IdVd @ T=150 C

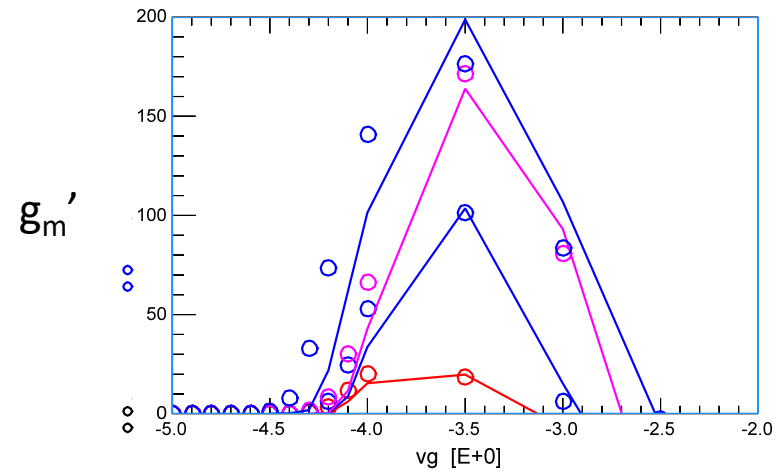
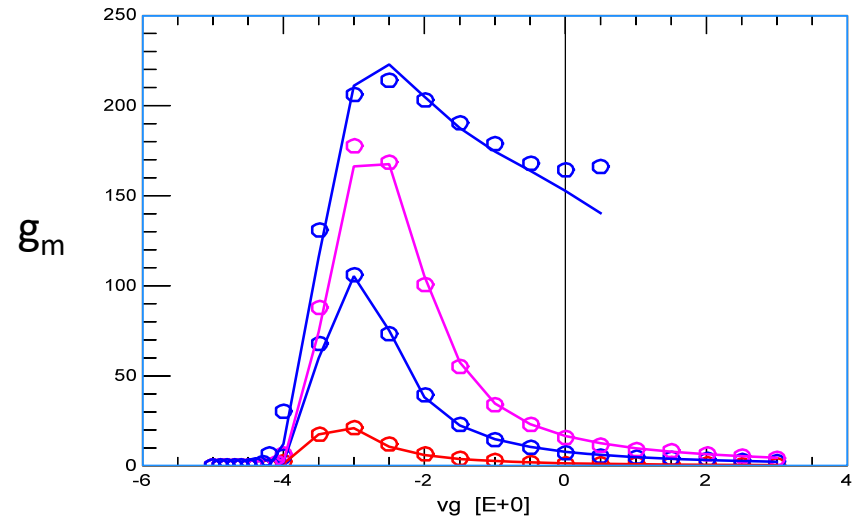
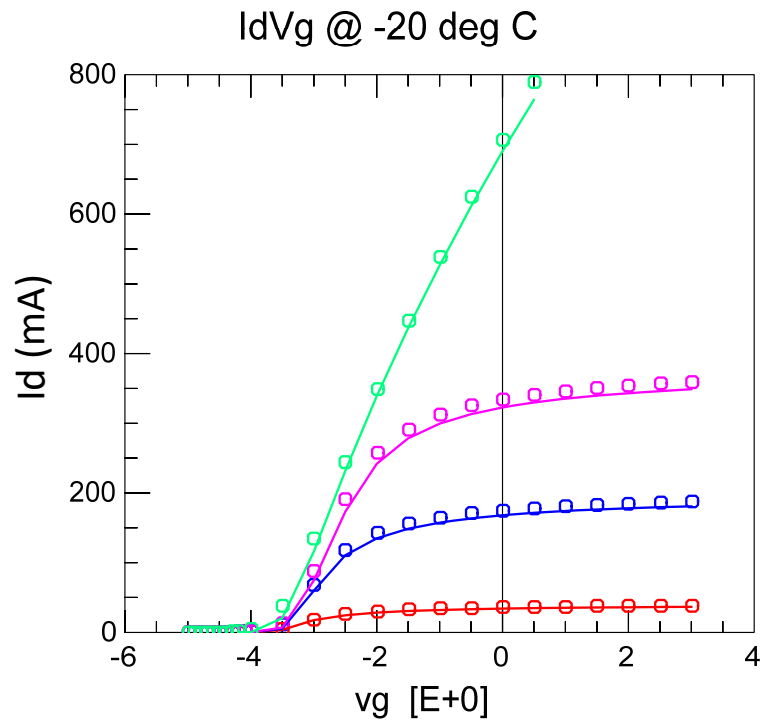


Rev IdVd @ T=-20 C

Vg from 12 to 5 V

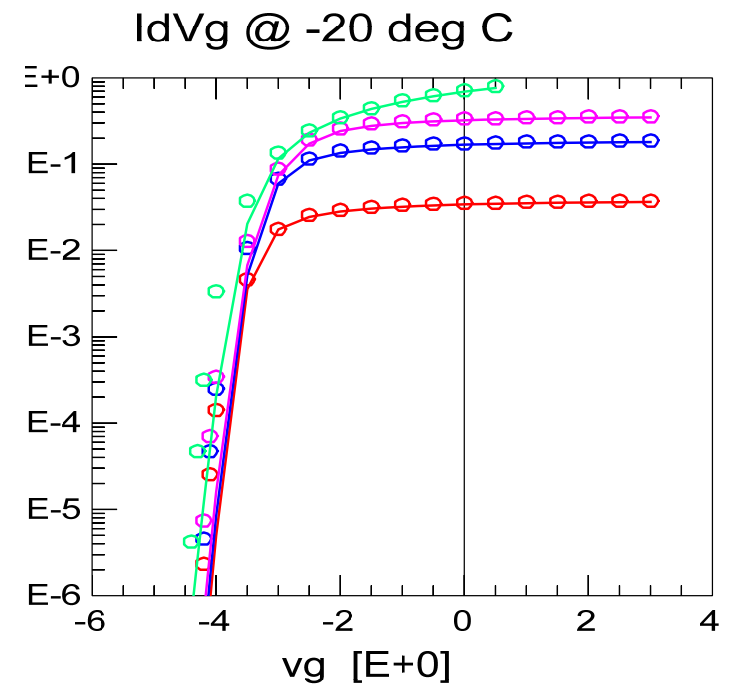
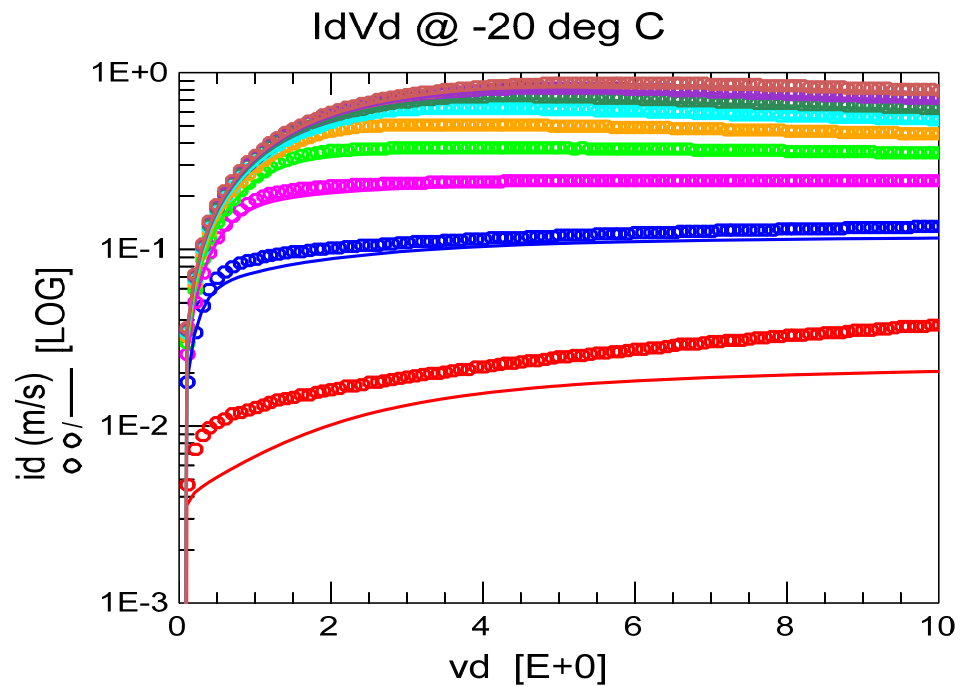


I-V @ -20 deg C

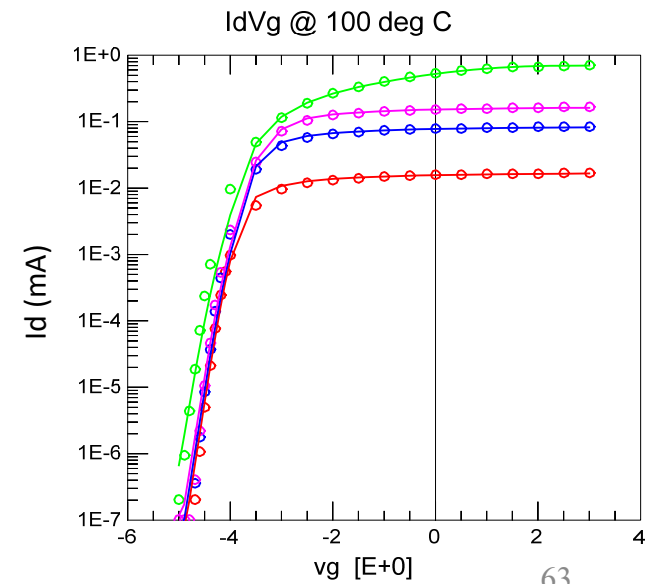
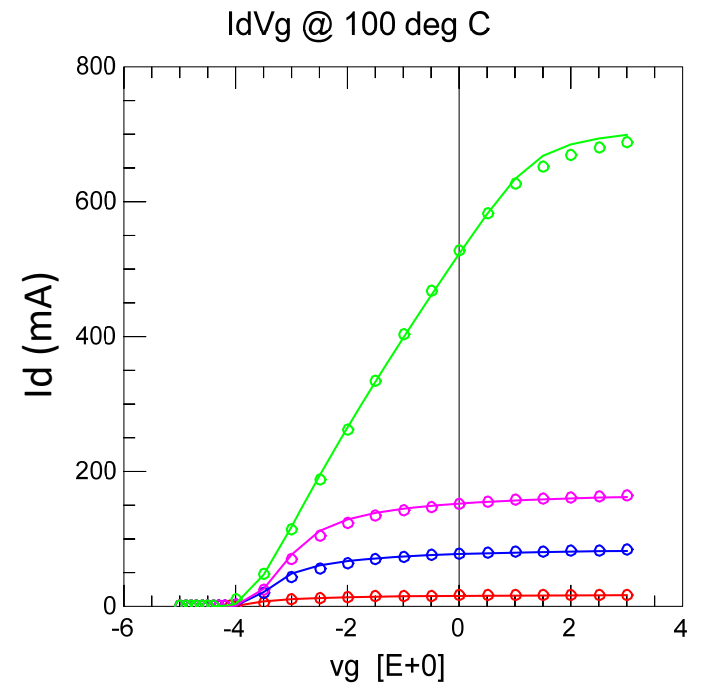
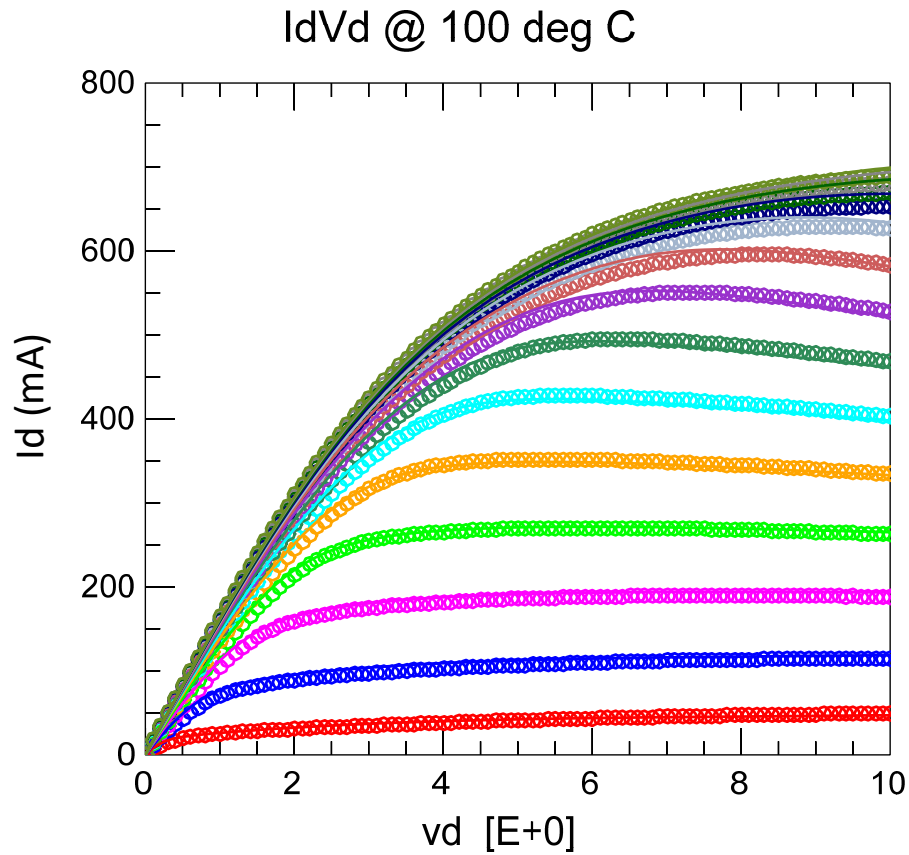


I-V @ -20 deg C

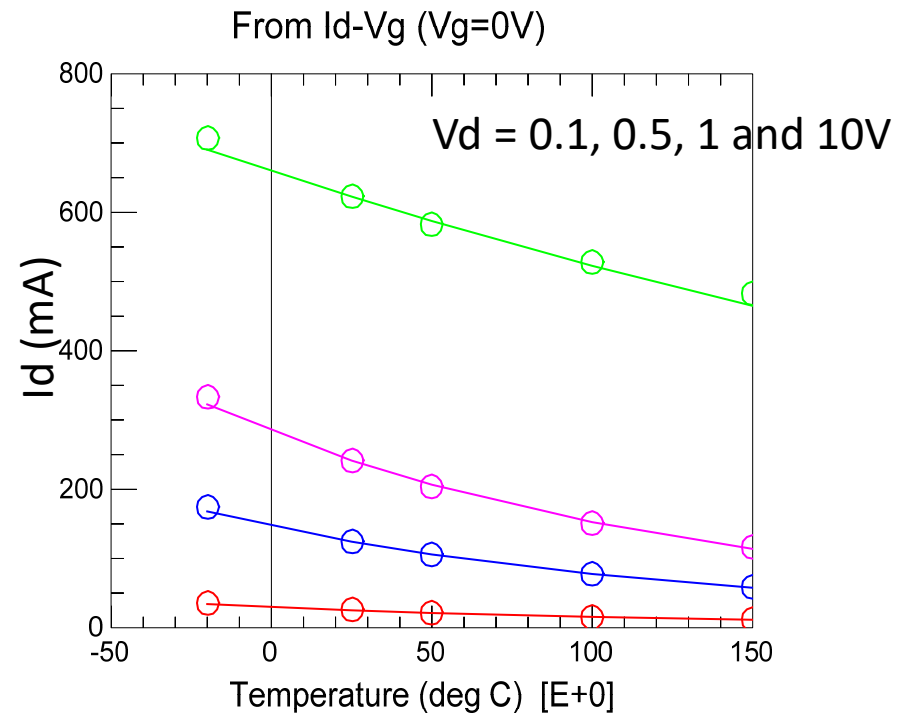
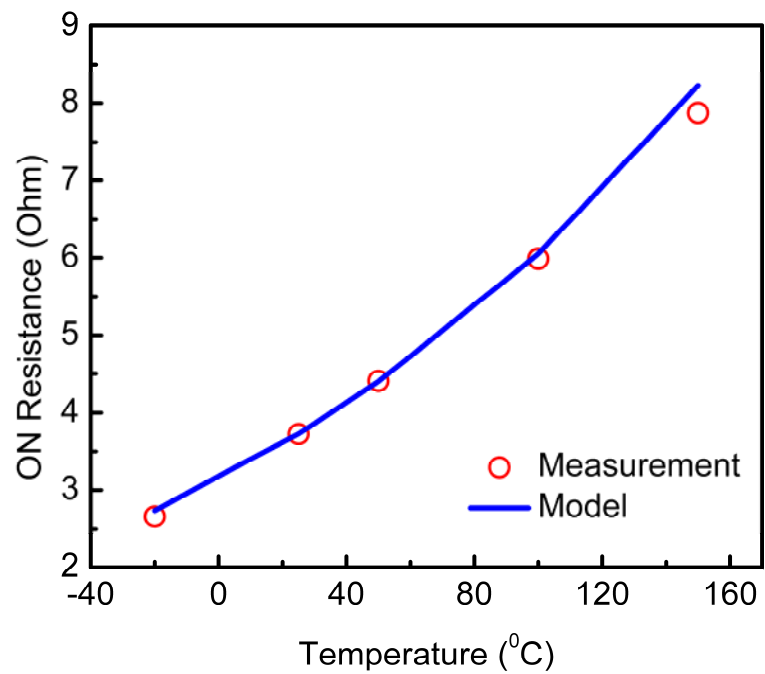
Log -Scale



I-V @ 100 deg C



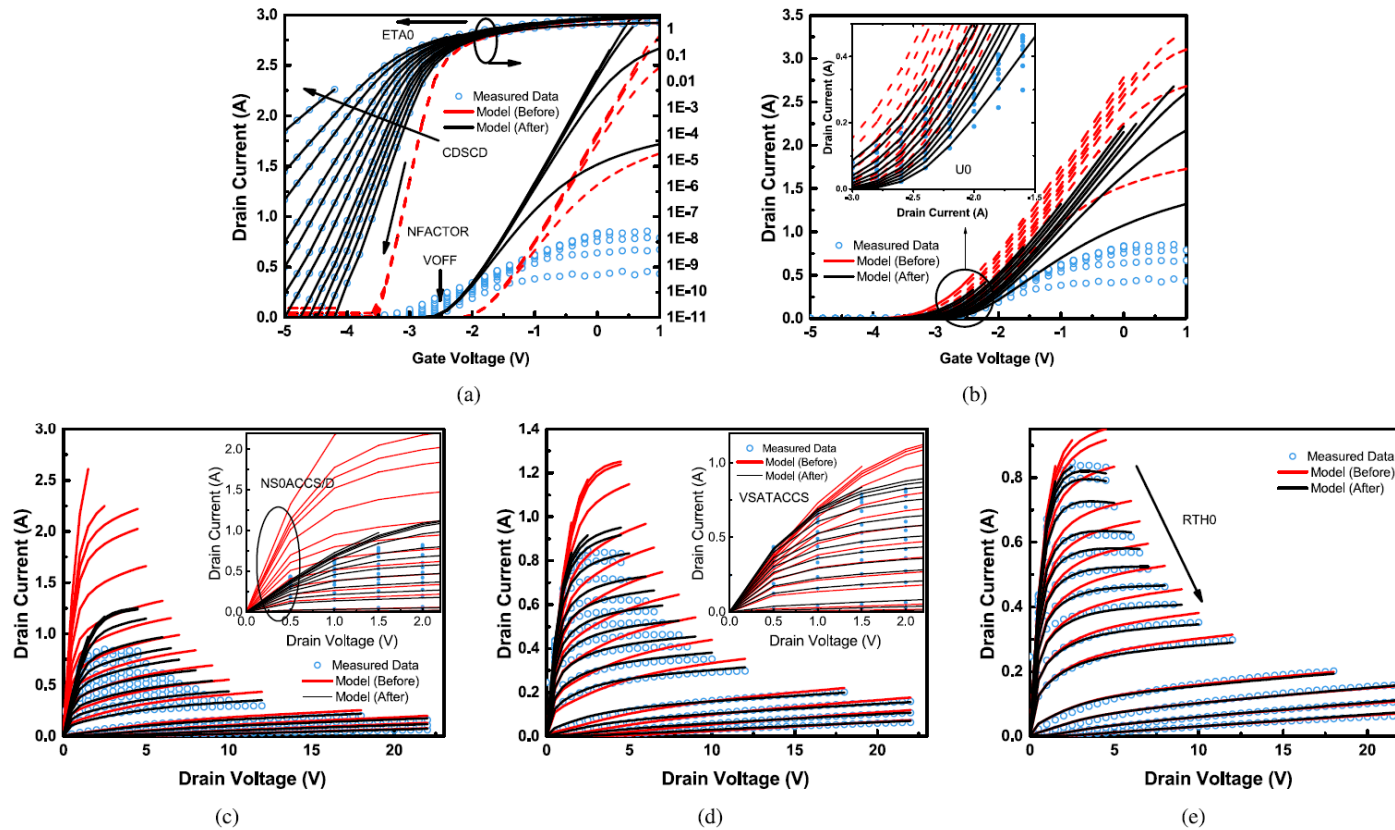
Temperature Scaling



DC I-V Results of Multifinger RF HEMT

$L_g = 125 \text{ nm}$, $W_g = 10 \times 90 \text{ }\mu\text{m}$, $L_{sg} = 200 \text{ nm}$, $L_{dg} = 1.7 \text{ }\mu\text{m}$

DC Parameter Extraction Flow



S. A. Ahsan, S. Ghosh, S. Khandelwal, and Y. S. Chauhan, "Physics-based Multi-bias RF Large-Signal GaN HEMT Modeling and Parameter Extraction Flow", IEEE Journal of the Electron Devices Society, Sept. 2017.

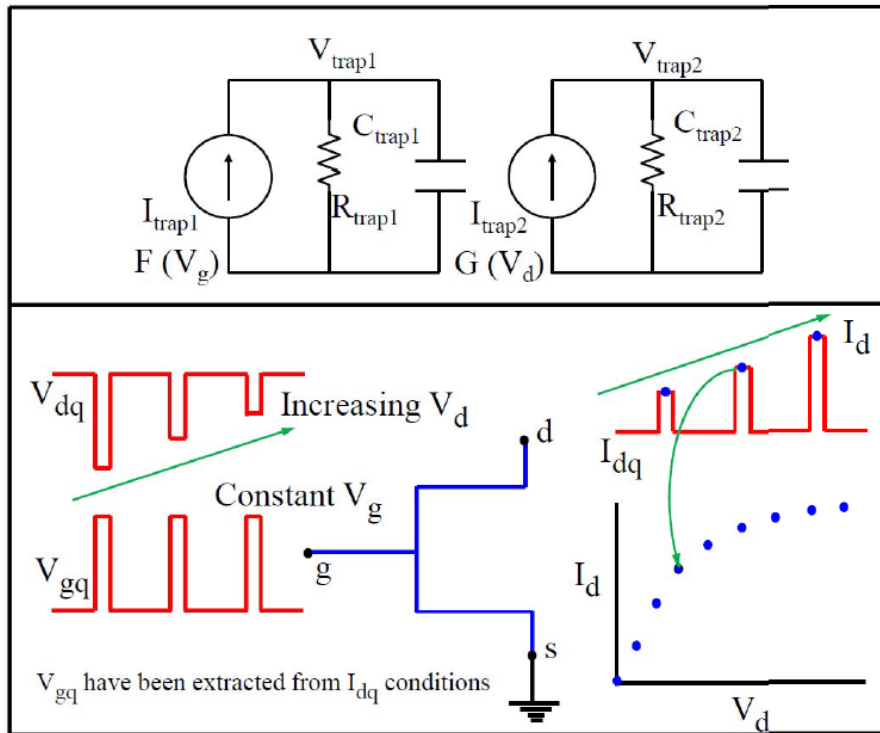


FIGURE 4. (I) Two R – C sub-circuits used for modeling trapping effects, one each for gate-lag and drain-lag. The voltages $V_{\text{trap}1,2}$ are fed back into the compact model to update its key parameters as shown in (5). (II) The dual-pulsed scheme to do the pulsed-IV simulation.

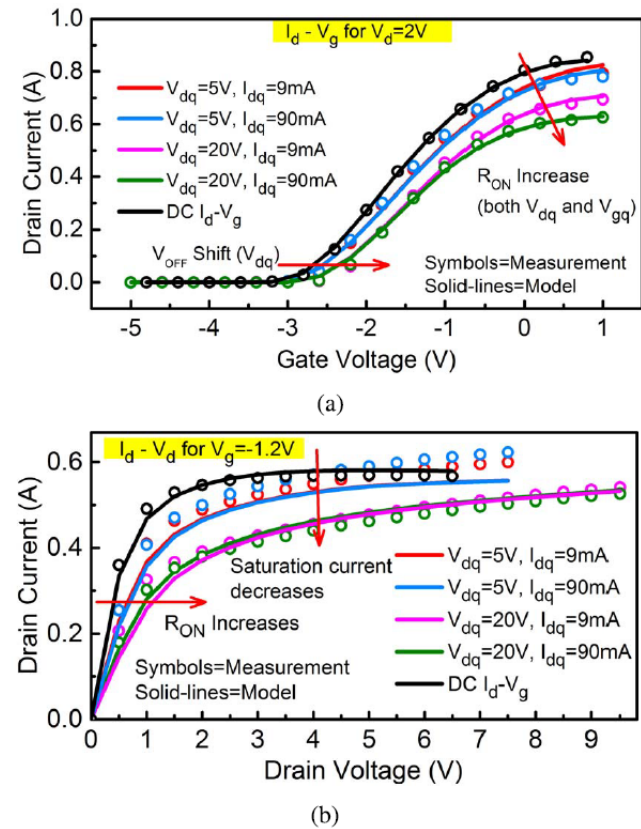
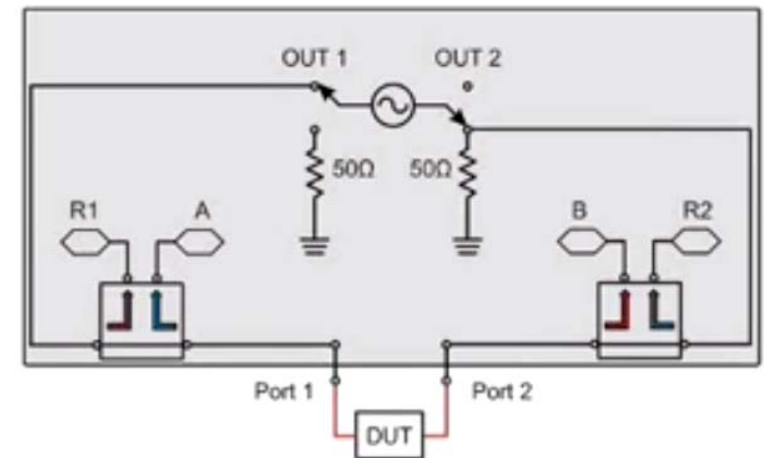
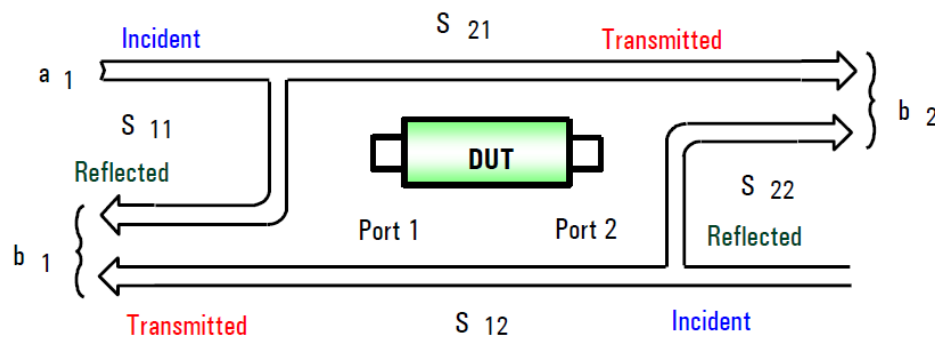


FIGURE 5. Correlation between measured and modeled (a) Pulsed $I_d - V_g$ and (b) Pulsed $I_d - V_d$ characteristics using the trap model. Accurate fits are seen for multiple quiescent bias conditions ($V_{dq} = 5, 20$ V and $I_{dq} = 10, 100$ mA/mm), which is essential for the non-linear RF behavior of the model.

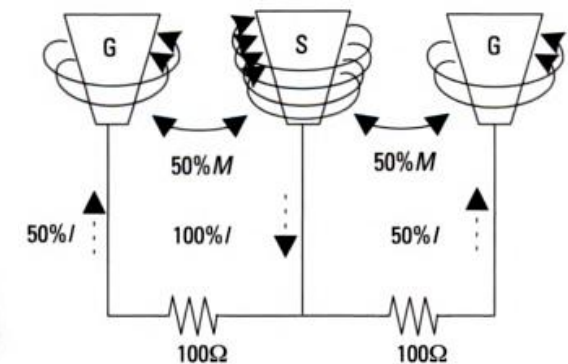
RF Measurements

S-Parameters

- Easy for high frequencies (hard to do open/short for Z/Y)
- Calculate other quantities
- Cascadable
- Transformation
- Compatibility with simulation tools



VNA Architecture

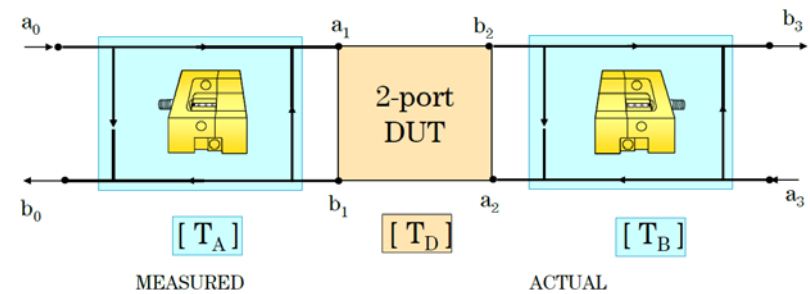
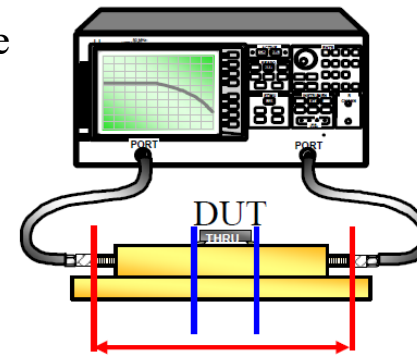
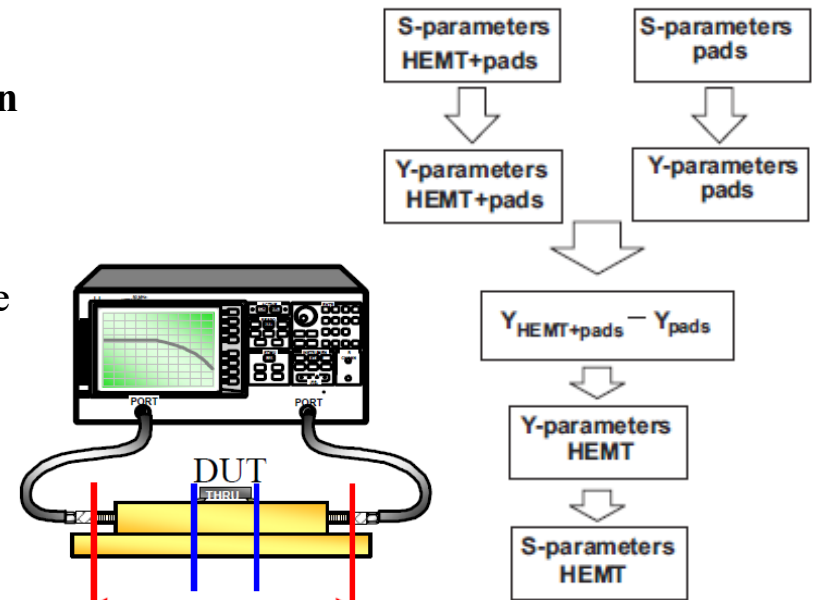
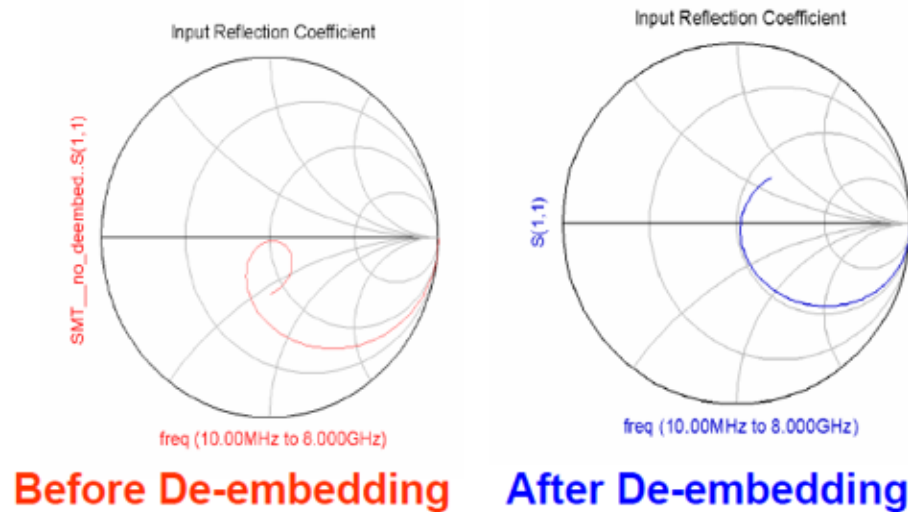


De-embedding

De-embedding : Negating effects of unwanted portion

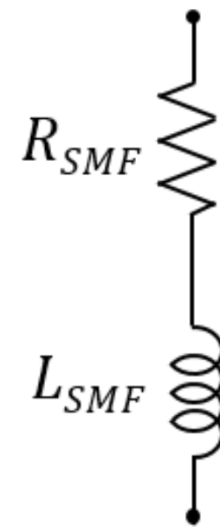
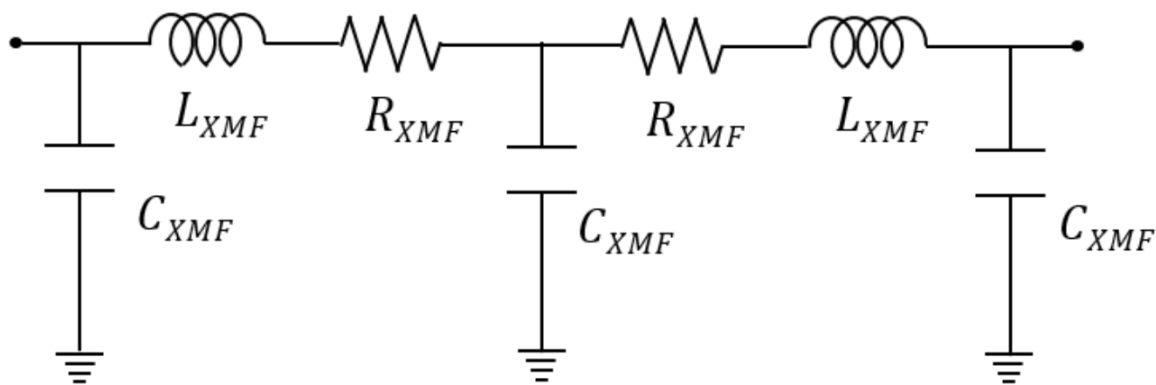
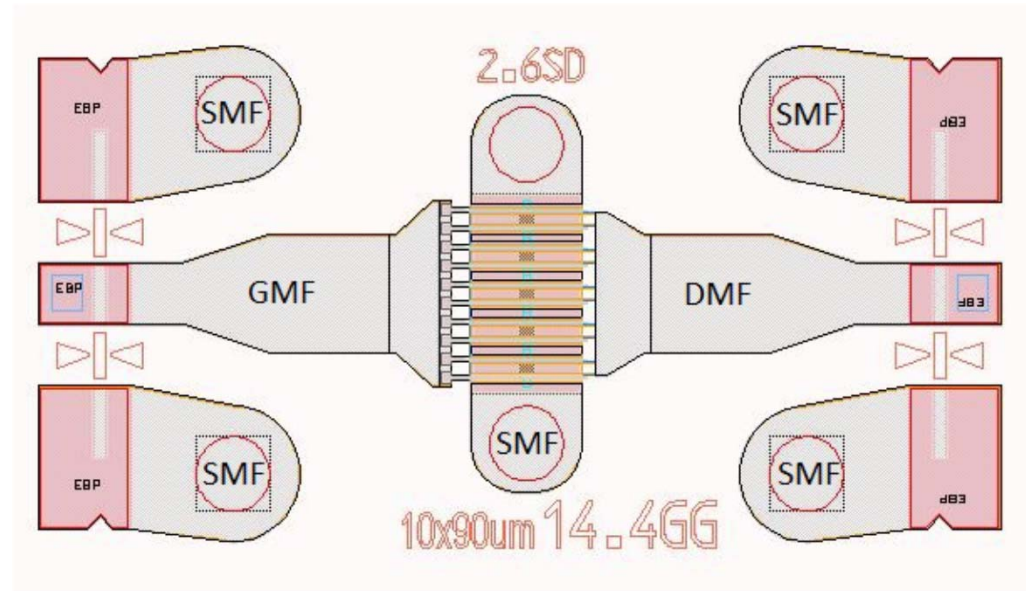
“Real” DUT SP= Measured SP–Fixture Characteristic

De-embedding is a mathematical process that removes the effects of unwanted embedded portions of the structure in the measured data by subtracting their contribution.

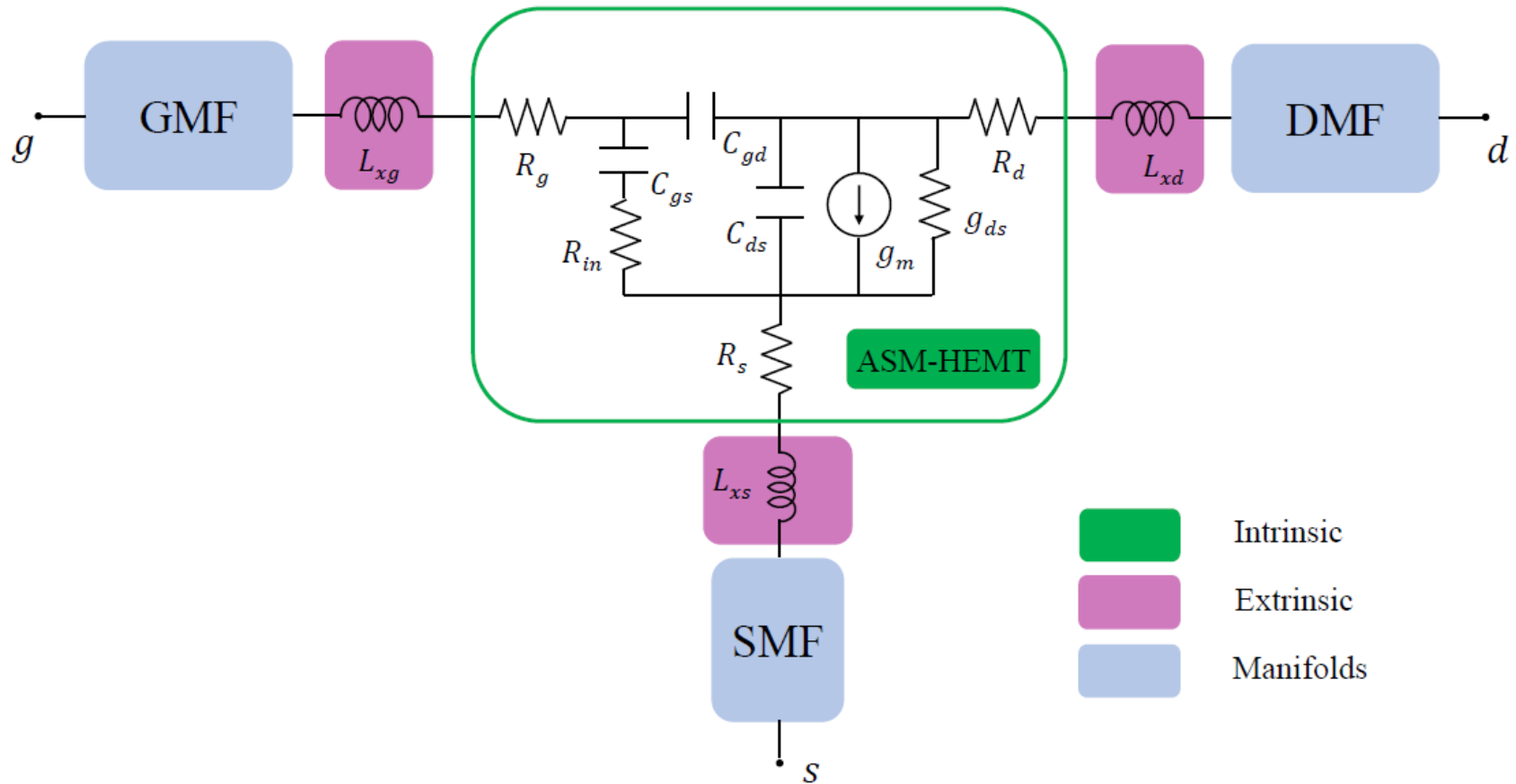


$$[T_m] = [T_A][T_D][T_B] \quad [T_D] = [T_A]^{-1}[T_m][T_B]^{-1}$$

Device Layout and Manifolds



Equivalent Circuit Model at RF



$$\begin{bmatrix} C_{gs} & C_{gd} & C_{ds} \\ g_m & g_{ds} & R_g \end{bmatrix} = \begin{bmatrix} (\text{Im}[Y_{11}] + \text{Im}[Y_{12}]) / \omega & -\text{Im}[Y_{12}] / \omega & \text{Im}[Y_{22}] / \omega - C_{gd} (1 + g_m R_g) \\ \text{Re}[Y_{21}] & \text{Re}[Y_{22}] & \text{Re}[Y_{11}] / (\omega^2 C_{gs}^2) \end{bmatrix}$$

11/08/2017

Yogesh S. Chauhan, IIT Kanpur

71

Small Signal Modeling

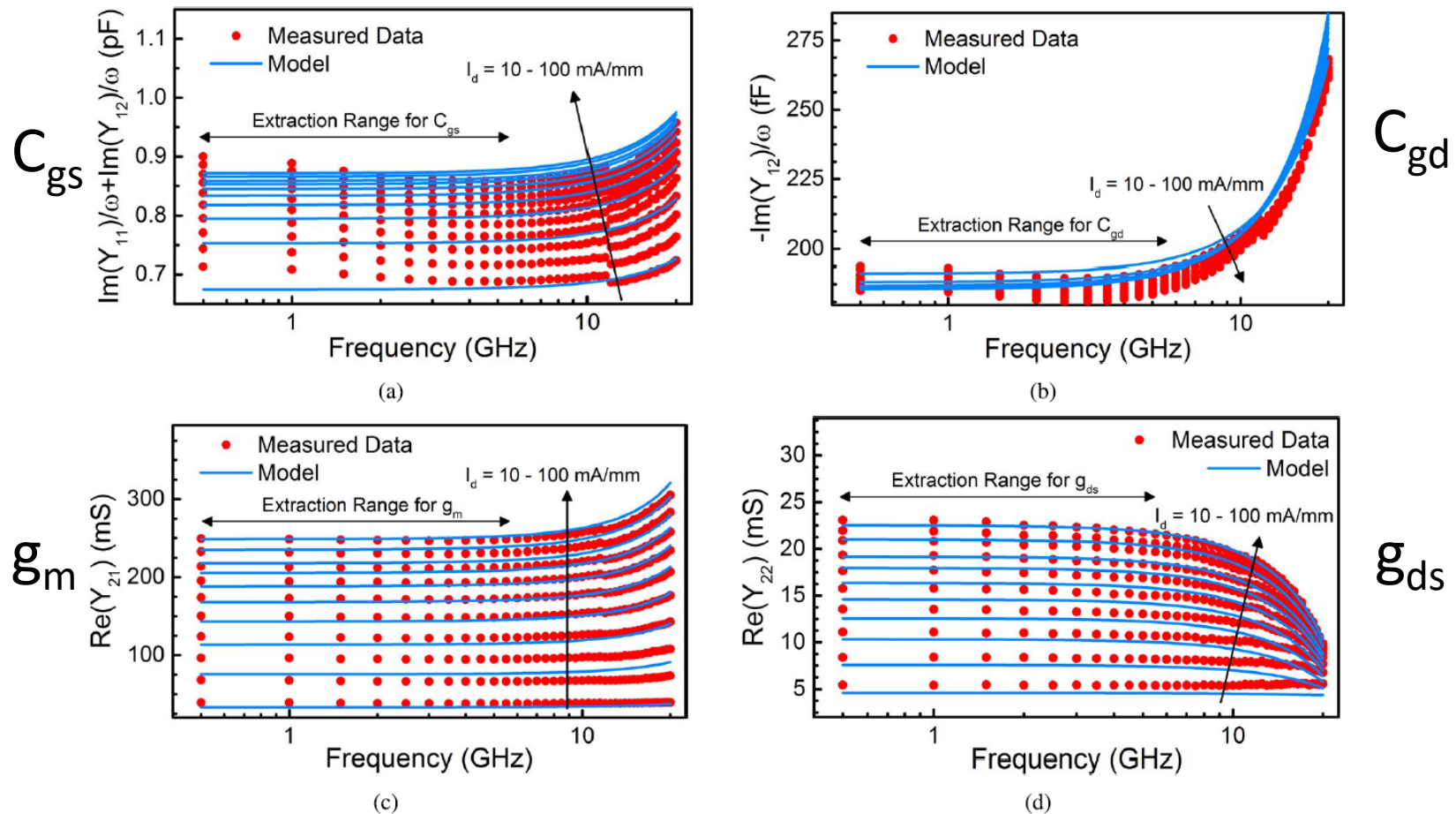
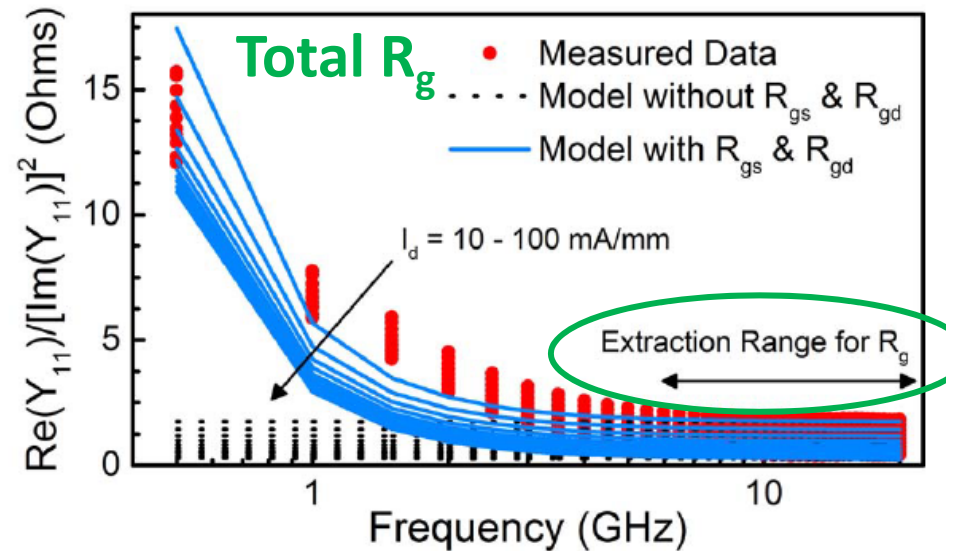
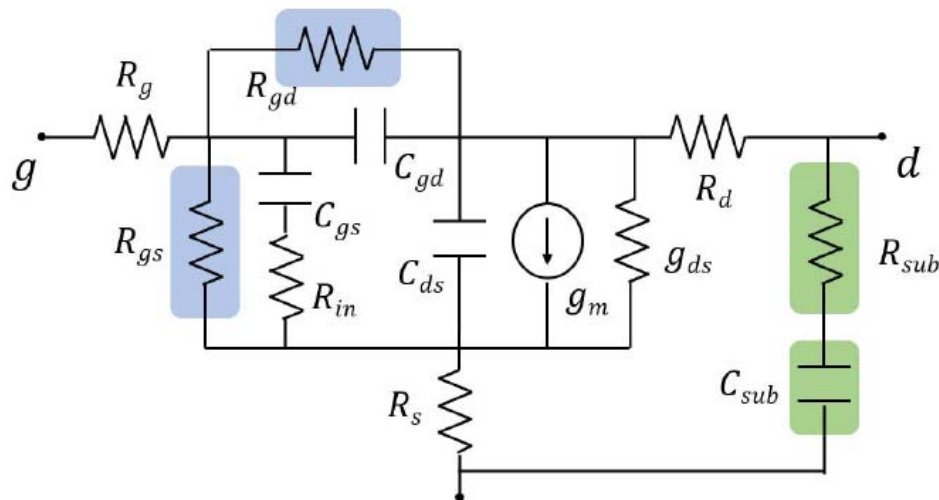


FIGURE 7. Extracted SS – EC (a) C_{gs} (b) C_{gd} (c) g_m and (d) g_{ds} for $V_d = 5$ V and 10 gate bias conditions. Parasitic capacitances are adjusted to values given in Table 2 to fit model and measured data for (a–b). A sufficiently broad frequency range (≈ 10 GHz) is observed for extraction for which frequency-independent behavior of SS – EC elements is seen after which inductive effects dominate.

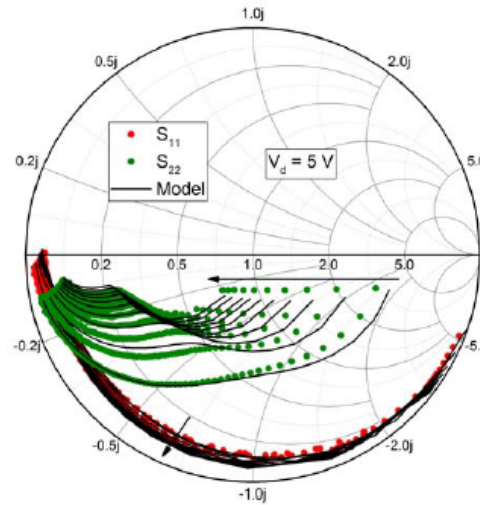
Impact of Gate Resistance

- **Large resistors R_{gs} and R_{gd}** – Capture the differential gate resistance for current flowing through the gate-source and gate-drain Schottky diodes.
- Their inclusion significantly impacts the overall gate resistance (R_g) at low frequencies as shown in Fig.
- **R_{sub} and C_{sub}** – Capture the substrate loss at the output port.

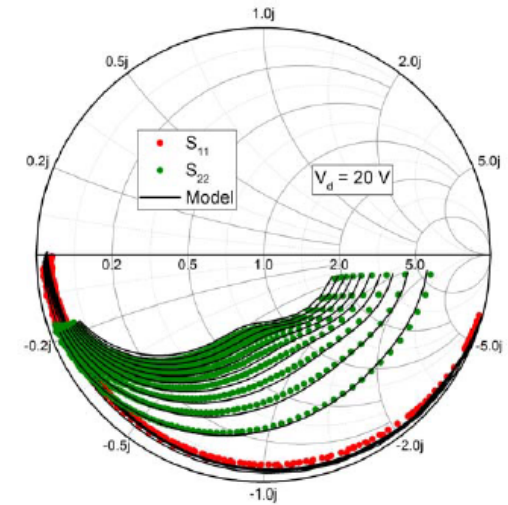


S-Parameters

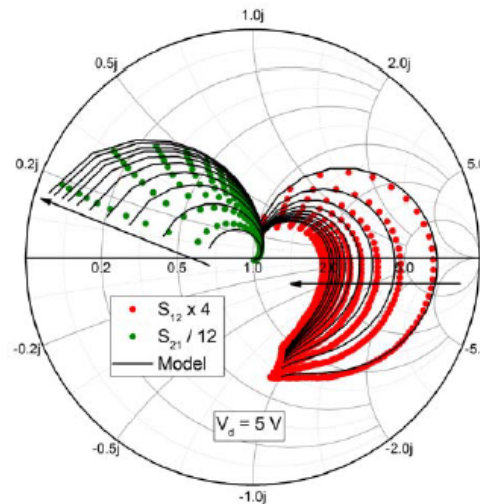
- Frequency: 0.5 – 50 GHz
- 2 different drain-bias conditions, with 10 different gate biases ($I_d = 10 - 100 \text{ mA/mm}$)



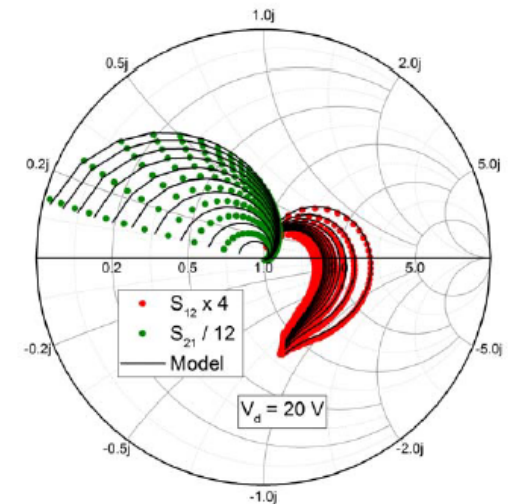
(a)



(b)



(c)

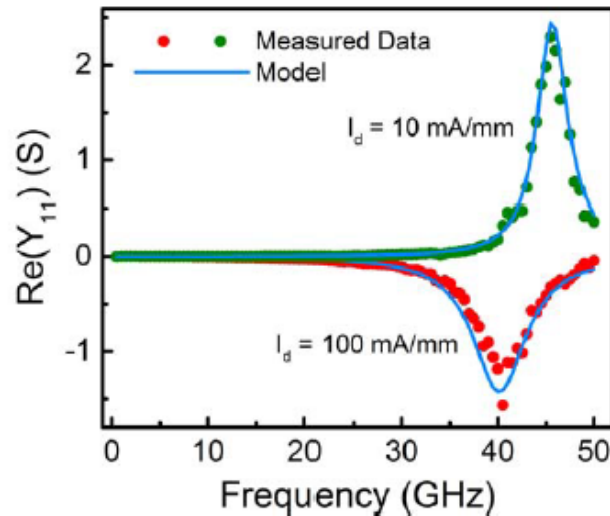


(d)

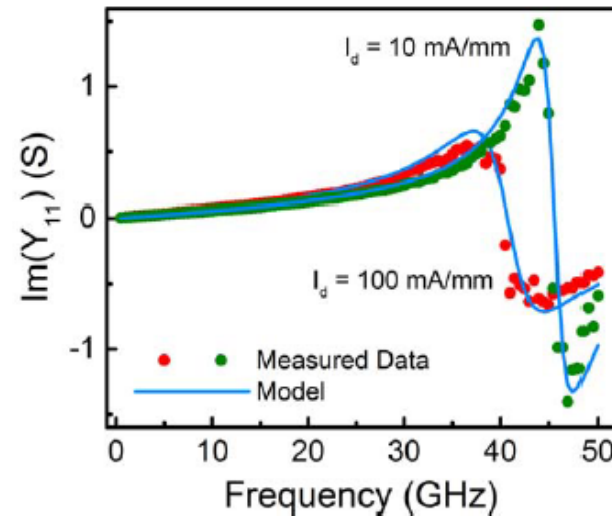
Lines – Model

Symbols – Measured Data 74

Y-Parameters



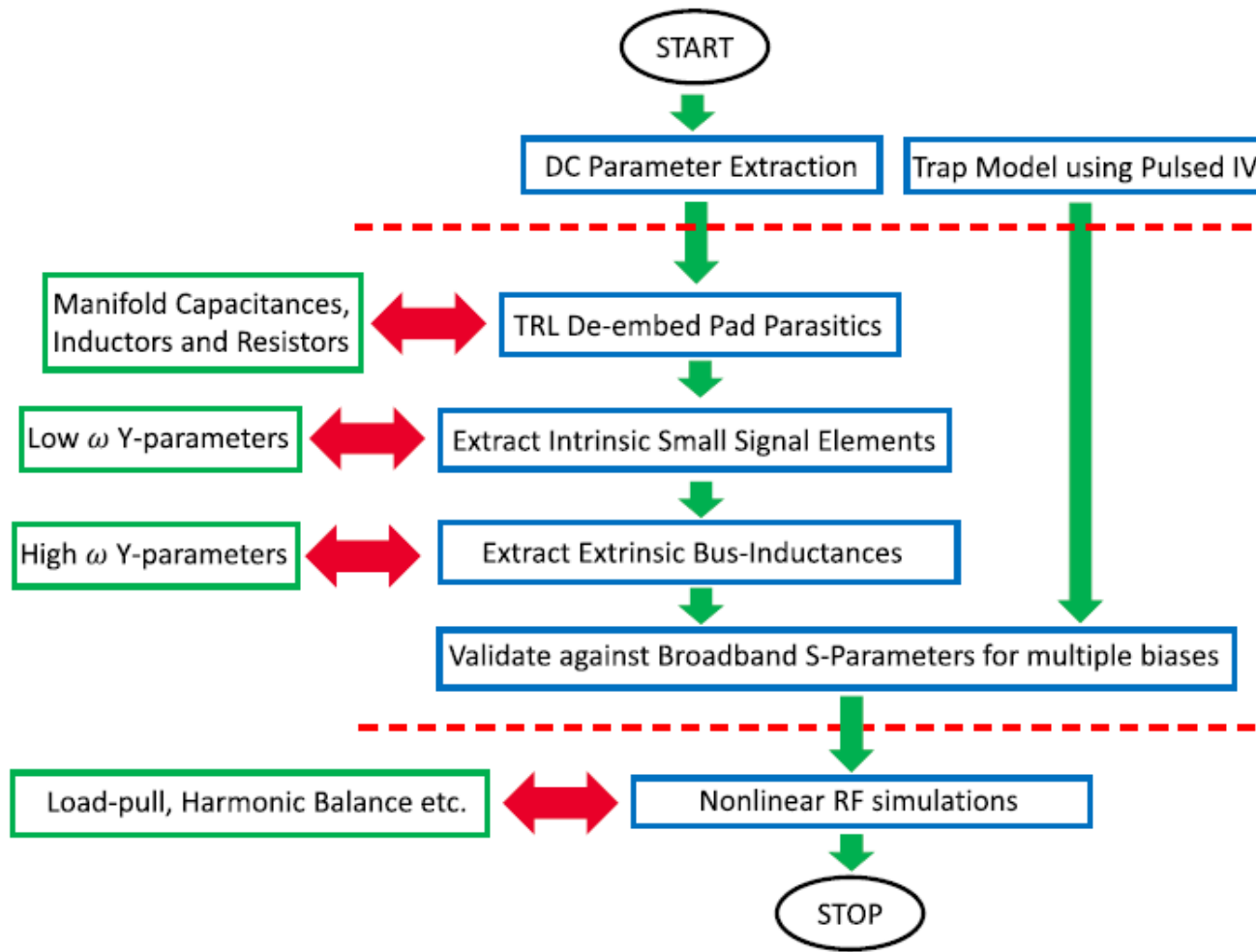
(a)



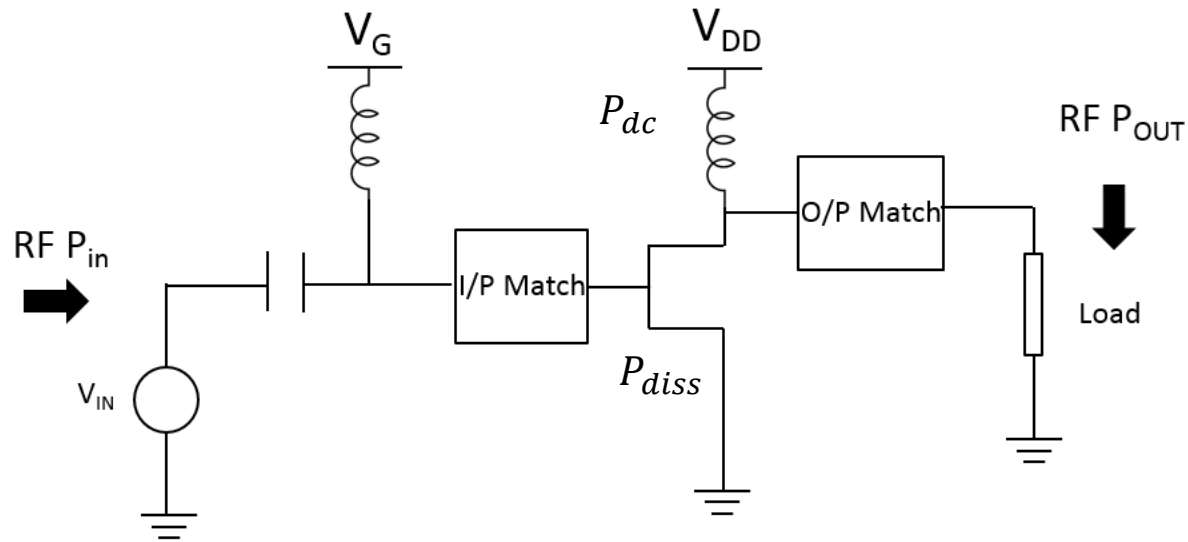
(b)

- The peaks and dips and their bias dependence is a manifestation of the interaction between the intrinsic capacitances and the extrinsic inductances.
- The values of bus-inductances can be fine-tuned to fit the peaks/dips in measured and modeled extrinsic-level Y-parameters.

RF Parameter Extraction Flow



Power Amplifier Design Goals



$$Gain = \frac{P_{out}}{P_{in}}$$

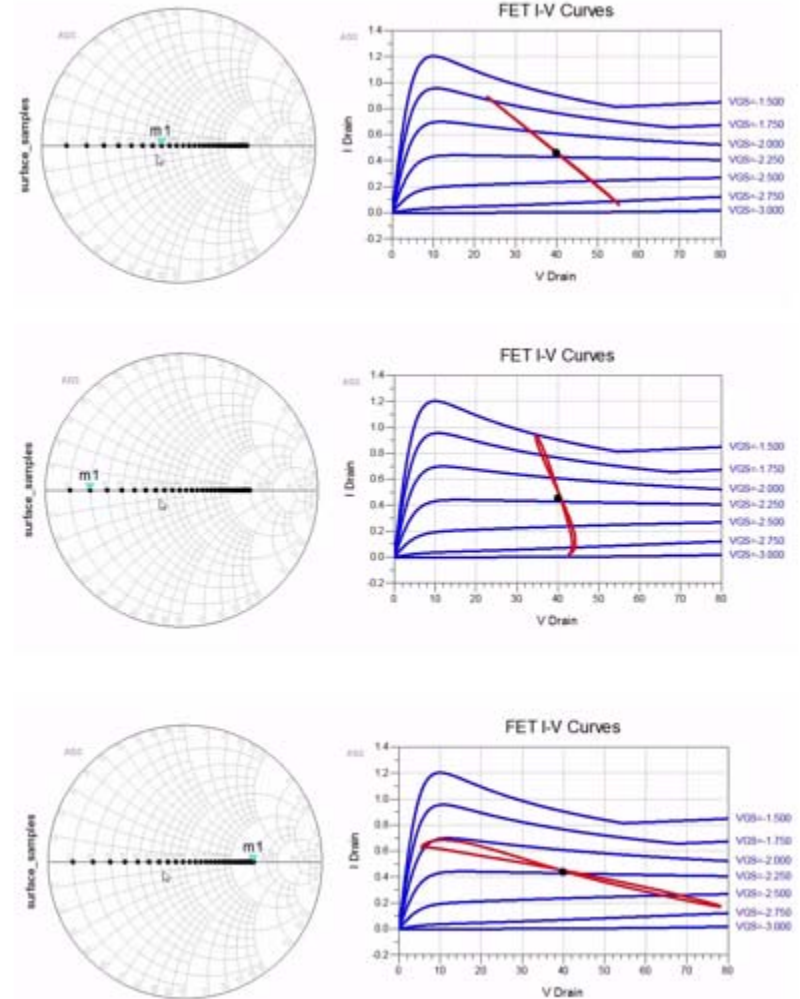
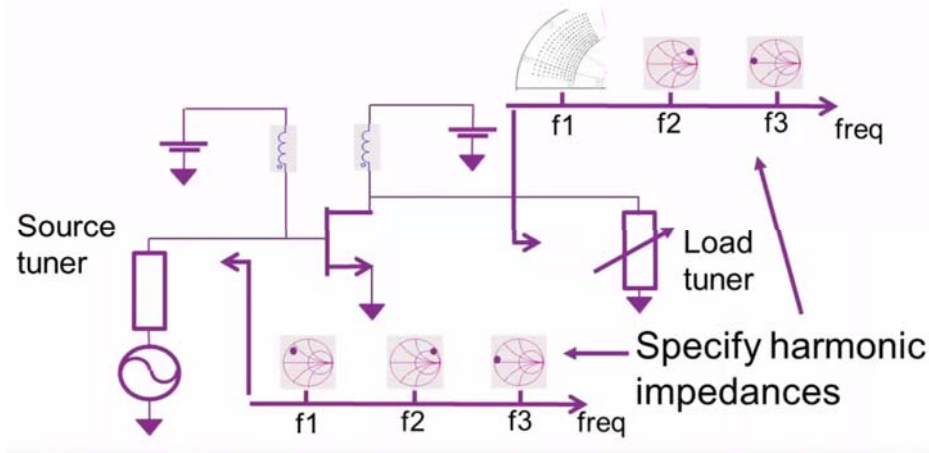
$$PAE = \frac{P_{out} - P_{in}}{P_{dc}}$$

$$Drain\ Efficiency = \frac{P_{out}}{P_{dc}}$$

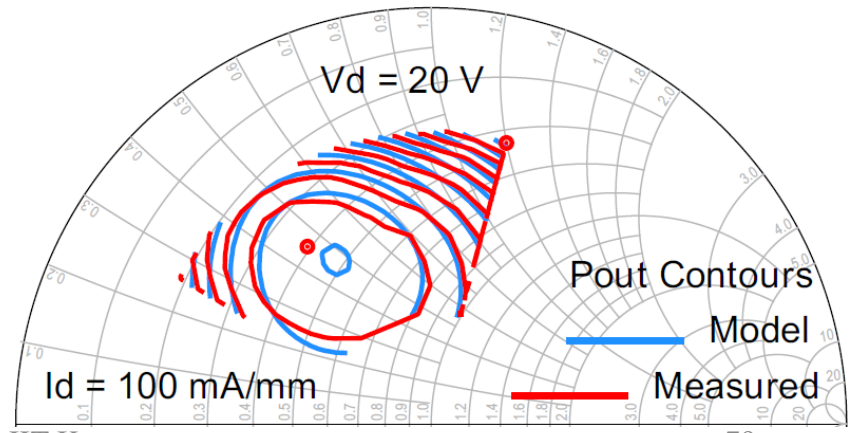
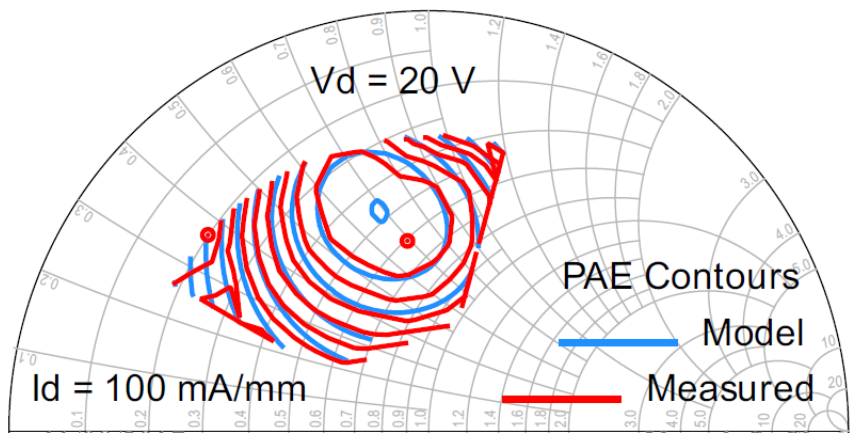
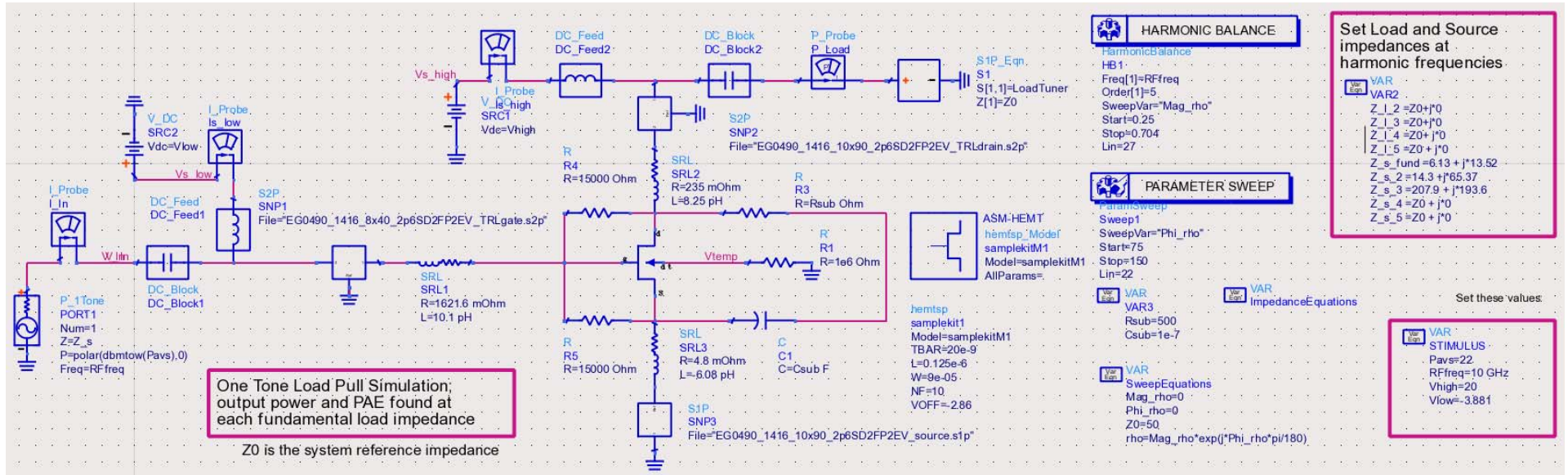
Load Pull Technique

Helps us:

- Determine Optimum load impedance for maximum Pout and PAE performance
- Matching networks
- Understand tradeoffs!



Load-Pull Schematic & Overlays



11/08/2017

Yogesh S. Chauhan, IIT Kanpur

S. A. Ahsan, et. al, *IEEE Trans. Microwave Theory Tech*, 2017.

79

Load Pull Contours

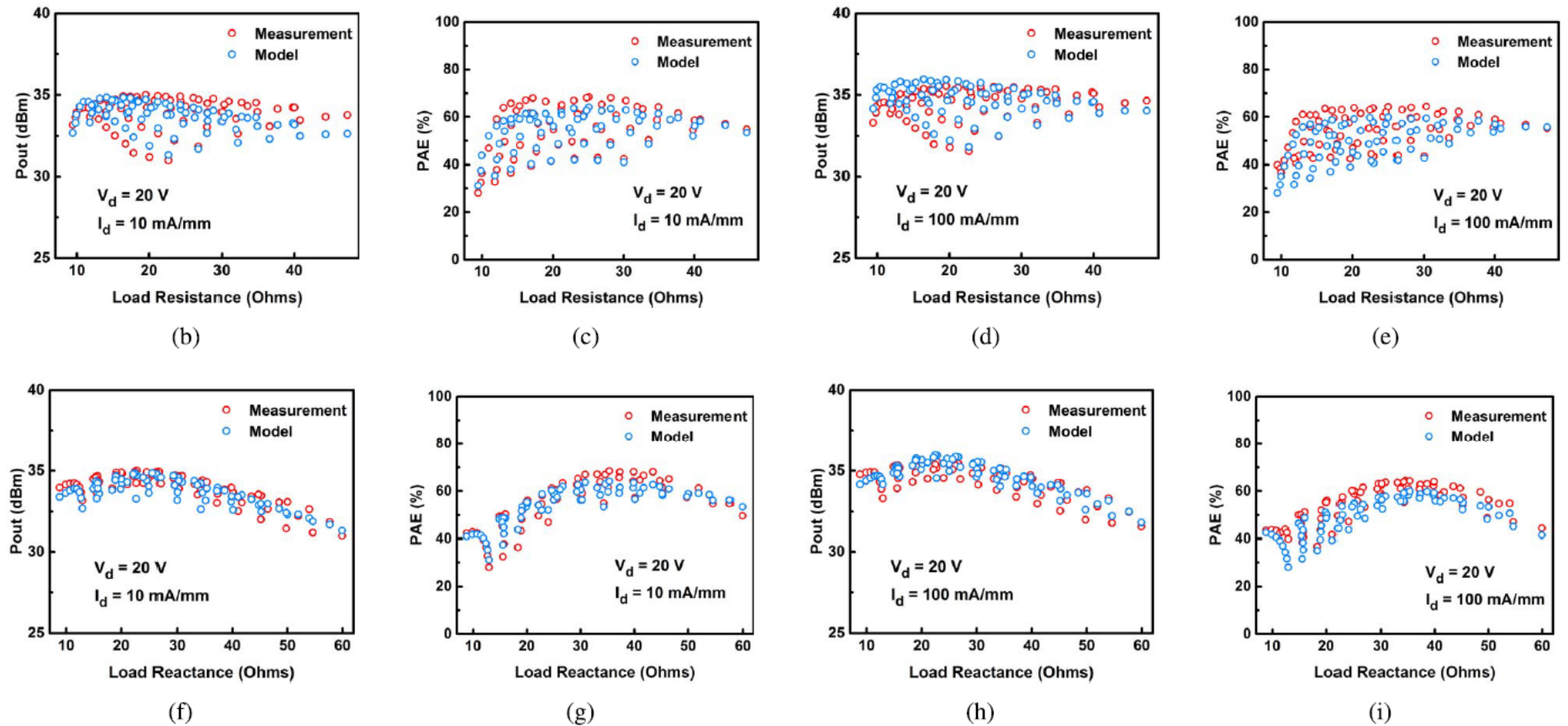
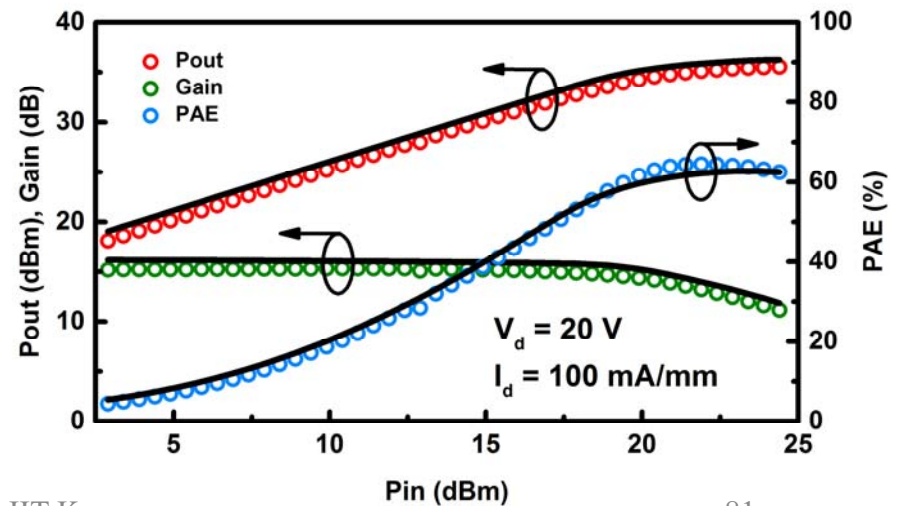
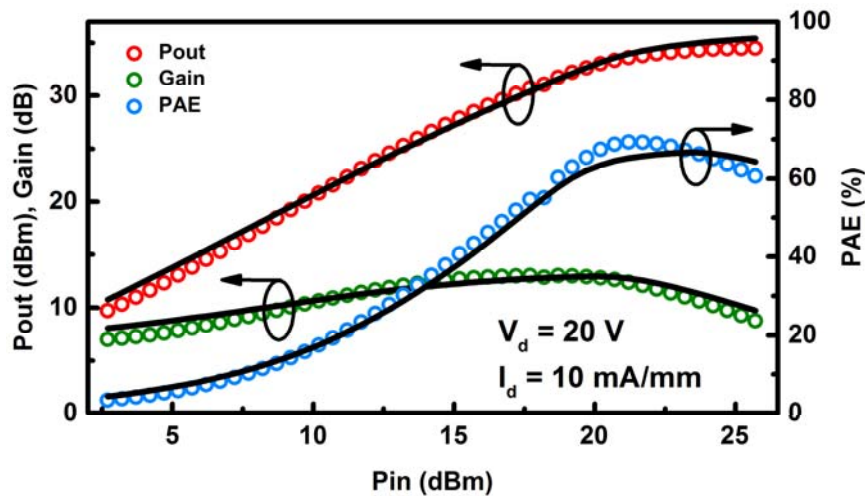
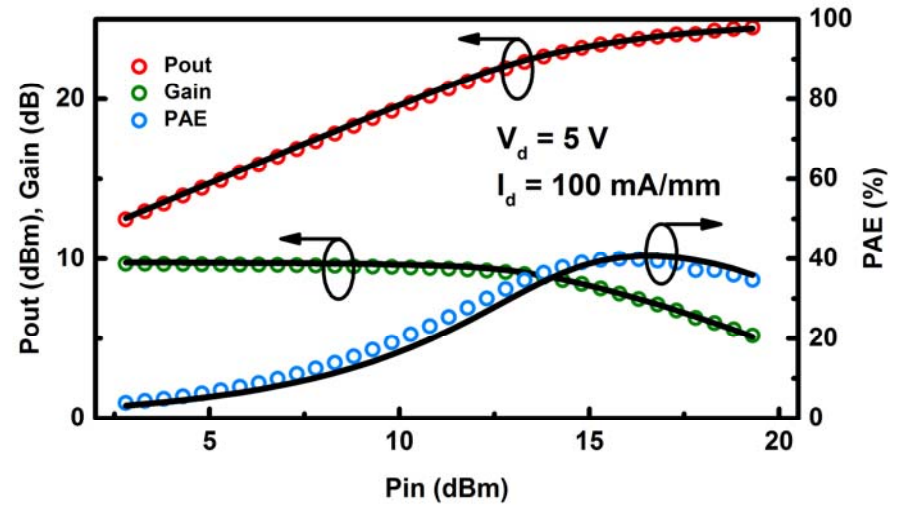
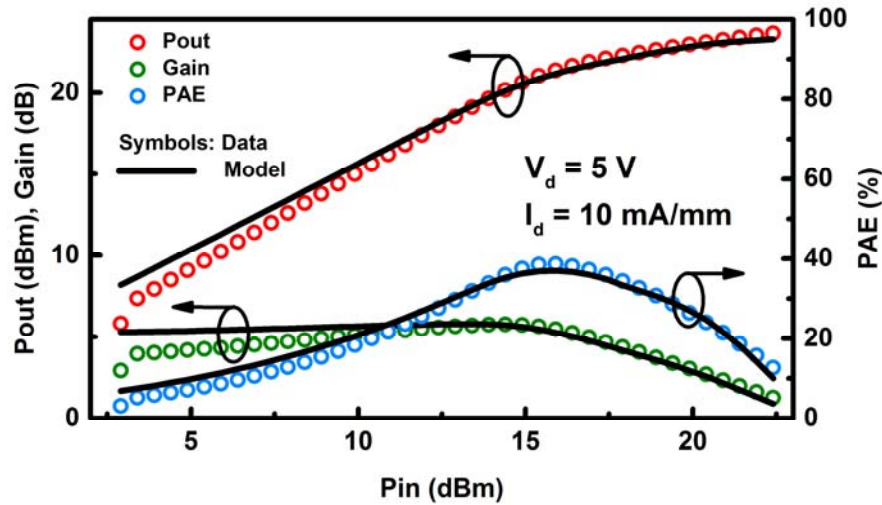


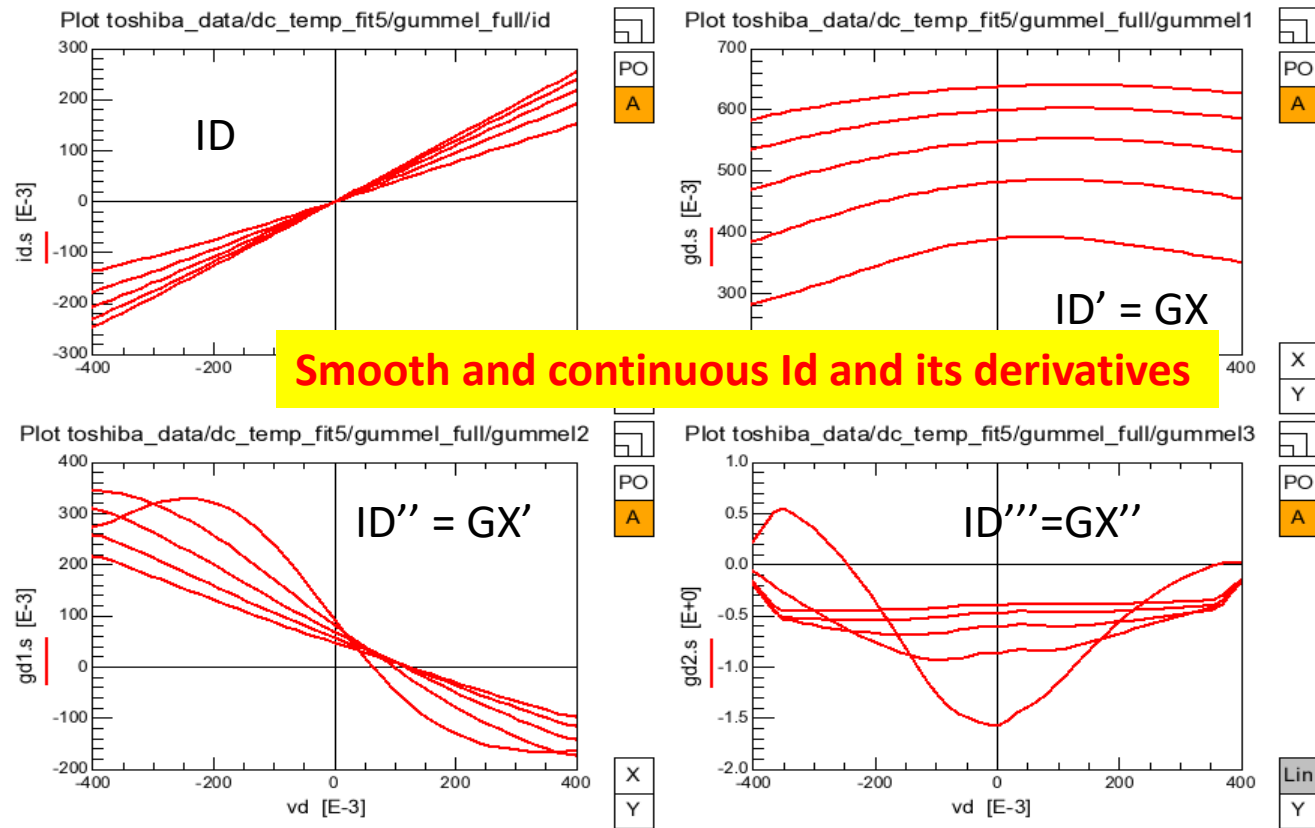
FIGURE 12. (a) ADS schematic for simulating load-pull contours using the embedded model. Pad level parasitics in the form of 2-port S-parameter components are added. Right in the centre is the DUT which is governed by the ASM-GaN-HEMT PDK. (b-i) Discrete load-sweeps for P_{OUT} and PAE against real and imaginary loads for multiple bias conditions, at 10 GHz signal frequency. The model accurately predicts the P_{OUT} and PAE maxima as well as their mutual tradeoffs upon varying the load resistance/reactance.

Harmonic Balance Power Sweeps



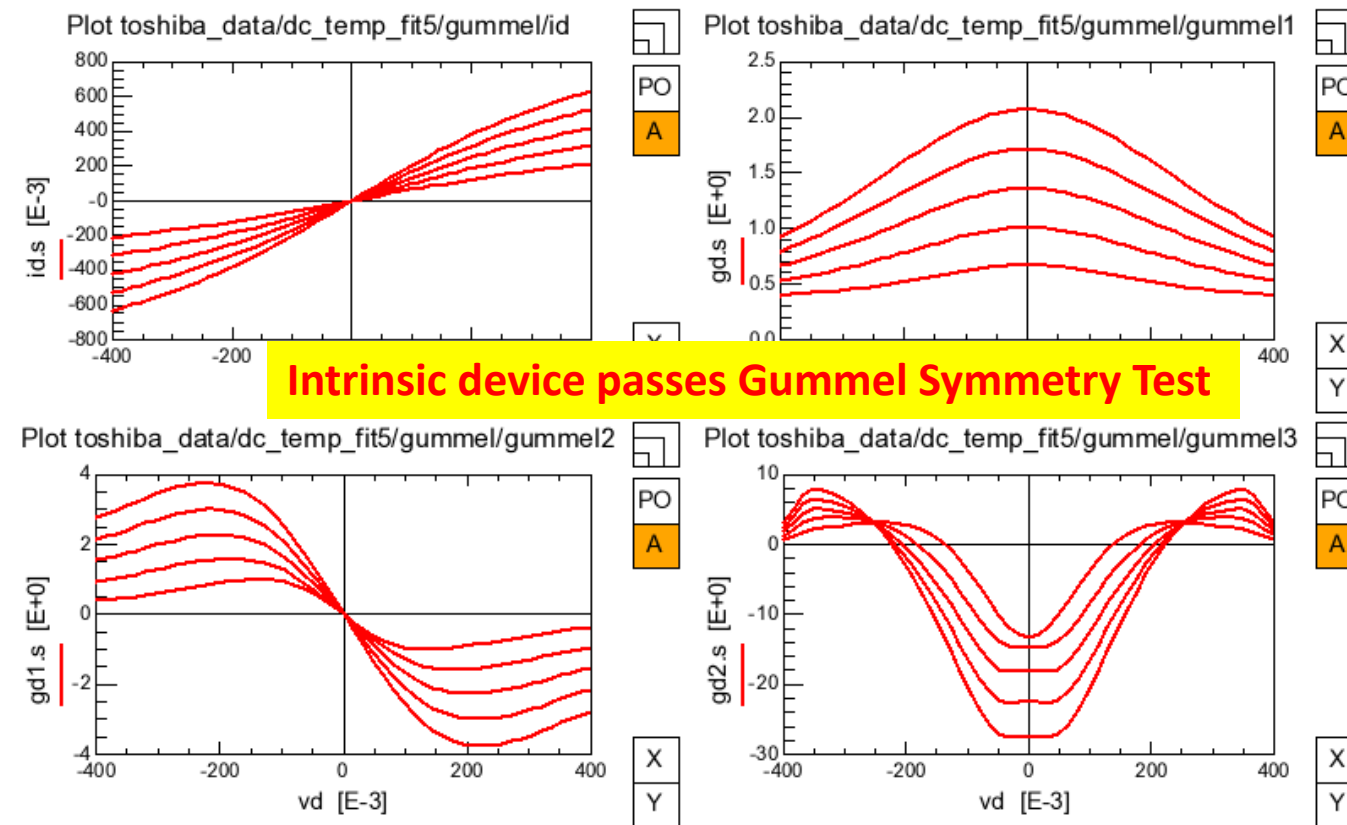
Model Quality

Toshiba device Id and derivatives



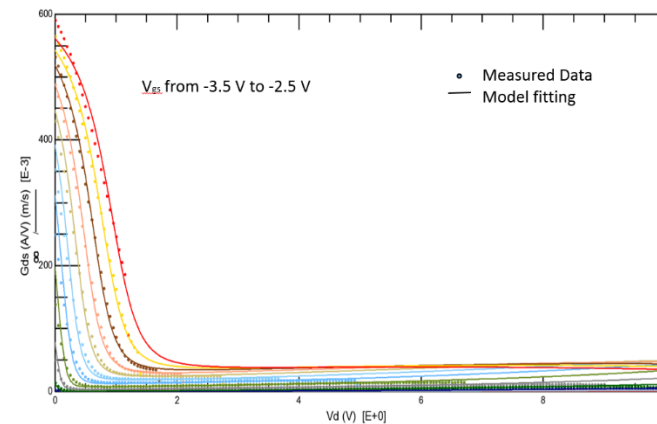
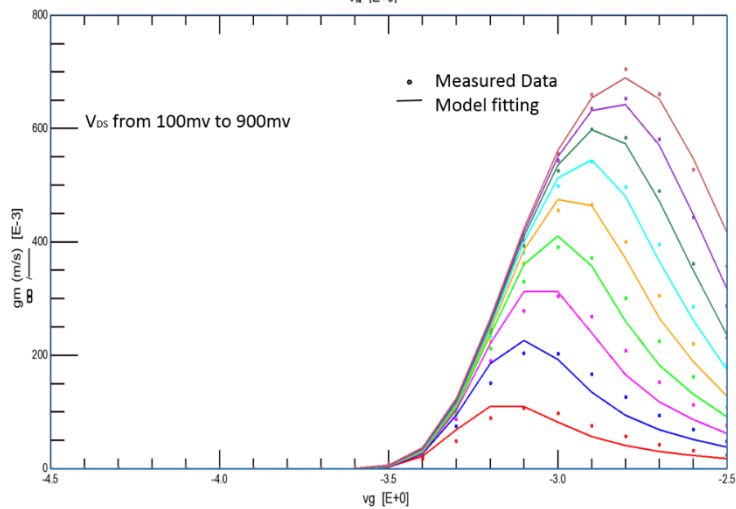
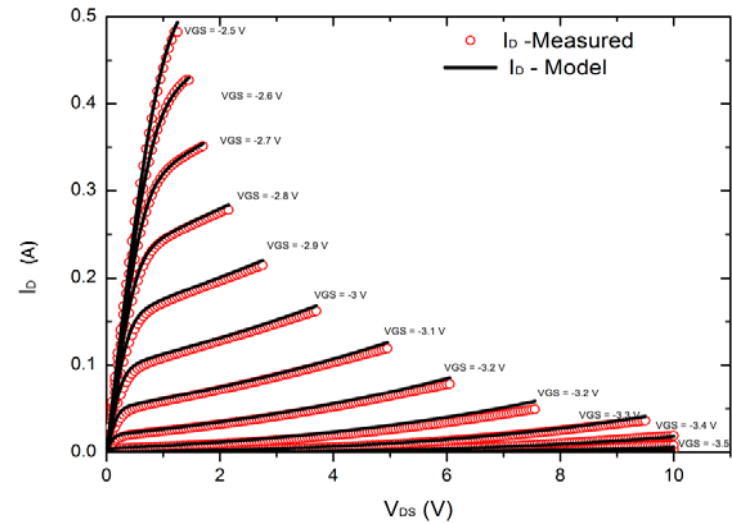
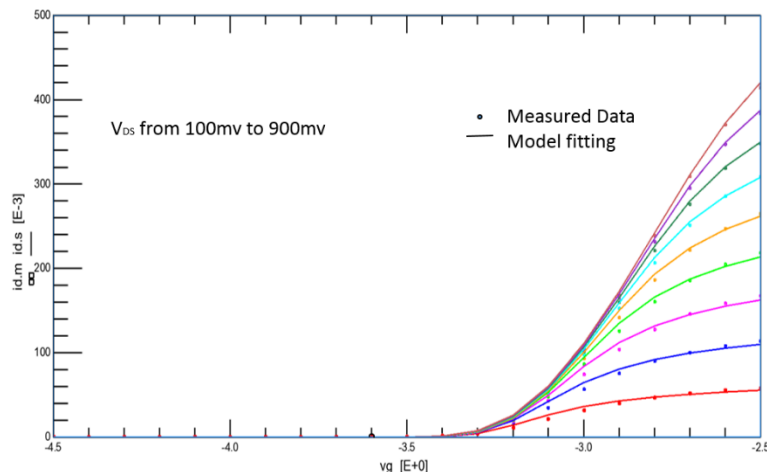
Toshiba device

Intrinsic device (simulation)



Characterization and Parameter Extraction for RFMD RF 3931 Device

(Devices received from ISRO)



Summary

- Physics-based fully analytical model for the GaN HEMTs
- Excellent agreement with the measured data at different temperatures for different channel length devices
- Model is implemented in the **Verilog - A** code
- Tested on Agilent ADS, Synopsys HSPICE and Cadence's Spectre **simulators**
- In final phase of industry standardization at CMC

My Group and Nanolab

Current members – 30

- Postdoc – 5
- Ph.D. – 17
- Three PhD graduated
 - Postdocs in UC Berkeley and U. Bordeaux France

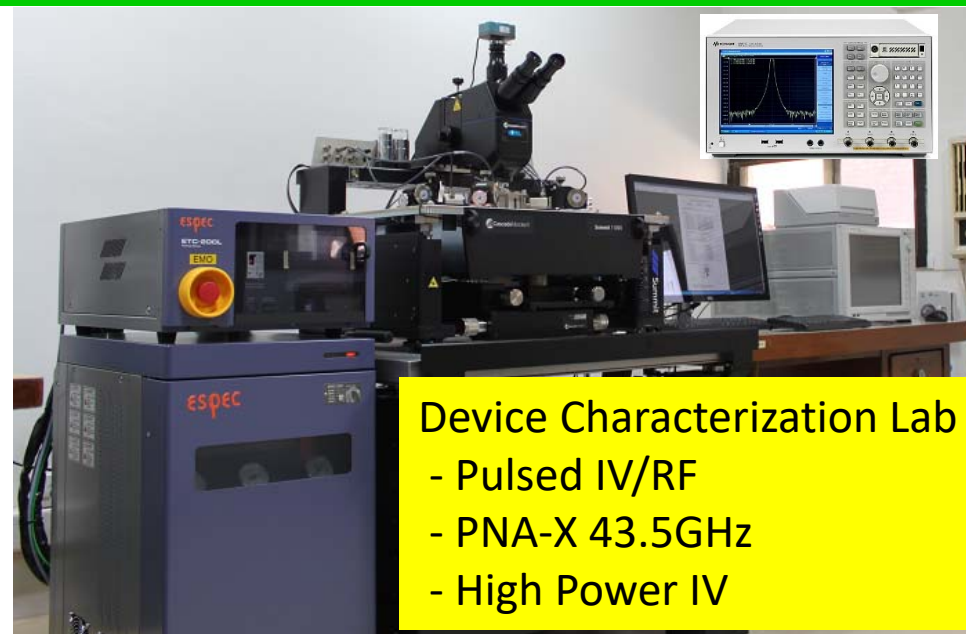


	2017	2016	2015	2014	2013	2012
Books	1		1			
Journal	20	18	9	5	3	3
Conference	8	30	30	8	4	6



Funding in last 5 years:
> Rs. 8.5 Crore

11/08/2017



Device Characterization Lab
 - Pulsed IV/RF
 - PNA-X 43.5GHz
 - High Power IV

GaN-HEMT Journal Publications

1. S. A. Ahsan, A. Pampori, S. Ghosh, S. Khandelwal, and Y. S. Chauhan, "A New Small-signal Parameter Extraction Technique for large gate-periphery GaN HEMTs", in [IEEE Microwave and Wireless Components Letters](#), Vol. 27, Issue 10, Oct. 2017.
2. S. A. Ahsan, S. Ghosh, S. Khandelwal, and Y. S. Chauhan, "Physics-based Multi-bias RF Large-Signal GaN HEMT Modeling and Parameter Extraction Flow", in [IEEE Journal of the Electron Devices Society](#), Vol. 5, Issue 5, Sept. 2017.
3. S. A. Ahsan, S. Ghosh, S. Khandelwal, and Y. S. Chauhan, "Pole-Zero Approach to Analyze and Model the Kink in Gain-Frequency Plot of GaN HEMTs", [IEEE Microwave and Wireless Components Letters](#), Vol. 27, Issue 3, Mar. 2017.
4. S. A. Ahsan, S. Ghosh, S. Khandelwal, and Y. S. Chauhan, "Analysis and Modeling of Cross-Coupling and Substrate Capacitance in GaN HEMTs for Power-Electronic Applications", [IEEE Transactions on Electron Devices \(Special Issue\)](#), Vol. 64, Issue 3, Mar. 2017.
5. A. Dasgupta and Y. S. Chauhan, "Modeling of Induced Gate Thermal Noise in HEMTs", [IEEE Microwave and Wireless Components Letters](#), Vol. 26, Issue 6, June 2016.
6. S. A. Ahsan, S. Ghosh, A. Dasgupta, K. Sharma, S. Khandelwal, and Y. S. Chauhan, "Capacitance Modeling in Dual Field Plate Power GaN HEMT for Accurate Switching Behaviour", [IEEE Transactions on Electron Devices](#), Vol. 63, Issue 2, Feb. 2016.
7. A. Dasgupta, S. Khandelwal, and Y. S. Chauhan, "Surface potential based Modeling of Thermal Noise for HEMT circuit simulation", [IEEE Microwave and Wireless Components Letters](#), Vol. 25, Issue 6, June 2015.
8. S. Ghosh, A. Dasgupta, S. Khandelwal, S. Agnihotri, and Y. S. Chauhan, "Surface-Potential-Based Compact Modeling of Gate Current in AlGa_N/Ga_N HEMTs", [IEEE Transactions on Electron Devices](#), Vol. 62, Issue 2, Feb. 2015.
9. A. Dasgupta, S. Khandelwal, and Y. S. Chauhan, "Compact Modeling of Flicker Noise in HEMTs", [IEEE Journal of Electron Devices Society](#), Vol. 2, Issue 6, Nov. 2014.
10. S. Khandelwal, C. Yadav, S. Agnihotri, Y. S. Chauhan, A. Curutchet, T. Zimmer, J.-C. Dejaeger, N. Defrance and T. A. Fjeldly, "A Robust Surface-Potential-Based Compact Model for GaN HEMT IC Design", [IEEE Transactions on Electron Devices](#), Vol. 60, Issue 10, Oct. 2013.
11. S. Khandelwal, Y. S. Chauhan, and T. A. Fjeldly, "Analytical Modeling of Surface-Potential and Intrinsic Charges in AlGa_N/Ga_N HEMT Devices", [IEEE Transactions on Electron Devices](#), Vol 59, Issue 8, Oct. 2012.

GaN-HEMT Conference Publications

1. S. Khandelwal, S. Ghosh, S. A. Ahsan and Y. S. Chauhan, "Dependence of GaN HEMT AM/AM and AM/PM Non-Linearity on AlGa_N Barrier Layer Thickness", IEEE Asia Pacific Microwave Conference (APMC), Kuala Lumpur, Malaysia, Nov. 2017.
2. S. A. Ahsan, S. Ghosh, S. Khandelwal and Y. S. Chauhan, "Surface-potential-based Gate-periphery-scalable Small-signal Model for GaN HEMTs", IEEE Compound Semiconductor IC Symposium (CSICS), Miami, USA, Oct. 2017.
3. S. Ghosh, S. A. Ahsan, A. Dasgupta, S. Khandelwal, and Y. S. Chauhan, "GaN HEMT Modeling for Power and RF Applications using ASM-HEMT", IEEE International Conference on Emerging Electronics (ICEE), Mumbai, India, Dec. 2016.
4. S. Ghosh, A. Dasgupta, A. K. Dutta, S. Khandelwal, and Y. S. Chauhan, "Physics based Modeling of Gate Current including Fowler-Nordheim Tunneling in GaN HEMT", IEEE International Conference on Emerging Electronics (ICEE), Mumbai, India, Dec. 2016.
5. S. A. Ahsan, S. Ghosh, S. Khandelwal, and Y. S. Chauhan, "Statistical Simulation for GaN HEMT Large Signal RF performance using a Physics-based Model", IEEE International Conference on Emerging Electronics (ICEE), Mumbai, India, Dec. 2016.
6. A. Dasgupta, S. Ghosh, S. A. Ahsan, S. Khandelwal, N. Defrance, and Y. S. Chauhan, "Modeling DC, RF and Noise behavior of GaN HEMTs using ASM-HEMT Compact Model", IEEE International Microwave and RF Conference (IMaRC), Delhi, India, Dec. 2016.
7. S. A. Ahsan, S. Ghosh, A. Dasgupta, S. Khandelwal, and Y. S. Chauhan, "ASM-HEMT: Advanced SPICE Model for Gallium Nitride High Electron Mobility Transistors", International Conference of Young Researchers on Advanced Materials (ICYRAM), Bangalore, India, Dec. 2016.
8. S. Ghosh, S. A. Ahsan, S. Khandelwal and Y. S. Chauhan, "Modeling of Source/Drain Access Resistances and their Temperature Dependence in GaN HEMTs", IEEE Conference on Electron Devices and Solid-State Circuits (EDSSC), Hong Kong, Aug. 2016.
9. S. A. Ahsan, S. Ghosh, S. Khandelwal and Y. S. Chauhan, "Modeling of Kink-Effect in RF Behaviour of GaN HEMTs using ASM-HEMT Model", IEEE Conference on Electron Devices and Solid-State Circuits (EDSSC), Hong Kong, Aug. 2016.
10. R. Nune, A. Anurag, S. Anand and Y. S. Chauhan, "Comparative Analysis of Power Density in Si MOSFET and GaN HEMT based Flyback Converters", IEEE International Conference on Compatibility and Power Electronics, Bydgoszcz, Poland, June 2016.
11. S. Agnihotri, S. Ghosh, A. Dasgupta, A. Ahsan, S. Khandelwal, and Y. S. Chauhan, "Modeling of Trapping Effects in GaN HEMTs", IEEE India Conference (INDICON), New Delhi, India, Dec. 2015.
12. S. Ghosh, S. Agnihotri, S. A. Ahsan, S. Khandelwal, and Y. S. Chauhan, "Analysis and Modeling of Trapping Effects in RF GaN HEMTs under Pulsed Conditions", International Workshop on Physics of Semiconductor Devices (IWPSD), Bangalore, India, Dec. 2015.
13. S. Agnihotri, S. Ghosh, S. Khandelwal, and Y. S. Chauhan, "Impact of Gate Field Plate on DC, C-V, and Transient Characteristics of Gallium Nitride HEMTs", International Workshop on Physics of Semiconductor Devices (IWPSD), Bangalore, India, Dec. 2015.
14. K. Sharma, S. Ghosh, A. Dasgupta, S. A. Ahsan, S. Khandelwal, and Y. S. Chauhan, "Capacitance Analysis of Field Plated GaN HEMT", International Workshop on Physics of Semiconductor Devices (IWPSD), Bangalore, India, Dec. 2015.
15. S. A. Ahsan, S. Ghosh, J. Bandrupalli, S. Khandelwal, and Y. S. Chauhan, "Physics based large signal modeling for RF performance of GaN HEMTs", International Workshop on Physics of Semiconductor Devices (IWPSD), Bangalore, India, Dec. 2015.
16. S. Khandelwal, S. Ghosh, Y. S. Chauhan, B. Iniguez, T. A. Fjeldly and C. Hu, "Surface-Potential-Based RF Large Signal Model for Gallium Nitride HEMTs", IEEE Compound Semiconductor IC Symposium (CSICS), New Orleans, USA, Oct. 2015.
17. S. A. Ahsan, S. Ghosh, K. Sharma, A. Dasgupta, S. Khandelwal, and Y. S. Chauhan, "Capacitance Modeling of a GaN HEMT with Gate and Source Field Plates", IEEE International Symposium on Compound Semiconductors (ISCS), Santa Barbara, USA, June 2015.
18. A. Dasgupta and Y. S. Chauhan, "Surface Potential Based Modeling of Induced Gate Thermal Noise for HEMTs", IEEE International Symposium on Compound Semiconductors (ISCS), Santa Barbara, USA, June 2015.
19. S. Khandelwal, Y. S. Chauhan, B. Iniguez, and T. Fjeldly, "RF Large Signal Modeling of Gallium Nitride HEMTs with Surface-Potential Based ASM-HEMT Model", IEEE International Symposium on Compound Semiconductors (ISCS), Santa Barbara, USA, June 2015. (Invited)
20. A. Dasgupta, S. Ghosh, S. Khandelwal, and Y. S. Chauhan, "ASM-HEMT: Compact model for GaN HEMTs", IEEE Conference on Electron Devices and Solid-State Circuits (EDSSC), Singapore, June 2015.
21. K. Sharma, A. Dasgupta, S. Ghosh, S. A. Ahsan, S. Khandelwal, and Y. S. Chauhan, "Effect of Access Region and Field Plate on Capacitance behavior of GaN HEMT", IEEE Conference on Electron Devices and Solid-State Circuits (EDSSC), Singapore, June 2015.
22. S. Ghosh, K. Sharma, S. Khandelwal, S. Agnihotri, T. A. Fjeldly, F. M. Yigletu, B. Iniguez, and Y. S. Chauhan, "Modeling of Temperature Effects in a Surface-Potential Based ASM-HEMT model", IEEE International Conference on Emerging Electronics (ICEE), Bangalore, India, Dec. 2014.
23. S. Agnihotri, S. Ghosh, A. Dasgupta, S. Khandelwal, and Y. S. Chauhan, "A Surface Potential based Model for GaN HEMTs", IEEE PrimeAsia, Visakhapatnam, Dec. 2013. (Gold Leaf Certificate)